ORTHOTROPIC CYLINDRICAL SHELLS UNDER DYNAMIC LOADING

By
ELMER MANGRUM, JR.

A DISSERTATION PRESENTED TO THE GRADUATE COUNCIL OF
THE UNIVERSITY OF FLORIDA
IN PARTIAL FULFILLMENT OF THE REQUIREMENTS FOR THE
DEGREE OF DOCTOR OF PHILOSOPHY

UNIVERSITY OF FLORIDA
1970

This dissertation is dedicated to

my wife Rita

and my daughter Gaila.

ACKNOWLEDGMENT

I would like to acknowledge the support and encouragement of General William M. Thames, K. A. Campbell, and N. E. Munch of the General Electric Company who made this research possible. I wish also to express my sincere gratitude to Dr. J. J. Burns for this guidance and suggestions during the course of this research.

TABLE OF CONTENTS

		Page
LIST OF TABLES		vii
LIST OF FIGURES		viii
KEY TO SYMBOLS		xi
ABSTRACT		xv
Chapter		
I	INTRODUCTION	1
	Statement of the Problem	1
	Specific Goals of This Research	2
	Review of Previous Work	3
	Contributions of This Work	3
II	GOVERNING EQUATIONS OF MOTION	5
	General Equations	5
	Axisymmetric Loading	15
	Pressure Loading Form	15
	Nondimensional Equations	16
III	TRANSFORMATION OF EQUATIONS	20
IV	INVESTIGATION OF THE CRITICAL VELOCITIES	23

TABLE OF CONTENTS (Continued)

Chapter		Page
V	SOLUTION FOR DISPLACEMENTS	42
	General Solution	42
	Transformed Displacements	42
	Inverse Transformation of the Rotation	43
	Inverse Transformation of the Radial Deflection	46
	Inverse Transformation of the Axial Deflection	51
	Summary of Deflection Expressions	55
	Solution for No External Damping	58
	Form of the Radial Deflection in Region IV	59
	Form of the Radial Deflection in Region VII	62
	Form of the Radial Deflection in Region V	63
	Form of the Radial Deflection in Region VI	63
	Comparison of Solution with Other Results	64
	Numerical Results	65
	Comparison of Results with Other Solutions for a Static Load	65
	Summary of Deflection Response for Shells under Various Load Velocities	69
	Region II Response	71
	Region IV Response	71
	Damping Effect on Regions V and VII Response	71
	Region VI Response	78
	Deflection Behavior in the Vicinity of λ_{1CR}^2	78
	Effect of Prestress on λ_{1CR}^2	78
	Superposition of Step Loads	82
	Study of Material Properties Variations	82

TABLE OF CONTENTS (Continued)

Chapter		Page
VI	STRESSES	92
	Development of Stress Equations	92
	Numerical Results	94
VII	CONCLUDING REMARKS	98
	Conclusions	98
	Suggestions for Future Work	99
Appendix		
A	FOURIER TRANSFORM OF THE FORCING FUNCTION	100
B	SOLUTION OF EQUATIONS FOR THE TRANSFORMED DEFLECTIONS	102
C	EVALUATION OF THE DISCRIMINANT OF A FOURTH ORDER POLYNOMIAL	106
D	DETERMINATION OF THE CRITICAL VELOCITY EQUATIONS	111
E	COMPUTER PROGRAM FOR SOLUTION OF LOAD VELOCITIES WHICH CAUSE REPEATED ROOTS IN THE UNDAMPED CHARACTERISTIC EQUATION	116
F	PARTIAL FRACTION EXPANSION OF A FOURTH ORDER POLYNOMIAL	123
G	CHECK TO SEE THAT SOLUTIONS SATISFY THE GOVERNING DIFFERENTIAL EQUATIONS	125
H	COMPUTER PROGRAM FOR DEFLECTION AND STRESS CALCULATIONS	130
I	RELATIONSHIPS BETWEEN ANALYSIS PARAMETERS	147
BIBLIOGRAPHY		149
ADDITIONAL REFERENCES		151

LIST OF TABLES

Table		Page
4-1	Correlation of Root Type with Region Numbers for Figures 4.2 through 4.8	27
H-1	Options Available for Program DEFSTR	131

LIST OF FIGURES

Figure		Page
2.1	Cylindrical Coordinate System	5
2.2	Pressure Loading	16
4.1	Flow Diagram of Computer Program VCRIT which Determines Load Velocities at which Repeated Roots Occur	28
4.2	Classification of Roots of the Undamped Characteristic Equation for Variations in the Thickness-to-Radius Ratio Including Prestress	29
4.3	Classification of Roots of the Undamped Characteristic Equation for Variations in the Thickness-to-Radius Ratio with No Prestress	30
4.4	Classification of Roots of the Undamped Characteristic Equation for Variations in E_{θ_o}/E_{x_o}	31
4.5	Classification of Roots of the Undamped Characteristic Equation for Variations in G_{xz_o}/E_{x_o}	32
4.6	Classification of Roots of the Undamped Characteristic Equation for Variations in E_{ν_o}/E_{x_o}	33
4.7	Classification of Roots of the Undamped Characteristic Equation for Variations in the Circumferential Prestress	34
4.8	Classification of Roots of the Undamped Characteristic Equation for Variations in the Axial Prestress	35
4.9	Path of the Roots of the Undamped Characteristic Equation for Increasing Load Speed (Beginning in Region I)	37
4.10	Path of the Roots of the Undamped Characteristic Equation for Increasing Load Speed (Beginning in Region V)	39
5.1	Contour Integration Path for Evaluating Rotation Integral . . .	44
5.2	Integration Contour for Radial Deflection for $\phi > 0$, $b_k > 0$ . .	47
5.3	Integration Contour for Evaluating Radial Deflection for $\phi < 0$, $b_k > 0$	49

Figure		Page
5.4	Loci of the Roots of the Characteristic Equation as the Damping Approaches Zero	60
5.5	Static Load Problem	64
5.6	Flow Diagram for Computer Program for Deflection and Stress Calculations	66
5.7	Radial Deflection for a Static Load on an Isotropic Shell ($\mu = 0.3$)	67
5.8	Displacements for a Static Load on an Isotropic Shell ($\mu = 0.3$, $h/R = 0.01$)	68
5.9	Radial Deflection Shape for Various Load Velocities	70
5.10	Radial Deflection Response for Variations in Radial Damping ($\lambda^2 = 2.0$)	72
5.11	Radial Deflection Pattern Immediately Above the First Critical Load Speed	73
5.12	Change in the Radial Deflection Pattern with Increasing Damping ($\lambda^2 = 2.7$)	74
5.13	Deflection Wave Form at $\lambda^2 = 5$ and 10	75
5.14	Effect of Damping for $\lambda^2 = 500$	76
5.15	Effect of Damping for $\lambda^2 = 2000$	77
5.16	Deflection Response for Variations in Circumferential and Axial Prestress	79
5.17	Maximum Radial Deflection in the Vicinity of the First Critical Load Speed	80
5.18	Effect of the Axial Prestress on the First Critical Load Speed	81
5.19	Variation of Pressure Pulse Length, d, at $\lambda^2 = 30$	83
5.20	Response from a Smooth Sine Wave Type Pressure Pulse Using Superposition	89
5.21	Response from a Sharp Pressure Front Using Superposition	90
5.22	Radial Deflection Response for Variations in the Circumferential Modulus	91

Figure		Page
6.1	Bending Stress in an Isotropic Shell Under a Static Load ($\mu = 0.3$, d = 1)	96
6.2	Surface Stresses in an Isotropic Shell Under a Static Load ($\mu = 0.3$, h/R = 0.1)	97

KEY TO SYMBOLS

x, θ, z	coordinate axes
$\overline{K}_\alpha$ $(\alpha = x, \theta, z)$	unit vectors in coordinate directions
R	radius of cylinder (to the middle surface)
h	thickness of cylinder
u, v, w	displacement in directions of coordinate axes
ψ, η	rotations
t	time
N_α, $N_{\alpha\beta}$ $(\alpha, \beta = x, \theta, z)$	stress resultants
M_α, $M_{\alpha\beta}$ $(\alpha, \beta = x, \theta, z)$	moment resultants
Q_α $(\alpha = x, \theta)$	shear force
T	axial prestress stress resultant
N	circumferential prestress stress resultant
I	moment of inertia
h_o	defined in Equation (2-7)
p_i	initial lateral pressure
ρ_o	mass density
ϵ_α $(\alpha = x, \theta)$	strain in α direction
$\gamma_{\alpha\beta}$ $(\alpha, \beta = x, \theta, z)$	shear strain
σ_α $(\alpha = x, \theta)$	stress in α direction
$\tau_{\alpha\beta}$ $(\alpha, \beta = x, \theta, z)$	shear stress
E_{x_o}	modulus in x direction
E_{θ_o}	modulus in θ direction
E_{ν_o}	modulus in normal direction

$G_{\alpha\beta_o}$ (α, β = x, θ, z)	shear moduli
D_α (α = x, θ, ν)	defined in Equation (2-12)
$D_{x\theta}$	defined in Equation (2-12)
E_α (α = x, θ, ν)	defined in Equation (2-12)
G_α (α = x, θ, ν)	defined in Equation (2-12)
$G_{x\theta}$	defined in Equation (2-12)
I_2	defined in Equation (2-12)
K_α (α = x, θ)	correction factors
q'(x, θ, t)	time varying lateral pressure load
ξ	damping coefficient
C_{ij}	coefficients of a matrix
H(y)	Heaviside step function
q	magnitude of lateral pressure load
V	constant velocity
t_o	constant
α	defined in Equation (2-29)
U, W	dimensionless displacements in axial and normal directions
ϕ	dimensionless axial distance
F	dimensionless axial stress resultant
P	dimensionless circumferential stress resultant
E_1	dimensionless normal modulus
G	dimensionless shear modulus
E_o	dimensionless tangential modulus
r	dimensionless inertia term
λ	dimensionless load velocity
I_o	dimensionless rotatory inertia term
ϵ	dimensionless damping term

r_o	thickness ratio depending upon pressure direction
D_1	dimensionless constant
$\bar{f}(s)$	transform of $f(\phi)$, $\mathbf{F}[f(\phi)] = \bar{f}(s)$
s	complex variable in transform space
c, c_i (i = integer)	constants
C_i	constants
$\overline{D}(s)$	characteristic equation
$\overline{\Delta}$	discriminant
e_i (i = integer)	coefficients
f_i (i = integer)	coefficients
λ_i (i = 1, . . . , 8)	load speeds giving repeated roots in undamped characteristic equation
λ_i'	approximate load speed roots
a	constant, real part of complex root
b	imaginary part of complex root
$s_{i, j}$	nomenclature used to trace root loci
λ_{iCR}	the i^{th} critical load speed
V_{CR}	dimensional critical load speed
E	Young's modulus
μ	Poisson ratio
q_o	dimensionless pressure load magnitude
c_i' (i = 5, . . . , 9)	coefficients
d	dimensionless load length
F_k	functions defined in analysis
a_k, b_k	real and imaginary part of complex root
$\overline{R}$	large radius defined in analysis
Res(a)	residue of a function at point a
α_k, β_k	coefficients in partial fraction expansions

ℓ_1, ℓ_2, ℓ_3	lengths defined in static problem analysis
K_1, K_2, K'_1	coefficients
β	coefficient, defined in Equation (6-24)
$(\sigma_\alpha)_o$ $(\alpha = x, \theta)$	outer surface stress
$(\sigma_\alpha)_i$ $(\alpha = x, \theta)$	inner surface stress
S_k	elements of determinant
Δ	determinant of a matrix of coefficients
n	integer

Abstract of Dissertation Presented to the Graduate Council in Partial Fulfillment of the Requirements for the Degree of Doctor of Philosophy

ORTHOTROPIC CYLINDRICAL SHELLS UNDER DYNAMIC LOADING

By

Elmer Mangrum, Jr.

August 1970

Chairman: Dr. J. J. Burns
Major Department: Engineering Science and Mechanics

An orthotropic right cylindrical shell is analyzed when subjected to a discontinuous, finite length pressure load moving in the axial direction at constant velocity. The analysis utilizes linear, small deflection shell theory which includes the effect of axial and circumferential prestress, transverse shear deformation, and external radial damping.

The problem is solved using Fourier transforms, and the inverse Fourier integrals are evaluated for the radial deflection, axial deflection and rotation by expanding the Characteristic Equation in partial fractions and using complex contour integration. By studying the discriminant of the undamped characteristic equation the load velocities which give repeated roots are determined. The loci of these load velocities separate regions in which the form of the displacement solutions differ. The behavior of these load velocity loci is studied for variations in the three nondimensionalized material moduli, the thickness-to-radius ratio, the axial prestress, and the circumferential prestress.

By tracing the root loci of the undamped characteristic equation and by inspection of the displacement expressions, it is determined that there are five critical load velocities (velocities at which the displacement becomes unbounded) for the specific example of an isotropic shell. An increase of the load velocity above the bar wave speed produces a deflection mode which is predominantly axial.

The deflection response is investigated for numerous combinations of load speed, material properties, length of pressure load, axial and circumferential prestress, and radial damping. The axial prestress has a significant effect on the first critical velocity of the cylinder; initial compression tends to lower the velocity. Circumferential prestress has no pronounced effect on the critical load speeds but does influence the response at higher velocities. Variation of material properties was found to cause a rapid change in deflection response.

Through superposition, the variation of pressure load length can be utilized to approximate the response to any desired pressure load. Examples of this application are demonstrated. A comparison of stresses and deflections against those predicted by the Timoshenko thin shell theory is shown for a static load.

All of the above numerical work was done using dimensionless parameters which can be applied to thin shells in general. The calculations were done utilizing a computer program developed from this research for the calculation of deflections and stresses in the shells. The program is written in Fortran and is operable on the General Electric Company Mark II time sharing service.

CHAPTER I

INTRODUCTION

Statement of the Problem

One of the most commonly used geometries for structural application is the right circular cylindrical shell. This is particularly true in the aerospace field and in undersea exploration vehicles. In many aerospace applications the cylindrical shell serves as the primary load carrying member for the rocket system and performs simultaneously as a portion of the pressurized fuel tank. In undersea applications the quest for greater depth range has brought about many refinements in structural optimization techniques. A result of the many stringent requirements being placed upon structural systems has resulted in two areas of rapid advancement: new material technologies and more sophisticated analysis techniques.

The material technologies for advanced design applications have in many cases moved away from the isotropic materials and are utilizing orthotropic and anisotropic materials to satisfy the demanding requirements for more efficient, lighter weight vehicles. Studies such as that reported in Reference (1)* have shown that there is indeed an incentive for the application of these advanced technologies.

Until recent years the mathematical complexity encountered when approaching the dynamic analysis of shells has been so formidable that few results were available for design applications.

*Denotes entries in the Bibliography.

The new technology demands mentioned previously have brought a response from the analysts in the past five to ten years and some of the more idealized dynamic shell problems have been investigated. The problem of particular interest in this work is that of a thin orthotropic cylindrical shell subjected to an axisymmetric pressure load moving in the axial direction. It is necessary to consider refinements to the theory such as the transverse shear deformation, axial inertia, and rotatory inertia effect so that the higher load velocities may be investigated.

It is known that axial prestress has an influence on results in dynamic analyses. In this work the effect of axial as well as circumferential prestress is investigated. The specific loading considered will be a constant pressure pulse finite in both magnitude and distance which moves along the cylinder at velocity V. The shell theory utilized is linear, assuming small deflections, and by superposition it is possible to investigate the effect of various pressure pulse shapes. External radial damping is also included.

Specific Goals of This Research

The major goal of this research was to obtain a solution for the deflections and stresses associated with the problem outlined above. The secondary goal, although perhaps not secondary in importance to those interested in utilizing the results, was that of developing a computer program for the calculation of deflections and stresses in the cylinder. Finally, the calculation and presentation of the effect of the many parameters included in the analysis conclude the goals to be reached in the study.

Review of Previous Work

A review of the early work on the response of a cylindrical shell to a moving load is given by Jones and Bhuta (2). Until the work by Nachbar (3), who considered the dynamic response of an infinitely long cylindrical shell to a semi-infinite step pressure load, the axial inertia was not considered. Nachbar included the axial inertia effect and also assumed an external damping effect. However, due to the damping included, the first resonance condition was missed. Jones and Bhuta solved the problem with a ring load moving on an infinitely long cylinder but did not include the transverse shear effect.

Other contributions were made by Reismann (4) who included the effect of axial prestress, which was significant as had been found in his work on plate strips (5). Hegemier (6) studied the stability problem for a large class of constant velocity moving loads but limited the velocity range to that lower than the first critical.

All of the work previewed above was done for an isotropic material. More recently Herrmann and Baker (7) solved the problem of a moving ring load on a cylindrical sandwich shell of infinite length. Numerical results were presented for a core material which is assumed to have material damping. Also, the problem of a ring load moving on a viscoelastic cylinder was solved by Tang (8).

Contributions of This Work

The following contributions are believed to be original with this work.

1. Analysis of orthotropic monocoque cylindrical shells including transverse shear deformation, axial and rotatory inertia, radial damping, circumferential and axial prestress under a finite length step load.
2. Presentation of the forms of the solution with no damping for the seven-dimensional space whose coordinates are the thickness-to-radius ratio,

the three material property ratios, axial prestress, circumferential prestress, and the load velocity parameter.

3. Results indicating the effect of a finite length pressure pulse, and the capability to approximate any load shape through superposition.
4. Indication of the effect of prestress on the critical velocities of an orthotropic monocoque shell.
5. Results which show the effects of external damping throughout the load velocity range.

CHAPTER II

GOVERNING EQUATIONS OF MOTION

General Equations

A cylindrical shell of thickness h and mean radius R is referred to the coordinate system shown in Figure 2.1.

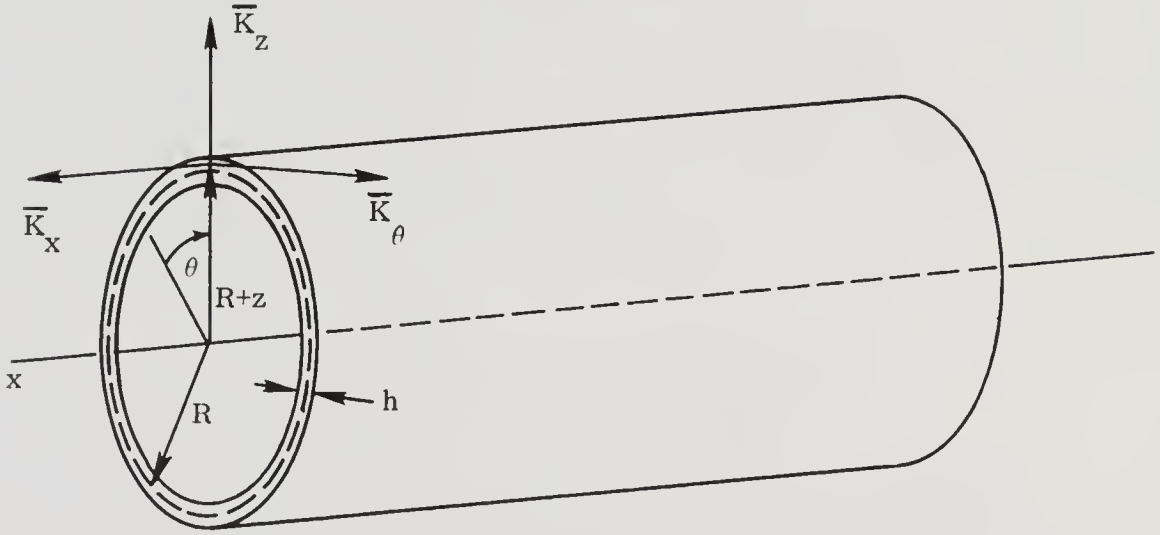

Figure 2.1. Cylindrical Coordinate System

Coordinate x is measured along the shell axis, θ along the circumference and z is perpendicular to the middle surface. The unit vectors tangent to the coordinate lines at a point (x, θ, z) are designated by $\overline{K}_x$, $\overline{K}_\rho$, $\overline{K}_z$. The displacements in these three directions are u_x, u_θ, and u_z respectively. It is

assumed that the displacements can be represented by the linear relationship in terms of z

$$u_x(x, \theta, z, t) = u(x, \theta, t) + z\psi(x, \theta, t)$$

$$u_\theta(x, \theta, z, t) = v(x, \theta, t) + z\eta(x, \theta, t)$$

$$u_z(x, \theta, z, t) = w(x, \theta, t) + z\psi_z(x, \theta, t) \qquad (2\text{-}1)$$

where u, v, w are the displacements on the middle surface (z = 0); t denotes time; ψ and η are the rotations of a line perpendicular to the normal surface in the x-z and θ-z planes respectively. ψ_z is referred to as the thickness stretch.

Equations (2-1) require that all straight lines normal to the middle surface of the shell before deformation remain straight after deformation. This is a good approximation if the shell is thin.

Herrmann and Armenakas (9) derived a linearized theory for the motion of isotropic cylindrical shells subjected to a general state of initial stress by assuming the final state of stress is reached by passing through an intermediate state, the state of initial stress. Subtracting the initial equilibrium equations from the non-linear equations of motion and then linearizing by disregarding all non-linear terms involving the additional stresses, the linearized equations of motion for a shell under initial stress are obtainable.

Following this procedure, Baker and Herrmann (10) derived a linearized set of equations for the motion of orthotropic shells. Assuming an orthotropic cylindrical monocoque shell is under initial lateral pressure p_i, an axial tension T, and is subjected to a time dependent radial load, the five equations of motion have the form:

$$\frac{\partial N_x}{\partial x} + \frac{1}{R}\frac{\partial N_{\theta x}}{\partial \theta} + T\frac{\partial^2 u}{\partial x^2} + \frac{N}{R^2}\frac{\partial^2 u}{\partial \theta^2} - \frac{N}{R}\frac{\partial w}{\partial x} = h\rho_o \ddot{u} + \frac{I}{R}\ddot{\psi} \qquad (2\text{-}2)$$

$$\frac{1}{R}\frac{\partial N_{\theta}}{\partial \theta} + \frac{\partial N_{x\theta}}{\partial x} + \frac{Q_{\theta}}{R} + T\frac{\partial^2 v}{\partial x^2} + \frac{N}{R^2}\left(\frac{\partial w}{\partial \theta} + \frac{\partial^2 v}{\partial \theta^2}\right) = h\rho_o \ddot{v}$$

$$+ \frac{I}{R}\ddot{\eta} - \frac{N}{R^2}\left[\frac{h_o}{R}\frac{\partial w}{\partial \theta} + h_o \eta\right] \tag{2-3}$$

$$- \frac{N_{\theta}}{R} + \frac{\partial Q_x}{\partial x} + \frac{1}{R}\frac{\partial Q_{\theta}}{\partial \theta} + T\frac{\partial^2 w}{\partial x^2} - \frac{N}{R^2}\left(w + \frac{\partial v}{\partial \theta} - \frac{\partial^2 w}{\partial \theta^2} + \frac{\partial v}{\partial \theta}\right)$$

$$+ \frac{N}{R}\left[\frac{1}{R}\left(1 - \frac{h_o}{R}\right)\left(w + \frac{\partial v}{\partial \theta}\right) + \left(\frac{h_o}{R} + \frac{h_o^2}{R^2}\right)\frac{\partial \eta}{\partial \theta} + \frac{\partial u}{\partial x} + h_o\frac{\partial \psi}{\partial x}\right]$$

$$+ q'(x, \theta, t) = \xi \dot{w} + \rho_o h \ddot{w} \tag{2-4}$$

$$\frac{\partial M_x}{\partial x} + \frac{1}{R}\frac{\partial M_{\theta x}}{\partial x} - Q_x - N\frac{h_o}{R}\left(\psi + \frac{\partial w}{\partial x}\right) = I\ddot{\psi} + \frac{I}{R}\ddot{u} \tag{2-5}$$

$$\frac{1}{R}\frac{\partial M_{\theta}}{\partial \theta} + \frac{\partial M_{x\theta}}{\partial x} - Q_{\theta}$$

$$+ \frac{Nh_o}{R^2}\left[v - \left(1 + \frac{h_o}{R}\right)\frac{\partial w}{\partial \theta} + (h_o - R)\eta\right] = I\ddot{\eta} + \frac{I}{R}\ddot{v} \tag{2-6}$$

where

$$h_o = \begin{cases} \frac{h}{2} \\ \\ -\frac{h}{2} \end{cases}, \qquad N = \begin{cases} -p_i R\left[1 + \frac{h}{2R}\right] & \text{for external pressure} \\ \\ +p_i R\left[1 - \frac{h}{2R}\right] & \text{for internal pressure} \end{cases} \tag{2-7}$$

$$I = \frac{h^3 \rho_o}{12} \tag{2-8}$$

These equations include the effect of external radial damping, axial and rotatory inertia, and transverse shear deformation.

The elongations, shears, and rotations have been assumed small in comparison with unity. The strain-displacement relations are therefore taken in the form of Hooke's law.

$$\epsilon_x = \frac{\partial u}{\partial x}$$

$$\epsilon_\theta = \frac{1}{R + z}\left(\frac{\partial v}{\partial \theta} + w\right)$$

$$\gamma_{x\theta} = \frac{1}{R + z}\frac{\partial u}{\partial \theta} + \frac{\partial v}{\partial x}$$

$$\gamma_{xz} = \frac{\partial u}{\partial z} + \frac{\partial w}{\partial x}$$

$$\gamma_{\theta z} = \frac{\partial v}{\partial z} + \frac{1}{R + z}\left(\frac{\partial w}{\partial \theta} - v\right) \qquad (2\text{-}9)$$

The stress strain relationships are assumed in the following form

$$\sigma_x = E_{x_o}\epsilon_x + E_{\nu_o}\epsilon_\theta$$

$$\sigma_\theta = E_{\nu_o}\epsilon_x + E_{\theta_o}\epsilon_\theta$$

$$\tau_{x\theta} = G_{x\theta_o}\gamma_{x\theta}$$

$$\tau_{\theta z} = G_{\theta z_o}\gamma_{\theta z}$$

$$\tau_{xz} = G_{xz_o}\gamma_{xz} \qquad (2\text{-}10)$$

Integrating the stresses through the shell thickness the z variable is eliminated and the stress and moment resultants are obtained.

$$N_x = E_x \frac{\partial u}{\partial x} + \frac{D_x}{R} \frac{\partial \psi}{\partial x} + \frac{E_\nu}{R} \left(w + \frac{\partial v}{\partial \theta} \right)$$

$$N_\theta = \left(\frac{E_\theta}{R} + \frac{D_\theta}{R^3} \right) \left(w + \frac{\partial v}{\partial \theta} \right) - \frac{D_\theta}{R^2} \frac{\partial \eta}{\partial \theta} + E_\nu \frac{\partial u}{\partial x}$$

$$N_{x\theta} = G_{x\theta} \frac{\partial v}{\partial x} + \frac{D_{x\theta}}{R} \frac{\partial \eta}{\partial x} + \frac{G_{x\theta}}{R} \frac{\partial u}{\partial \theta}$$

$$N_{\theta x} = G_{x\theta} \frac{\partial v}{\partial x} - \frac{D_{x\theta}}{R^2} \frac{\partial \psi}{\partial \theta} + \left(\frac{G_{x\theta}}{R} + \frac{D_{x\theta}}{R^3} \right) \frac{\partial u}{\partial \theta}$$

$$M_x = \frac{D_x}{R} \frac{\partial u}{\partial x} + D_x \frac{\partial \psi}{\partial x} + \frac{D_\nu}{R} \frac{\partial \eta}{\partial \theta}$$

$$M_\theta = \frac{D_\theta}{R} \left(\frac{\partial \eta}{\partial \theta} - \frac{w}{R} - \frac{1}{R} \frac{\partial v}{\partial \theta} \right) + D_\nu \frac{\partial \psi}{\partial x}$$

$$M_{x\theta} = \frac{D_{x\theta}}{R} \left(\frac{\partial \psi}{\partial \theta} + \frac{\partial v}{\partial x} \right) + D_{x\theta} \frac{\partial \eta}{\partial x}$$

$$M_{\theta x} = \frac{D_{x\theta}}{R} \left(\frac{\partial \psi}{\partial \theta} - \frac{1}{R} \frac{\partial u}{\partial \theta} \right) + D_{x\theta} \frac{\partial \eta}{\partial x}$$

$$Q_x = G_x \left(\psi + \frac{\partial w}{\partial x} \right)$$

$$Q_\theta = \frac{G_\theta}{R} \left(R\eta + \frac{\partial w}{\partial \theta} - v \right) \qquad (2\text{-}11)$$

where

$$D_x = E_{x_o} I_2, \quad D_\theta = E_{\theta_o} I_2, \quad D_\nu = E_{\nu_o} I_2$$

$$D_{x\theta} = G_{x\theta_o} I_2, \quad E_x = E_{x_o} h, \quad E_\theta = E_{\theta_o} h$$

$$E_\nu = E_{\nu_o} h, \quad G_{x\theta} = G_{x\theta_o} h, \quad G_x = K_x^2 G_{xz_o} h$$

$$G_\theta = K_\theta^2 G_{\theta z_o} h \left[1 + \frac{h^2}{12R^2}\right], \quad I_2 = \frac{h^3}{12} \tag{2-12}$$

The coefficients K_x and K_θ are constants for adjustment and can be taken as $\pi/\sqrt{12}$ as discussed by Mirsky and Herrmann (11).

Substituting Equations (2-11) into the Equations of Motion, (2-2) through (2-6), yields

$$E_x \frac{\partial^2 u}{\partial x^2} + \frac{D_x}{R} \frac{\partial^2 \psi}{\partial x^2} + \frac{E_\nu}{R}\left(\frac{\partial w}{\partial x} + \frac{\partial^2 v}{\partial x \partial \theta}\right)$$

$$+ \frac{1}{R}\left[G_{x\theta} \frac{\partial^2 v}{\partial x \partial \theta} - \frac{D_{x\theta}}{R^2} \frac{\partial^2 \psi}{\partial \theta^2} + \left(\frac{G_{x\theta}}{R} + \frac{D_{x\theta}}{R^3}\right) \frac{\partial^2 u}{\partial \theta^2}\right]$$

$$+ T \frac{\partial^2 u}{\partial x^2} + \frac{N}{R^2} \frac{\partial^2 u}{\partial \theta^2} - \frac{N}{R} \frac{\partial w}{\partial x} = h \rho_o \ddot{u} + \frac{I}{R} \ddot{\psi} \tag{2-13}$$

$$\frac{1}{R}\left(\frac{E_\theta}{R} + \frac{D_\theta}{R^3}\right)\left(\frac{\partial w}{\partial \theta} + \frac{\partial^2 v}{\partial \theta^2}\right) - \frac{D_\theta}{R^3} \frac{\partial^2 \eta}{\partial \theta^2} + \frac{E_\nu}{R} \frac{\partial^2 u}{\partial x \partial \theta} + G_{x\theta} \frac{\partial^2 v}{\partial x^2}$$

$$+ \frac{D_{x\theta}}{R} \frac{\partial^2 \eta}{\partial x^2} + \frac{G_{x\theta}}{R} \frac{\partial^2 u}{\partial x \partial \theta} + \frac{G_\theta}{R}\left(\eta + \frac{1}{R} \frac{\partial w}{\partial \theta} - \frac{v}{R}\right) + T \frac{\partial^2 v}{\partial x^2}$$

$$+ \frac{N}{R^2}\left[\frac{\partial w}{\partial \theta} + \frac{\partial^2 v}{\partial \theta^2} + h_o\left(\frac{1}{R} \frac{\partial w}{\partial \theta} + \eta\right)\right] = \rho_o h \ddot{v} + \frac{I}{R} \ddot{\eta} . \tag{2-14}$$

$$-\left(\frac{E_\theta}{R^2}+\frac{D_\theta}{R^4}\right)\left(w+\frac{\partial v}{\partial\theta}\right)+\frac{D_\theta}{R^3}\frac{\partial\eta}{\partial\theta}-\frac{E_\nu}{R}\frac{\partial u}{\partial x}+G_x\left(\frac{\partial\psi}{\partial x}+\frac{\partial^2 w}{\partial x^2}\right)$$

$$+\frac{G_\theta}{R}\left[\frac{\partial\eta}{\partial\theta}+\frac{1}{R}\left(\frac{\partial^2 w}{\partial\theta^2}-\frac{\partial v}{\partial\theta}\right)\right]+T\frac{\partial^2 w}{\partial x^2}-\frac{N}{R^2}\left(w+2\frac{\partial v}{\partial\theta}-\frac{\partial^2 w}{\partial\theta^2}\right)$$

$$+\frac{N}{R^2}\left[\left(1-\frac{h_o}{R}\right)\left(w+\frac{\partial v}{\partial\theta}\right)+h_o\left(1+\frac{h_o}{R}\right)\frac{\partial\eta}{\partial\theta}+R\frac{\partial u}{\partial x}+Rh_o\frac{\partial\psi}{\partial x}\right]$$

$$+q'(x,\theta,t)=\xi\dot{w}+\rho_o h\ddot{w} \qquad (2\text{-}15)$$

$$\frac{D_x}{R}\frac{\partial^2 u}{\partial x^2}+D_x\frac{\partial^2\psi}{\partial x^2}+\frac{D_\nu}{R}\frac{\partial^2\eta}{\partial x\partial\theta}+\frac{D_{x\theta}}{R^2}\left(\frac{\partial^2\psi}{\partial\theta^2}-\frac{1}{R}\frac{\partial^2 u}{\partial\theta^2}\right)$$

$$+\frac{D_{x\theta}}{R}\frac{\partial^2\eta}{\partial x\partial\theta}-G_x\left(\psi+\frac{\partial w}{\partial x}\right)-\frac{Nh_o}{R}\left(\psi+\frac{\partial w}{\partial x}\right)=I\ddot{\psi}+\frac{I}{R}\ddot{u} \qquad (2\text{-}16)$$

$$\frac{D_\theta}{R^2}\left(\frac{\partial^2\eta}{\partial\theta^2}-\frac{1}{R}\frac{\partial w}{\partial\theta}-\frac{1}{R}\frac{\partial^2 v}{\partial\theta^2}\right)+\frac{D_\nu}{R}\frac{\partial^2\psi}{\partial x\partial\theta}+\frac{D_{x\theta}}{R}\left(\frac{\partial^2\psi}{\partial x\partial\theta}+\frac{\partial^2 v}{\partial x^2}\right)$$

$$+D_{x\theta}\frac{\partial^2\eta}{\partial x^2}-\frac{G_\theta}{R}\left(R\eta+\frac{\partial w}{\partial\theta}-v\right)$$

$$+\frac{Nh_o}{R^2}\left[v-\left(1+\frac{h_o}{R}\right)\frac{\partial w}{\partial\theta}+(h_o-R)\eta\right]=I\ddot{\eta}+\frac{I}{R}\ddot{v} \qquad (2\text{-}17)$$

Collecting coefficients on deflections gives

$$\left[E_x\frac{\partial^2}{\partial x^2}+\frac{1}{R^2}\left(G_{x\theta}+\frac{D_{x\theta}}{R^2}\right)\frac{\partial^2}{\partial\theta^2}+T\frac{\partial^2}{\partial x^2}+\frac{N}{R^2}\frac{\partial^2}{\partial\theta^2}-\rho_o h\frac{\partial^2}{\partial t^2}\right]u$$

$$+\left[\frac{1}{R}(E_\nu+G_{x\theta})\frac{\partial^2}{\partial x\partial\theta}\right]v+\left[\frac{1}{R}(E_\nu-N)\frac{\partial}{\partial x}\right]w$$

$$+\left[\frac{D_x}{R}\frac{\partial^2}{\partial x^2}-\frac{D_{x\theta}}{R^3}\frac{\partial^2}{\partial\theta^2}-\frac{I}{R}\frac{\partial^2}{\partial t^2}\right]\psi=0 \qquad (2\text{-}18)$$

$$\left[\frac{1}{R}\left(E_\nu + G_{x\theta}\right)\frac{\partial^2}{\partial x \partial \theta}\right] u + \left[\frac{1}{R^2}\left(E_\theta + \frac{D_\theta}{R^2} + N\right)\frac{\partial^2}{\partial \theta^2} + \left(G_{x\theta} + T\right)\frac{\partial^2}{\partial x^2} - \frac{G_\theta}{R^2} - \rho_o h \frac{\partial^2}{\partial t^2}\right] v$$

$$+ \left\{\left[\frac{1}{R^2}\left(E_\theta + \frac{D_\theta}{R^2}\right) + \frac{G_\theta}{R^2} + \frac{N}{R^2}\left(1 + \frac{h_o}{R}\right)\right]\frac{\partial}{\partial \theta}\right\} w$$

$$\left[-\frac{D_\theta}{R^3}\frac{\partial^2}{\partial \theta^2} + \frac{D_{x\theta}}{R}\frac{\partial^2}{\partial x^2} + \frac{G_\theta}{R} + \frac{h_o N}{R^2} - \frac{I}{R}\frac{\partial^2}{\partial t^2}\right]\eta = 0 \qquad (2\text{-}19)$$

$$\left[\frac{1}{R}\left(E_\nu - N\right)\frac{\partial}{\partial x}\right] u + \left\{\left[\frac{1}{R^2}\left(E_\theta + \frac{D_\theta}{R^2}\right) + \frac{G_\theta}{R^2} + \left(1 + \frac{h_o}{R}\right)\frac{N}{R^2}\right]\frac{\partial}{\partial \theta}\right\} v$$

$$+ \left[\frac{1}{R^2}\left(E_\theta + \frac{D_\theta}{R^2} + N\frac{h_o}{R}\right) - \left(G_x + T\right)\frac{\partial^2}{\partial x^2} - \frac{1}{R^2}\left(G_\theta + N\right)\frac{\partial^2}{\partial \theta^2} + \xi\frac{\partial}{\partial t} + \rho_o h \frac{\partial^2}{\partial t^2}\right] w + \left[-\left(G_x + \frac{Nh_o}{R}\right)\frac{\partial}{\partial x}\right]\psi$$

$$+ \left\{-\frac{1}{R^2}\left[\frac{D_\theta}{R} + RG_\theta + Nh_o\left(1 + \frac{h_o}{R}\right)\right]\frac{\partial}{\partial \theta}\right\}\eta = q'(x, \theta, t) \qquad (2\text{-}20)$$

$$\left[\frac{D_x}{R}\frac{\partial^2}{\partial x^2} - \frac{D_{x\theta}}{R^3}\frac{\partial^2}{\partial \theta^2} - \frac{I}{R}\frac{\partial^2}{\partial t^2}\right] u + \left[-\left(G_x + \frac{Nh_o}{R}\right)\frac{\partial}{\partial x}\right] w$$

$$+ \left[-\left(\frac{Nh_o}{R} + G_x\right) + D_x\frac{\partial^2}{\partial x^2} + \frac{D_{x\theta}}{R^2}\frac{\partial^2}{\partial \theta^2} - I\frac{\partial^2}{\partial t^2}\right]\psi$$

$$+ \left[\frac{1}{R}\left(D_\nu + D_{x\theta}\right)\frac{\partial^2}{\partial x \partial \theta}\right]\eta = 0 \qquad (2\text{-}21)$$

$$\left[\frac{D_{x\theta}}{R} \frac{\partial^2}{\partial x^2} - \frac{D_\theta}{R^3} \frac{\partial^2}{\partial \theta^2} + \frac{1}{R}\left(G_\theta + \frac{Nh_o}{R} \right) - \frac{I}{R} \frac{\partial^2}{\partial t^2} \right] v$$

$$+ \left\{ - \frac{1}{R}\left[\frac{D_\theta}{R^2} + G_\theta + \frac{Nh_o}{R}\left(1 + \frac{h_o}{R} \right) \right] \frac{\partial}{\partial \theta} \right\} w$$

$$+ \left[\frac{1}{R}(D_\nu + D_{x\theta}) \frac{\partial^2}{\partial x \partial \theta} \right] \psi$$

$$+ \left[D_{x\theta} \frac{\partial^2}{\partial x^2} + \frac{D_\theta}{R^2} \frac{\partial^2}{\partial \theta^2} - G_\theta - \frac{Nh_o}{R}\left(- \frac{h_o}{R} + 1 \right) - I \frac{\partial^2}{\partial t^2} \right] \eta = 0 \quad (2\text{-}22)$$

Equations (2-16), (2-17), and (2-18) express the principle of linear momentum in the x, θ, and z directions, respectively, while Equations (2-21) and (2-22) express the principle of angular momentum about an axis through the middle surface in the direction of $\overline{K}_\theta$ and $\overline{K}_x$, respectively.

These equations can be written in the form

$$C_{ij}\, u_j = q_i, \qquad C_{ij} = C_{ji} \quad (2\text{-}23)$$

In matrix notation the set has the form

$$\begin{bmatrix} C_{11} & C_{12} & C_{13} & C_{14} & 0 \\ C_{12} & C_{22} & C_{23} & 0 & C_{25} \\ C_{13} & C_{23} & C_{33} & C_{34} & C_{35} \\ C_{14} & 0 & C_{34} & C_{44} & C_{45} \\ 0 & C_{25} & C_{35} & C_{45} & C_{55} \end{bmatrix} \begin{bmatrix} u \\ v \\ w \\ \psi \\ \eta \end{bmatrix} = \begin{bmatrix} 0 \\ 0 \\ q'(x, \theta, t) \\ 0 \\ 0 \end{bmatrix} \quad (2\text{-}24)$$

where the coefficients are defined as follows:

$$C_{11} = (E_x + T)\frac{\partial^2}{\partial x^2} + \frac{1}{R^2}\left(G_{x\theta} + \frac{D_{x\theta}}{R^2} + N\right)\frac{\partial^2}{\partial \theta^2} - \rho_o h \frac{\partial^2}{\partial t^2}$$

$$C_{12} = \frac{1}{R}(E_\nu + G_{x\theta})\frac{\partial^2}{\partial x \partial \theta}$$

$$C_{13} = \frac{1}{R}(E_\nu - N)\frac{\partial}{\partial x}$$

$$C_{14} = \frac{D_x}{R}\frac{\partial^2}{\partial x^2} - \frac{D_{x\theta}}{R^3}\frac{\partial^2}{\partial \theta^2} - \frac{I}{R}\frac{\partial^2}{\partial t^2}$$

$$C_{22} = (G_{x\theta} + T)\frac{\partial^2}{\partial x^2} + \frac{1}{R^2}\left(E_\theta + \frac{D_\theta}{R^2} + N\right)\frac{\partial^2}{\partial \theta^2} - \frac{G_\theta}{R^2} - \rho_o h \frac{\partial^2}{\partial t^2}$$

$$C_{23} = \frac{1}{R^2}\left[E_\theta + \frac{D_\theta}{R^2} + G_\theta + N\left(1 + \frac{h_o}{R}\right)\right]\frac{\partial}{\partial \theta}$$

$$C_{25} = \frac{D_{x\theta}}{R}\frac{\partial^2}{\partial x^2} - \frac{D_\theta}{R^3}\frac{\partial^2}{\partial \theta^2} + \frac{G_\theta}{R} + \frac{Nh_o}{R^2} - \frac{I}{R}\frac{\partial^2}{\partial t^2}$$

$$C_{33} = -(G_x + T)\frac{\partial^2}{\partial x^2} - \frac{1}{R^2}(G_\theta + N)\frac{\partial^2}{\partial \theta^2} + \frac{1}{R^2}\left(E_\theta + \frac{D_\theta}{R^2} + N\frac{h_o}{R}\right) + \xi\frac{\partial}{\partial t} + \rho_o h \frac{\partial^2}{\partial t^2}$$

$$C_{34} = -\left(G_x + N\frac{h_o}{R}\right)\frac{\partial}{\partial x}$$

$$C_{35} = -\frac{1}{R^2}\left[\frac{D_\theta}{R} + RG_\theta + Nh_o\left(1 + \frac{h_o}{R}\right)\right]\frac{\partial}{\partial \theta}$$

$$C_{44} = D_x\frac{\partial^2}{\partial x^2} + \frac{D_{x\theta}}{R^2}\frac{\partial^2}{\partial \theta^2} - G_x - N\frac{h_o}{R} - I\frac{\partial^2}{\partial t^2}$$

$$C_{45} = \frac{1}{R}(D_\nu + D_{x\theta})\frac{\partial^2}{\partial x \partial \theta}$$

$$C_{55} = D_{x\theta}\frac{\partial^2}{\partial x^2} + \frac{D_\theta}{R^2}\frac{\partial^2}{\partial \theta^2} - G_\theta - N\frac{h_o}{R}\left(1 - \frac{h_o}{R}\right) - I\frac{\partial^2}{\partial t^2} \qquad (2\text{-}25)$$

Axisymmetric Loading

Assuming the loading on the cylinder is axisymmetric, the set of Equations (2-24) reduces to the following.

$$(E_x + T)\frac{\partial^2 u}{\partial x^2} - \rho_o h \frac{\partial^2 u}{\partial t^2} + \frac{1}{R}(E_\nu - N)\frac{\partial w}{\partial x} + \frac{D_x}{R}\frac{\partial^2 \psi}{\partial x^2} - \frac{I}{R}\frac{\partial^2 \psi}{\partial t^2} = 0$$

$$\frac{1}{R}(E_\nu - N)\frac{\partial u}{\partial x} - (G_x + T)\frac{\partial^2 w}{\partial x^2} + \xi \frac{\partial w}{\partial t} + \rho_o h \frac{\partial^2 w}{\partial t^2}$$

$$+ \frac{1}{R^2}\left(E_\theta + \frac{D_\theta}{R^2} + N\frac{h_o}{R}\right) w - \left(G_x + N\frac{h_o}{R}\right)\frac{\partial \psi}{\partial x} = q'(x, t)$$

$$\frac{D_x}{R}\frac{\partial^2 u}{\partial x^2} - \frac{I}{R}\frac{\partial^2 u}{\partial t^2} - \left(G_x + N\frac{h_o}{R}\right)\frac{\partial w}{\partial x} + D_x \frac{\partial^2 \psi}{\partial x^2} - I\frac{\partial^2 \psi}{\partial t^2}$$

$$- \left(G_x + N\frac{h_o}{R}\right)\psi = 0 \qquad (2\text{-}26)$$

Pressure Loading Form

A step input in external pressure which is finite in both magnitude and time and which travels down the length of the cylinder at constant velocity V can be represented in the form

$$q'(x, t) = -q\{H[Vt - x] - H[V(t - t_o) - x]\} \qquad (2\text{-}27)$$

where H(y) is the Heaviside step function, defined as

$$H(y) = \begin{cases} 0, & y < 0 \\ 1, & y > 0 \end{cases} \qquad (2\text{-}28)$$

This pressure loading is represented schematically in Figure 2.2.

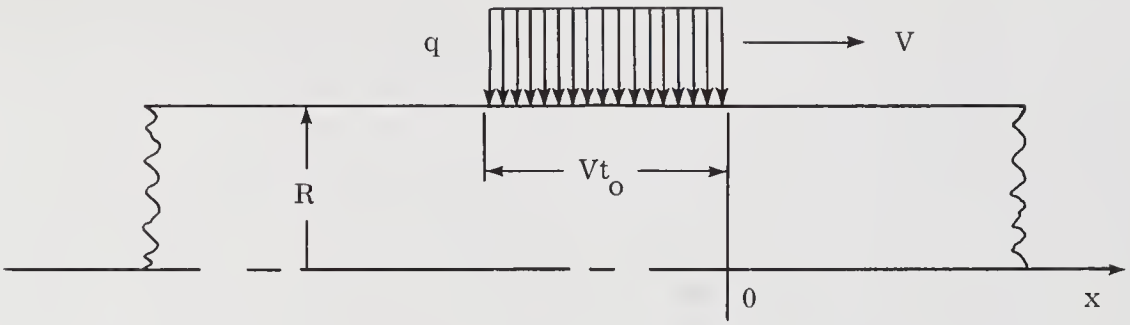

Figure 2.2. Pressure Loading

Nondimensional Equations

The steady state solution will be investigated. Making the transformation

$$\alpha = x - Vt \tag{2-29}$$

the partial derivatives may be written in terms of α.

$$\frac{\partial}{\partial x} = \frac{\partial}{\partial \alpha}\frac{\partial \alpha}{\partial x} = \frac{\partial}{\partial \alpha}$$

$$\frac{\partial}{\partial t} = \frac{\partial}{\partial \alpha}\frac{\partial \alpha}{\partial t} = -V\frac{\partial}{\partial \alpha}$$

$$\frac{\partial^2}{\partial t^2} = V^2\frac{\partial^2}{\partial \alpha^2} \tag{2-30}$$

Using these relationships in Equations (2-26), letting

$$U = \frac{u}{R}$$

$$W = \frac{w}{R}$$

$$\phi = \frac{\alpha}{R} \tag{2-31}$$

multiplying by R/E_x in the first two equations and $1/E_x$ in the third gives

$$\left(1 + \frac{T}{E_x}\right)\frac{d^2U}{d\phi^2} - \frac{\rho_o h V^2}{E_x}\frac{d^2U}{d\phi^2} + \left(\frac{E_\nu}{E_x} - \frac{N}{E_x}\right)\frac{dW}{d\phi} + \frac{D_x}{R^2E_x}\frac{d^2\psi}{d\phi^2}$$

$$- \frac{IV^2}{E_x R^2}\frac{d^2\psi}{d\phi^2} = 0$$

$$\left(\frac{E_\nu}{E_x} - \frac{N}{E_x}\right)\frac{dU}{d\phi} - \left(\frac{G_x}{E_x} + \frac{T}{E_x}\right)\frac{d^2W}{d\phi^2} - \frac{\xi VR}{E_x}\frac{dW}{d\phi} + \frac{\rho_o h V^2}{E_x}\frac{d^2W}{d\phi^2}$$

$$+ \left(\frac{E_\theta}{E_x} + \frac{D_\theta}{E_x R^2} + \frac{N}{E_x}\frac{h_o}{R}\right)W$$

$$- \left(\frac{G_x}{E_x} + \frac{N}{E_x}\frac{h_o}{R}\right)\frac{d\psi}{d\phi} = -\frac{Rq}{E_x}[H(-R\phi) - H(-R\phi - Vt_o)]$$

$$\frac{D_x}{R^2E_x}\frac{d^2U}{d\phi^2} - \frac{V^2I}{R^2E_x}\frac{d^2U}{d\phi^2} - \left(\frac{G_x}{E_x} + \frac{N}{E_x}\frac{h_o}{R}\right)\frac{dW}{d\phi} + \frac{D_x}{R^2E_x}\frac{d^2\psi}{d\phi^2}$$

$$- \frac{IV^2}{E_x R^2}\frac{d^2\psi}{d\phi^2} - \left(\frac{G_x}{E_x} + \frac{N}{E_x}\frac{h_o}{R}\right)\psi = 0 \qquad (2\text{-}32)$$

Now the following dimensionless ratios are defined.

$$\frac{T}{E_x} = F$$

$$\frac{N}{E_x} = P$$

$$\frac{Rq}{E_x} = q_o$$

$$\frac{E_\nu}{E_x} = E_1, \quad \frac{G_x}{E_x} = G, \quad E_o = \frac{E_\theta}{E_x}\left(1 + \frac{D_\theta}{E_\theta R^2}\right), \quad \frac{D_x}{R^2 E_x} = D_1$$

$$\frac{h_o}{R} = r_o$$

$$\lambda^2 = \frac{V^2 \rho_o R}{E_x}$$

$$r = \frac{\rho_o h}{\rho_o R} = \frac{h}{R}$$

$$I_o = \frac{I}{\rho_o R^3} = \frac{h^3 \rho_o}{12R^3 \rho_o} = \frac{h^3}{12R^3}$$

$$\epsilon^2 = \frac{\xi^2 R}{E_x \rho_o} \qquad (2\text{-}33)$$

The dimensionless velocity parameter is denoted by λ and r refers to the inertia. A distinction will be made in the axial and radial inertia terms for later investigation, r_1 denoting axial and r denoting the radial inertia terms.

Using the dimensionless ratios given in Equations (2-33), the equations of motion now take the form

$$(1 + F - r_1 \lambda^2) \frac{d^2U}{d\phi^2} + (E_1 - P) \frac{dW}{d\phi} + (D_1 - I_o \lambda^2) \frac{d^2\psi}{d\phi^2} = 0 \qquad (2\text{-}34a)$$

$$(E_1 - P) \frac{dU}{d\phi} - (G + F - r\lambda^2) \frac{d^2W}{d\phi^2} - \epsilon\lambda \frac{dW}{d\phi} + (E_o + P r_o)W$$

$$- (G + P r_o) \frac{d\psi}{d\phi} = - q_o[H(-R\phi) - H(-R\phi - Vt_o)] \qquad (2\text{-}34b)$$

$$(D_1 - I_o \lambda^2) \frac{d^2U}{d\phi^2} - (G + P r_o) \frac{dW}{d\phi} + (D_1 - I_o \lambda^2) \frac{d^2\psi}{d\phi^2}$$

$$- (G + P r_o)\psi = 0 \qquad (2\text{-}34c)$$

CHAPTER III

TRANSFORMATION OF EQUATIONS

Equations (2-34) will be transformed using the Fourier transform

$$\mathbf{F}[f(\phi)] = \bar{f}(s) = \int_{-\infty}^{\infty} f(\phi)\, e^{-is\phi}\, d\phi \tag{3-1}$$

The inverse transform is

$$\mathbf{F}^{-1}[\bar{f}(s)] = f(\phi) = \frac{1}{2\pi} \int_{-\infty}^{\infty} \bar{f}(s)\, e^{is\phi}\, ds \tag{3-2}$$

where $i = \sqrt{-1}$.

Assuming all the derivatives of $f(\phi)$ through order (r-1) vanish as $\phi \to \pm\infty$ the transforms of derivatives of $f(\phi)$ are given by

$$\bar{f}^{k}(s) = (is)^{k}\, \bar{f}(s) \tag{3-3}$$

so

$$\mathbf{F}\left[\frac{df(\phi)}{d\phi}\right] = is\, \bar{f}(s) \tag{3-4}$$

$$\mathbf{F}\left[\frac{d^2 f(\phi)}{d\phi^2}\right] = -s^2\, \bar{f}(s) \tag{3-5}$$

Applying this to Equations (2-34) gives

$$(1 + F - r_1\lambda^2)\, s^2\, \bar{U}(s) - i(E_1 - P)\, s\, \bar{W}(s) + (D_1 - I_0\lambda^2)\, s^2\, \bar{\psi}(s) = 0$$

$$i(E_1 - P)\, s\, \bar{U}(s) + (G + F - r\lambda^2)\, s^2\, \bar{W}(s) - i\epsilon\lambda\, s\, \bar{W}(s)$$

$$+ (E_0 + P r_0)\, \bar{W}(s) - i(G + P r_0)\, s\, \bar{\psi}(s) = -\frac{q_0}{i s}\left[e^{isd} - 1\right] *$$

$$(D_1 - I_0\lambda^2)\, s^2\, \bar{U}(s) + i(G + P r_0)\, s\, \bar{W}(s) + (D_1 - I_0\lambda^2)\, s^2\, \bar{\psi}(s)$$

$$+ (G + P r_0)\, \bar{\psi}(s) = 0 \qquad (3\text{-}6)$$

Collecting coefficients on like displacements allows this set of equations to be written in the following matrix notation.

$$\begin{bmatrix} [(1+F-r_1\lambda^2)s^2] & [-i(E_1-P)s] & [(D_1-I_0\lambda^2)s^2] \\ [i(E_1-P)s] & [(G+F-r\lambda^2)s^2 - i\epsilon\lambda s + (E_0+Pr_0)] & [-i(G+Pr_0)s] \\ [(D_1-I_0\lambda^2)s^2] & [i(G+Pr_0)s] & [(D_1-I_0\lambda^2)s^2 + (G+Pr_0)] \end{bmatrix} \begin{bmatrix} \bar{U}(s) \\ \bar{W}(s) \\ \bar{\psi}(s) \end{bmatrix} = \begin{bmatrix} 0 \\ -\frac{q_0}{is}\left[e^{isd} - 1\right] \\ 0 \end{bmatrix} \qquad (3\text{-}7)$$

*See Appendix A for the derivation of the transform of the forcing function.

This set of equations can now be solved for $\overline{U}$, $\overline{W}$, and $\overline{\psi}$. This work is carried out in Appendix B and the results are

$$\frac{\overline{U}(s)}{q_o} = \frac{(1 - e^{isd})}{s^2 \overline{D}(s)} [(D_1 - I_o \lambda^2)(G + P r_o + E_1 - P)s^2 + (G + P r_o)(E_1 - P)]$$

$$\frac{\overline{W}(s)}{q_o} = \frac{(1 - e^{isd})}{i s \overline{D}(s)} [(D_1 - I_o \lambda^2)c s^2 + (G + P r_o)(1 + F - r_1 \lambda^2)]$$

$$\frac{\overline{\psi}(s)}{q_o} = - \frac{(1 - e^{isd})}{\overline{D}(s)} [(E_1 - P)(D_1 - I_o \lambda^2) + (G + P r_o)(1 + F - r_1 \lambda^2)] \tag{3-8}$$

where

$$\overline{D}(s) = c_4 s^4 + i c_3 s^3 + c_2 s^2 + i c_1 s + c_o \tag{3-9}$$

and

$$c_o = (G + P r_o)[(1 + F - r_1 \lambda^2)(E_o + P r_o) - (E_1 - P)^2]$$

$$c_1 = - \epsilon \lambda (G + P r_o)(1 + F - r_1 \lambda^2)$$

$$c_2 = (D_1 - I_o \lambda^2)\{(E_o + P r_o)c - (E_1 - P)[(E_1 - P) + 2(G + P r_o)]\}$$
$$+ (G + P r_o)(1 + F - r_1 \lambda^2)(F - P r_o - r \lambda^2)$$

$$c_3 = - \epsilon \lambda (D_1 - I_o \lambda^2)c$$

$$c_4 = (G + F - r \lambda^2)(D_1 - I_o \lambda^2)c$$

$$c = 1 + F - D_1 - r_1 \lambda^2 + I_o \lambda^2 \tag{3-10}$$

The displacements are found by inverting Equations (3-8) using transformation (3-2). In order to evaluate these integrals the roots of the characteristic equation $\overline{D}(s) = 0$ must be determined.

CHAPTER IV

INVESTIGATION OF THE CRITICAL VELOCITIES

It is known that the inverse of the deflections [given by integral (3-2), where $\overline{f}(s)$ represents the deflection expressions (3-8)] does not exist when there are repeated roots of the characteristic equation

$$\overline{D}(s) = 0$$

on the real axis. This can occur when there is no external damping and corresponds to a resonant condition as discussed by Jones and Bhuta (2). There are specific load velocities corresponding to these points and they will be referred to as critical velocities. The condition which must be satisfied in order to have repeated roots is that the discriminant of the undamped characteristic equation

$$c_4 s^4 + c_2 s^2 + c_o = 0 \tag{4-1}$$

must be zero. The discriminant of this equation is determined in Appendix C as

$$\overline{\Delta} = 16 c_o c_4 (c_2^2 - 4c_o c_4)^2 \tag{4-2}$$

Therefore, the three conditions which will make the discriminant zero are

$$c_2^2 - 4c_o c_4 = 0 \tag{4-3}$$

$$c_4 = 0 \tag{4-4}$$

$$c_o = 0 \tag{4-5}$$

Substituting the required coefficients from (3-10) into (4-3) gives*

$$C_8 \lambda^8 + C_6 \lambda^6 + C_4 \lambda^4 + C_2 \lambda^2 + C_o = 0 \tag{4-6}$$

*See Appendix D for the detailed calculations.

where

$$C_8 = e_9^2 - e_{14}$$

$$C_6 = 2e_8 e_9 - e_{13}$$

$$C_4 = e_8^2 + 2e_7 e_9 - e_{12}$$

$$C_2 = 2e_7 e_8 - e_{11}$$

$$C_0 = e_7^2 - e_{10} \qquad (4\text{-}7)$$

The e_i are defined as

$$e_7 = D_1 e_5 + e_3 f_0 f_2$$

$$e_8 = D_1 e_0 e_4 - I_0 e_5 - e_3 f_5$$

$$e_9 = e_3 r r_1 - I_0 e_0 e_4$$

$$e_{10} = 4e_3 e_6 f_3 D_1 f_1$$

$$e_{11} = 4e_3 [e_6 (f_3 f_9 - r D_1 f_1) - e_0 r_1 f_3 D_1 f_1]$$

$$e_{12} = -4e_3 [e_6 (r f_9 + f_3 I_0 e_4) + e_0 r_1 (f_3 f_9 - r D_1 f_1)]$$

$$e_{13} = 4e_3 [e_6 r I_0 e_4 + e_0 r_1 (r f_9 + f_3 I_0 e_4)]$$

$$e_{14} = -4e_3 e_0 r_1 r I_0 e_4 \qquad (4\text{-}8)$$

and the f_i coefficients are defined in Appendix D.

If the axial and rotatory inertia are neglected the equation for determining the location of the repeated roots reduces to

$$\bar{C}_4 \lambda^4 + \bar{C}_2 \lambda^2 + \bar{C}_0 = 0 \qquad (4\text{-}9)$$

where

$$\bar{C}_4 = e_3^2 r^2 f_0^2$$

$$\bar{C}_2 = 2r e_3 [2e_6 D_1 f_1 - f_0 (D_1 e_5 + e_3 f_0 f_2)]$$

$$\bar{C}_0 = (D_1 e_5 + e_3 f_0 f_2)^2 - 4e_3 f_3 D_1 f_1 e_6 \qquad (4\text{-}10)$$

The solution of Equation (4-9) gives two roots $(\lambda_1')^2$ and $(\lambda_2')^2$ which are approximations for λ_1^2 and λ_2^2. These are the square of the two lowest load velocities at which repeated roots occur.

The second condition which gives repeated roots is that given by Equation (4-4). Substituting for the c_4 coefficient gives

$$(G + F - r\lambda^2)(D_1 - I_o\lambda^2)[1 + F - D_1 + (I_o - r_1)\lambda^2] = 0 \qquad (4\text{-}11)$$

This can be written

$$(f_3 - r\lambda^2)(D_1 - I_o\lambda^2)(f_1 + e_4\lambda^2) = 0 \qquad (4\text{-}12)$$

Expanding this and collecting coefficients on λ^2 yields

$$[f_3 D_1 - (r D_1 + f_3 I_o)\lambda^2 + I_o r\lambda^4](f_1 + e_4\lambda^2) = 0$$

$$f_1 f_3 D_1 + [e_4 f_3 D_1 - f_1 (r D_1 + f_3 I_o)]\lambda^2$$

$$+ [f_1 r I_o - e_4 (r D_1 + f_3 I_o)]\lambda^4 + e_4 I_o r\lambda^6 = 0$$

Finally

$$C_6'\lambda^6 + C_4'\lambda^4 + C_2'\lambda^2 + C_o' = 0 \qquad (4\text{-}13)$$

where

$$C_6' = e_4 I_o r$$

$$C_4' = f_1 r I_o - e_4 (r D_1 + f_3 I_o)$$

$$C_2' = e_4 f_3 D_1 - f_1 (r D_1 + f_3 I_o)$$

$$C_o' = f_1 f_3 D_1 \qquad (4\text{-}14)$$

If rotatory and axial inertia are neglected Equation (4-13) reduces to give one root

$$(\lambda_3')^2 = -\frac{C_o'}{C_2'} = \frac{f_3}{r} = \frac{R}{r}(G + F) \tag{4-15}$$

The third condition ($c_o = 0$) from Equation (4-5) is now investigated. Substituting for c_o gives

$$(1 + F - r_1\lambda^2)(E_o + Pr_o) - (E_1 - P)^2 = 0 \tag{4-16}$$

or

$$(f_o - r_1\lambda^2)e_o = e_1^2 \tag{4-17}$$

thus

$$\lambda_4^2 = \frac{e_o f_o - e_1^2}{e_o r_1}$$

$$\lambda_4^2 = \frac{e_6}{e_o r_1} \tag{4-18}$$

Therefore, Equations (4-6), (4-13) and (4-18) can be solved to give eight roots in λ^2 which satisfy the conditions for repeated roots. Equation (4-6) gives four values of λ^2 and these values are labeled λ_1^2, λ_2^2, λ_7^2, and λ_8^2. The condition which lead to these roots was that

$$c_2^2 - 4c_o c_4 = 0$$

Solving Equation (4-1) directly gives

$$s^2 = \frac{-c_2 \pm \sqrt{c_2^2 - 4c_o c_4}}{2c_4} \tag{4-19}$$

If the radical in (4-19) is zero, the roots are

$$s_{1,2} = \sqrt{-\frac{c_2}{2c_4}}, \qquad s_{3,4} = -\sqrt{-\frac{c_2}{2c_4}} \tag{4-20}$$

The repeated roots are either real or imaginary depending upon the sign of the coefficients.

Equation (4-13) gives three more roots which will be labeled λ_3^2, λ_5^2, and λ_6^2. These roots come from the statement that $c_4 = 0$ and if $c_2 \neq 0$ the repeated roots in this case will occur at an infinite value.

Equation (4-18) adds one more root, making a total of eight. This root is designated λ_3^2. The condition leading to this root was that $c_0 = 0$. From Equation (4-1) it is observable that the characteristic equation becomes

$$s^2(c_4 s^2 + c_2) = 0 \qquad (4\text{-}21)$$

which shows a repeated root at the origin.

A computer program was written for the solution of these equations. A simplified flow diagram of the program is shown in Figure 4.1 and the details of the program, named VCRIT, are presented in Appendix E.

The results of a parametric study using the computer program VCRIT are presented in Figures 4.2 through 4.8. The locus of each of the roots $\lambda_i (i = 1, \ldots 8)$ is shown on these figures. These curves are the boundaries which separate these plots into distinct regions which are labeled as Regions I through VIII. In each of the regions the roots of the undamped characteristic equation have a particular form as noted on the figures and as listed in Table 4-1.

Table 4-1

Correlation of Root Type with Region Numbers for Figures 4.2 through 4.8

Region	Form of Root
I, III, VI	$\pm ib_1, \pm ib_2$
II	$a \pm ib, -a \pm ib$
IV, VII	$\pm a_1, \pm a_2$
V, VIII	$\pm a, \pm ib$

a, b are real

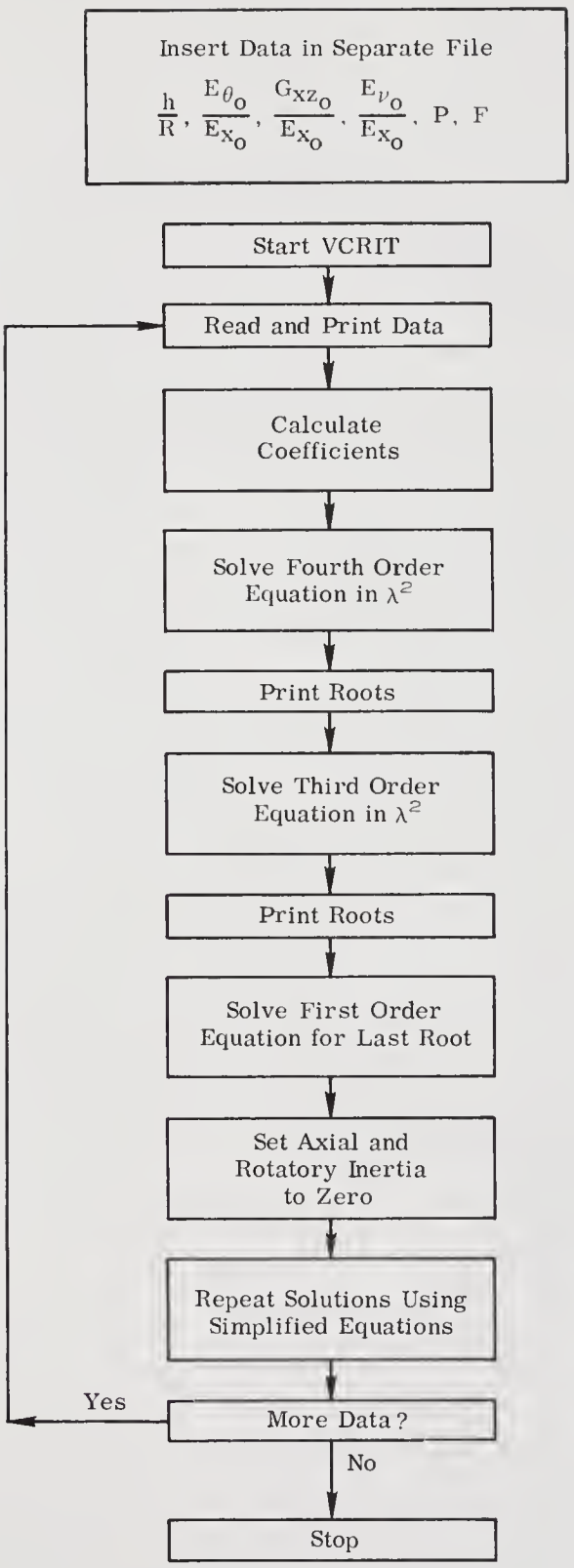

Figure 4.1. Flow Diagram of Computer Program VCRIT which Determines Load Velocities at which Repeated Roots Occur

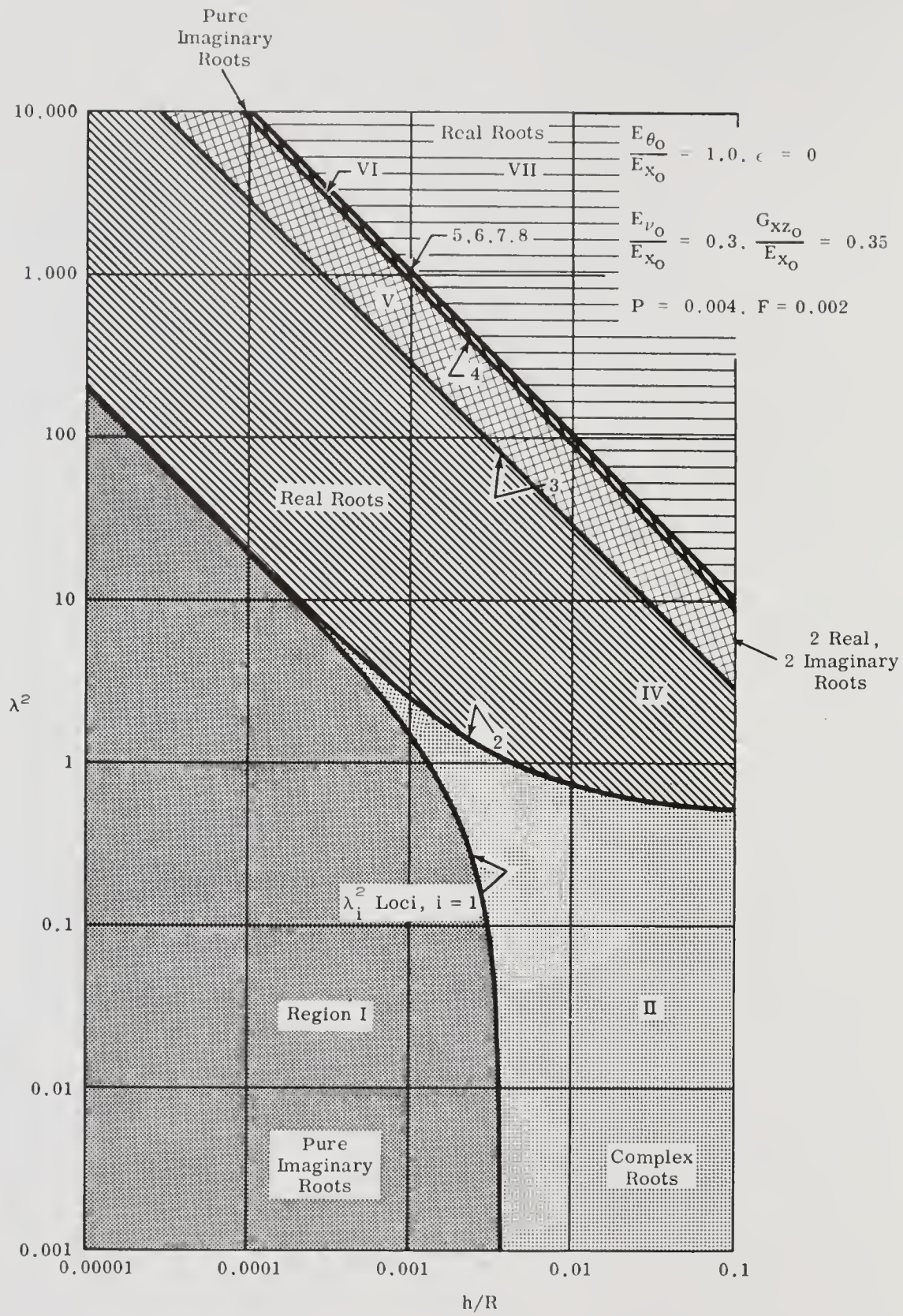

Figure 4.2. Classification of Roots of the Undamped Characteristic Equation for Variations in the Thickness to Radius Ratio Including Prestress

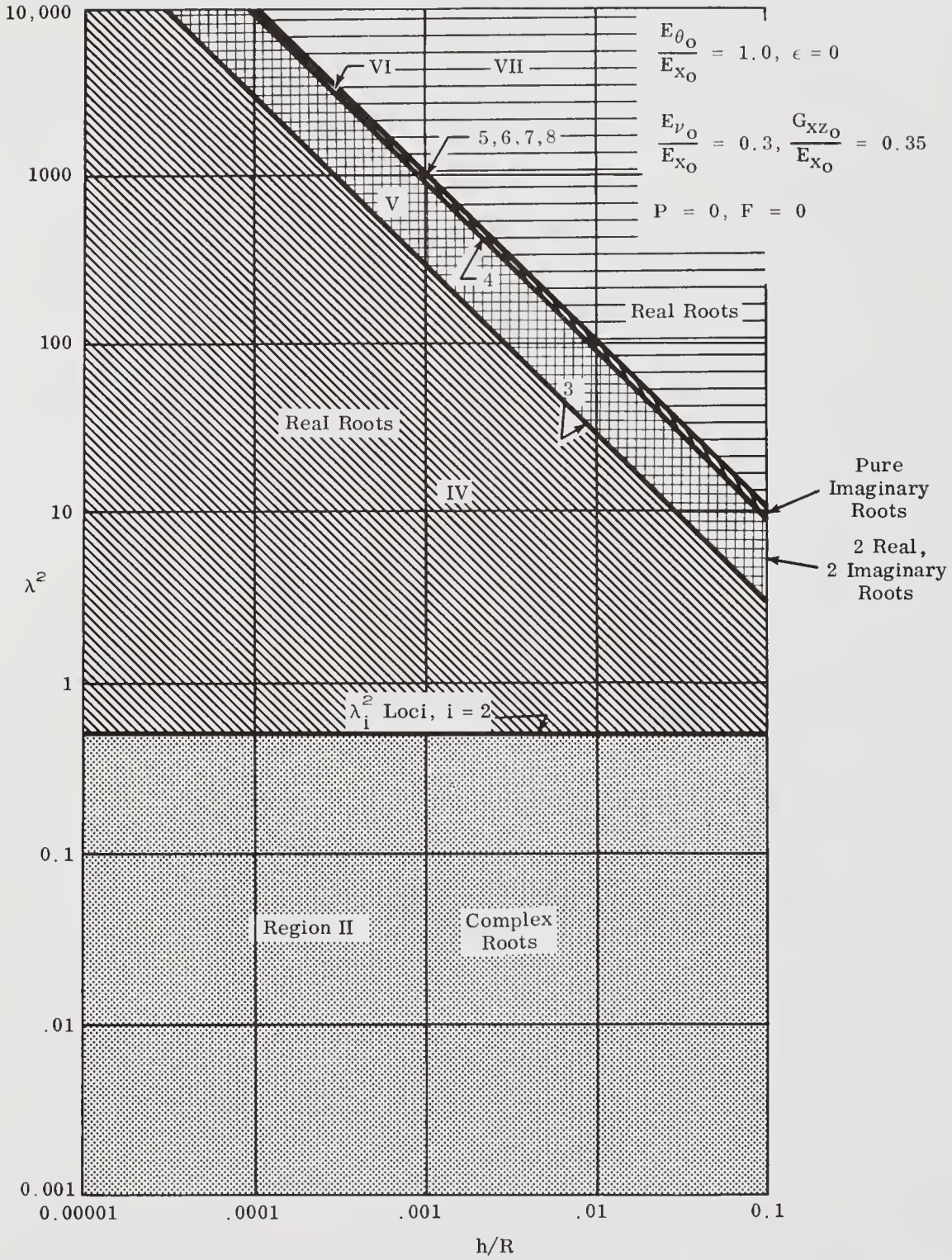

Figure 4.3. Classification of Roots of the Undamped Characteristic Equation for Variations in the Thickness to Radius Ratio with No Prestress

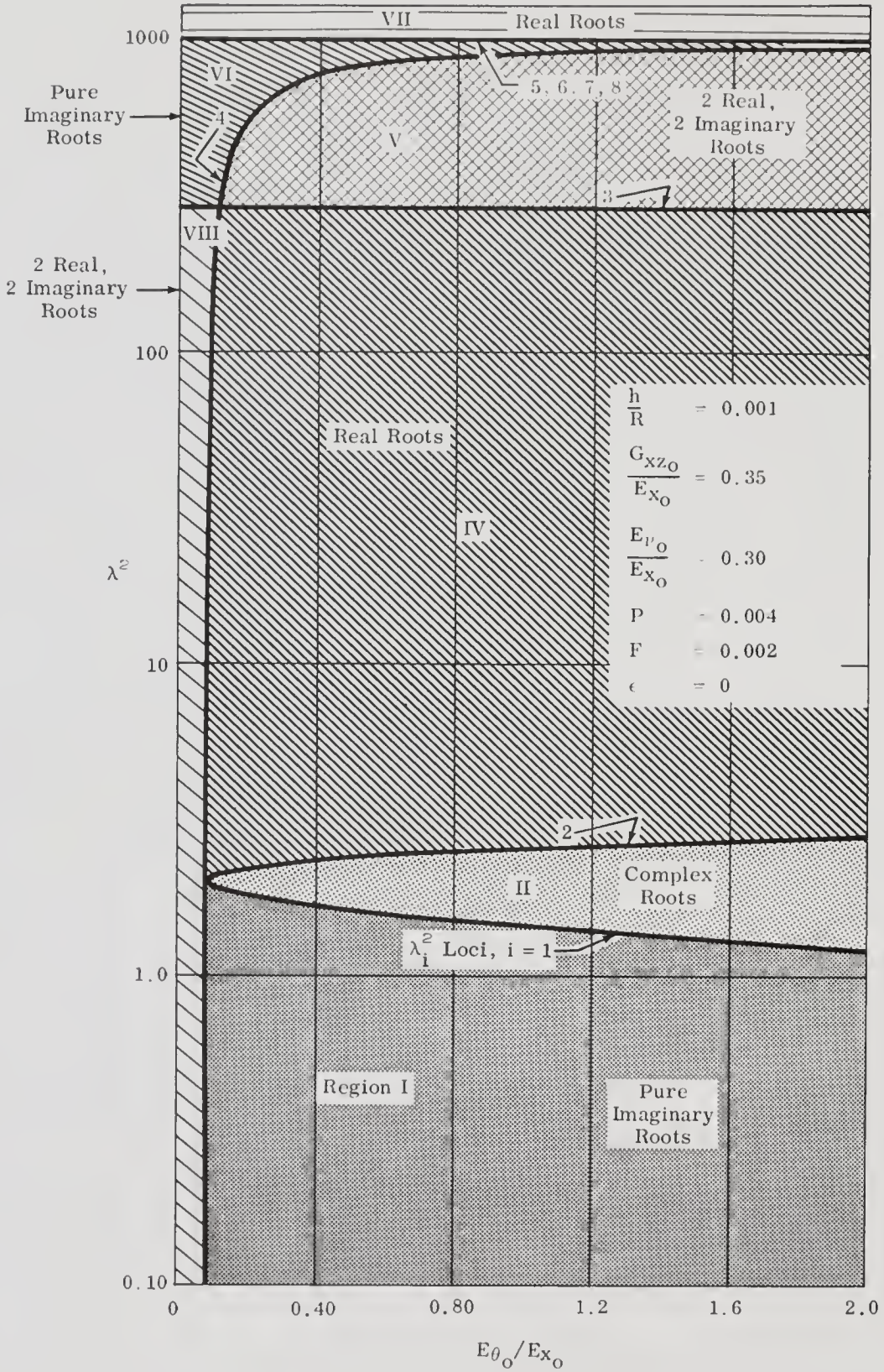

Figure 4.4. Classification of Roots of the Undamped Characteristic Equation for Variations in E_{θ_o}/E_{x_o}

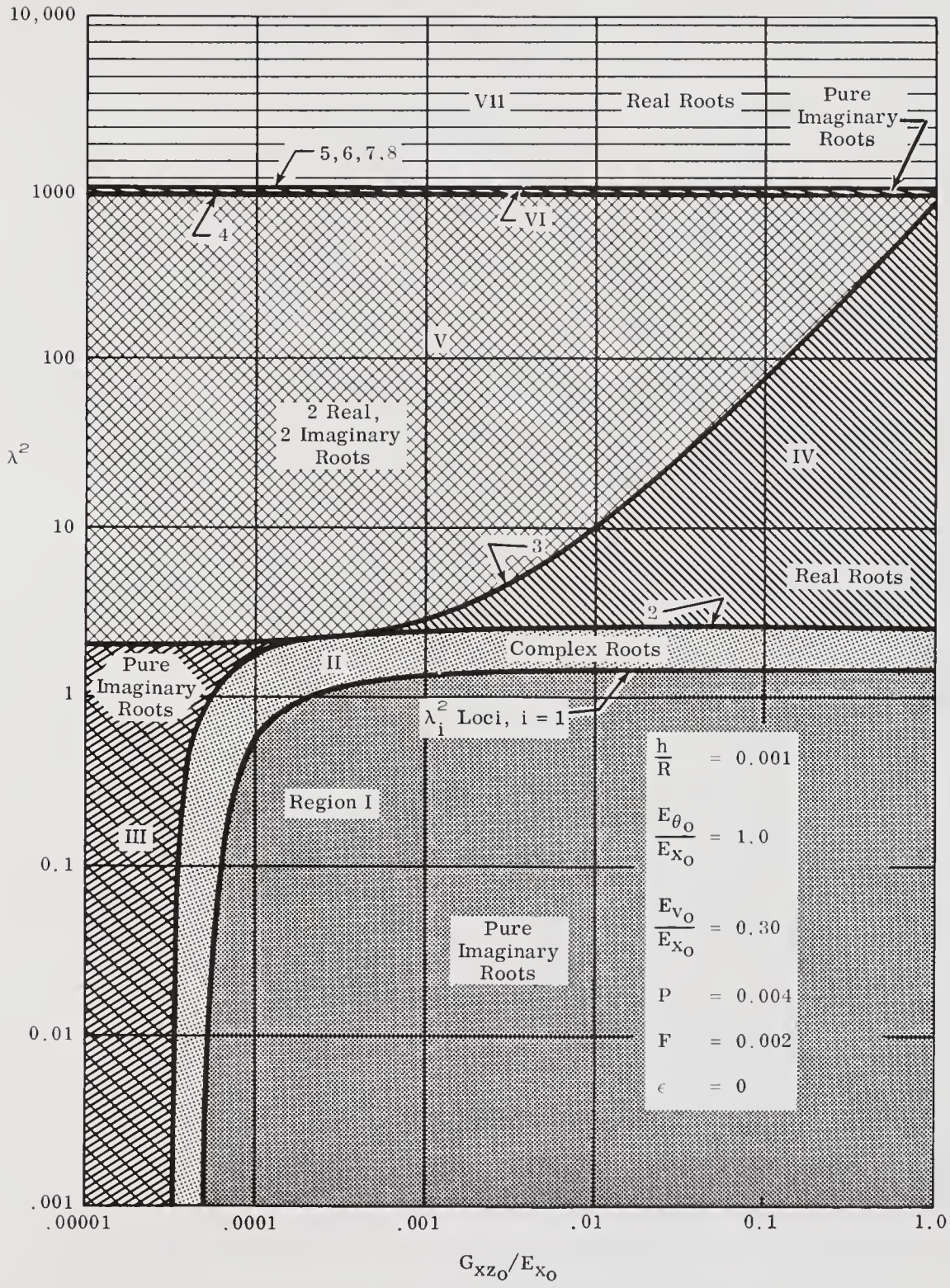

Figure 4.5. Classification of Roots of the Undamped Characteristic Equation for Variations in G_{xz_o}/E_{x_o}

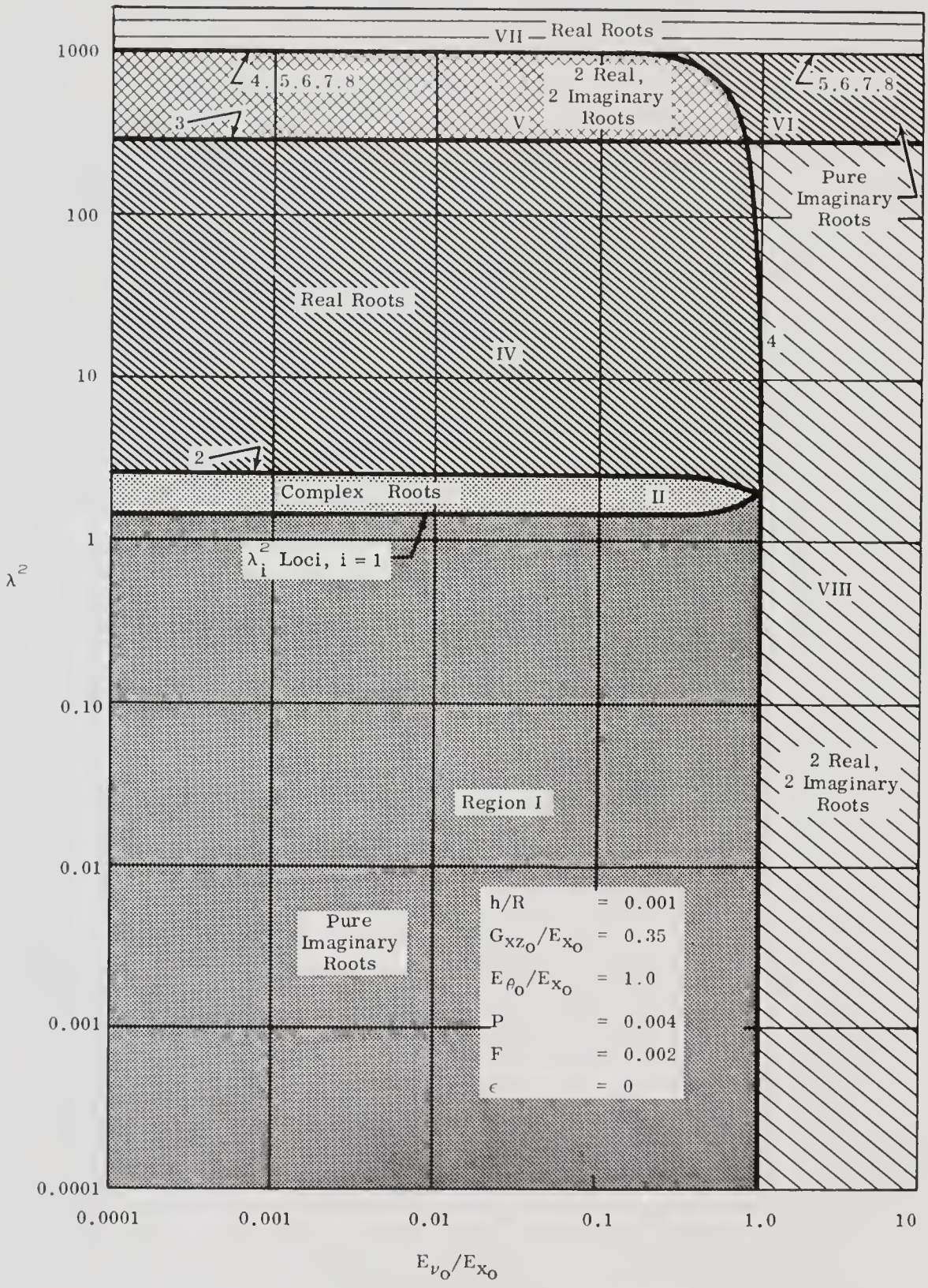

Figure 4.6. Classification of Roots of the Undamped Characteristic Equation for Variations in the E_{ν_o}/E_{x_o}

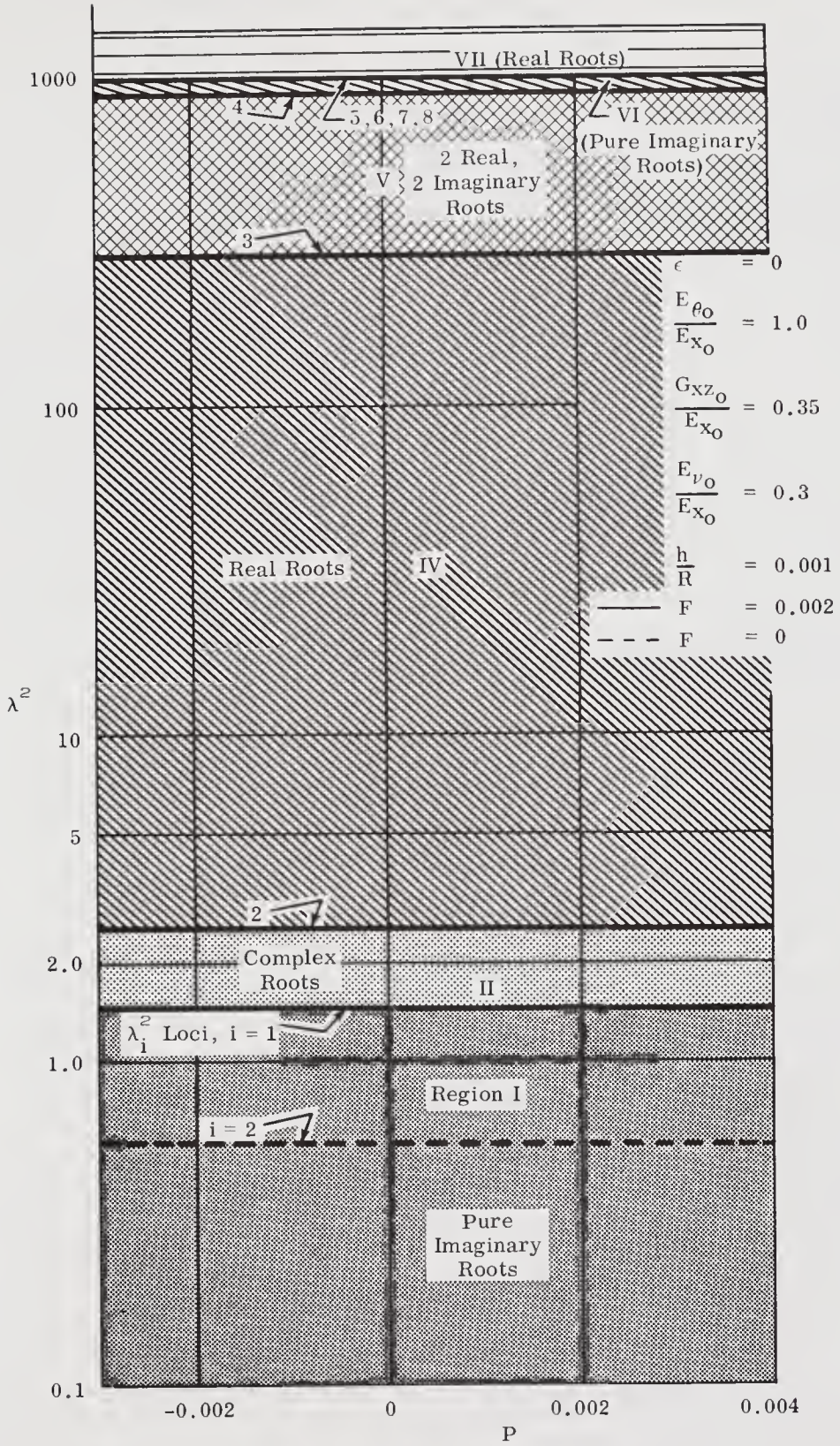

Figure 4.7. Classification of Roots of the Undamped Characteristic Equation for Variations in the Circumferential Prestress

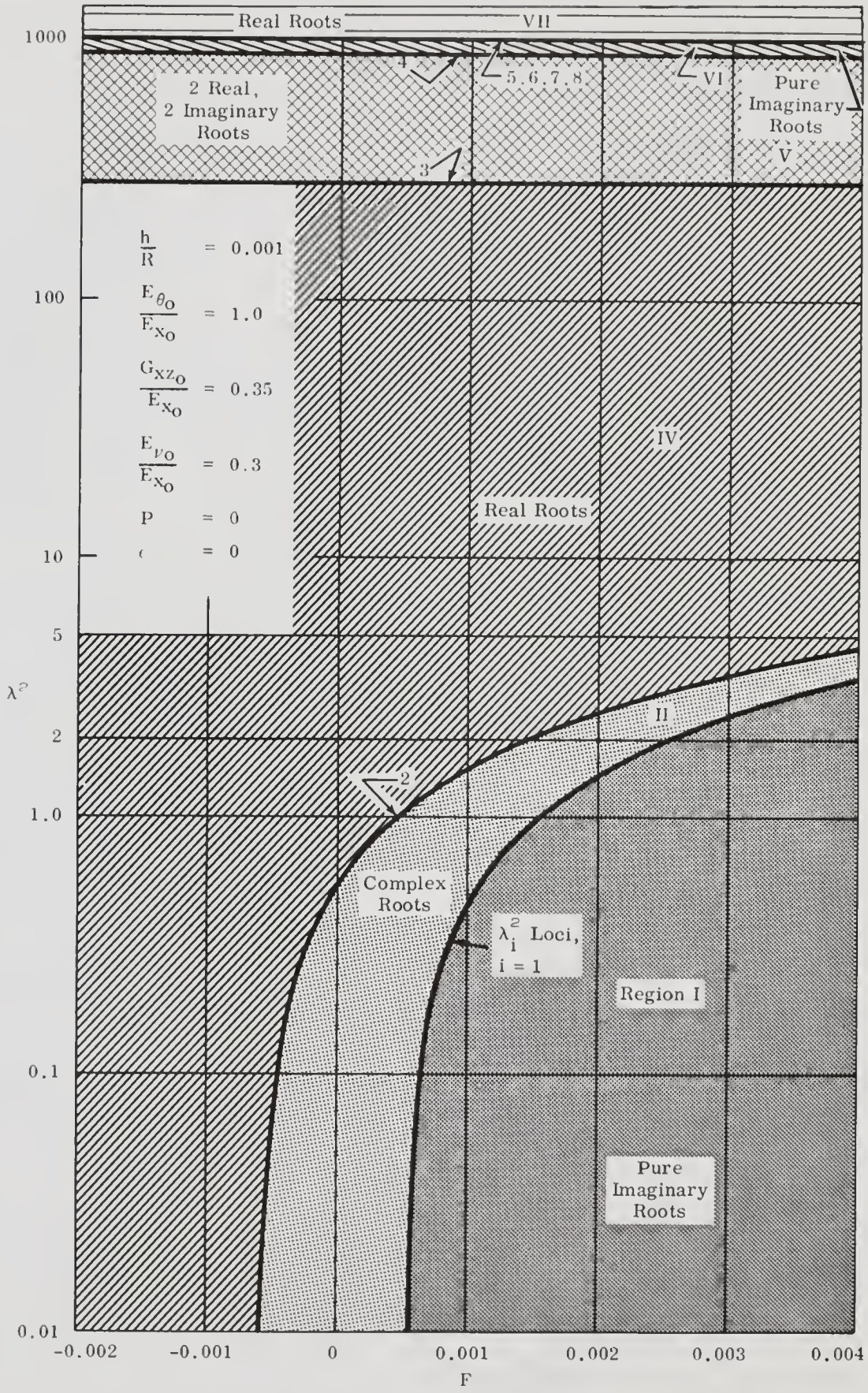

Figure 4.8. Classification of Roots of the Undamped Characteristic Equation for Variations in the Axial Prestress

The lower three values of λ_i are approximated by Expressions (4-9) and (4-15) by neglecting the axial and rotatory inertia. The approximations are quite good over the range of parameters studied.

The critical load speeds are denoted as those speeds at which the displacements become unbounded for an undamped system. This corresponds to the load speeds which produce a double root on the real axis as will be shown later. It is instructive to follow the path of the roots of the undamped characteristic equation in the complex plane as the load speed increases. As an example, the roots will be traced for material properties corresponding to an isotropic shell with h/R = 0.001 and positive axial and circumferential prestress.

Following the vertical line for h/R = 0.001 in Figure 4.2 for increasing λ^2 will give a path crossing all of the boundaries separating different types of roots. Starting at the low load speed, the roots are all on the imaginary axis. (This would not be the case if prestress were not included, as shown by Figure 4.3.) As a means of tracing the location of the roots, Figure 4.9 is utilized which shows the complex plane. The roots in Region I appear on the plane on the imaginary axis and these particular roots are designated $s_{1,1}$, $s_{2,1}$, $s_{3,1}$, and $S_{4,1}$. The nomenclature $s_{i,j}$ denotes the i^{th} root location and j indicates the relative position of the roots. For instance $s_{1,4}$ denotes the position of the first root and at that time (load speed) the other roots are located at points $s_{2,4}$, $s_{3,4}$, and $s_{4,4}$. The arrows indicate the direction in which the root is moving for an increasing load speed. At the first speed two pairs of roots are moving toward one another on the positive and negative parts of the imaginary axis. They meet, and the first repeated root location is established which corresponds to λ_1 in Figure 4.2. As the load speed increases Region II is entered. The roots are complex as can be seen in Figure 4.9. Next, the complex roots approach one another in pairs on the negative and positive real axis. This gives

the first repeated roots on the real axis and this load speed is designated as the first critical load speed, $\lambda_{1_{CR}}$.

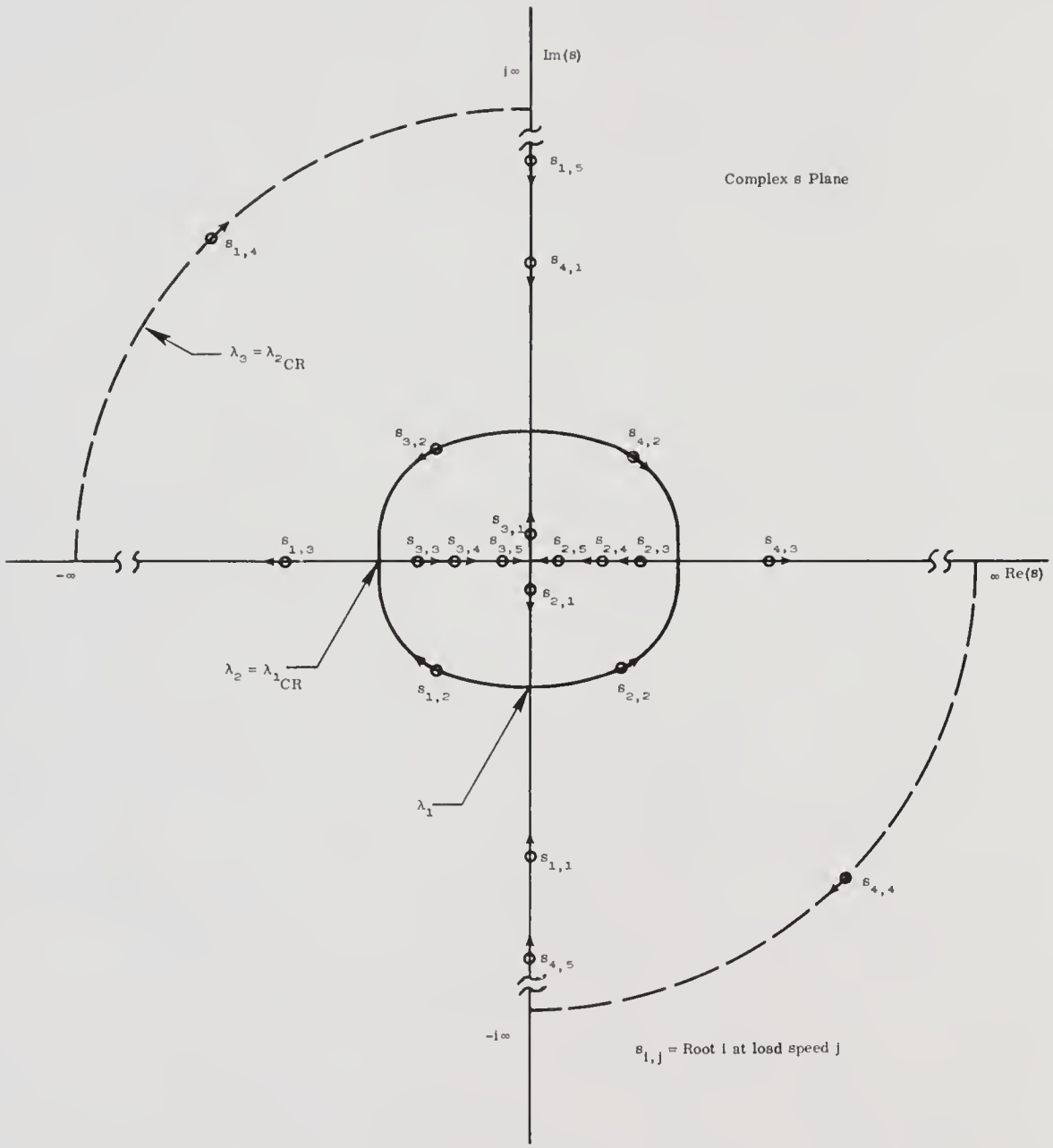

Figure 4.9. Path of the Roots of the Undamped Characteristic Equation for Increasing Load Speed (Beginning in Region I)

Now the roots separate and go in opposite directions along the real axis, the larger roots eventually becoming unbounded. This speed corresponds to the boundary line between Regions IV and V. The condition causing this occurrence is that $c_4 \rightarrow 0$. Repeated roots occur at infinity and the second critical load speed has been determined. As the load speed increases further, the large roots come in from $\pm i\infty$ along the imaginary axis. At location 5 the two large roots are imaginary and the other two are still on the real axis approaching the origin. This corresponds to Region V in Figure 4.2.

The locations of the roots are now transferred to Figure 4.10 to avoid undue complication of the picture. Two roots meet at the origin while the other two are yet large and imaginary. This double root corresponds to λ_4 in Figure 4.2 and is the third critical load speed. An increase in load speed now causes the roots to become all imaginary which is in Region VI. The last four values of λ_i^2 (i = 5, 6, 7, 8) are very close together. In fact λ_5^2 is approximately 1000, and λ_6^2, λ_7^2, and λ_8^2 are almost nondistinguishable at 1002. Increasing the load speed past λ_5^2 causes the large imaginary roots to proceed to an unbounded imaginary value and reappear on the real axis so that the roots are now two real and two imaginary. Also λ_5 must be a critical speed because Condition (4-4) is satisfied at load speed λ_5. This region is not distinguishable on Figures 4.2 through 4.8 and is not given a number.

Further increase in load speed moves the imaginary roots out and eventually they reappear on the real axis with the other pair, there to remain. This position is indicated by $s_{i,10}$ (i = 1, 2, 3, 4). It is interesting to note that $\lambda_{6,7,8}$ also must correspond to a critical load speed, λ_{5CR}.

The lowest critical load speed for an isotropic shell is therefore $\lambda_{1CR} = \lambda_2$. Figure 4.5 shows that for a material with a very low shear modulus, the first critical speed becomes $\lambda_3 = \lambda_{2CR}$ which corresponds to the shear wave speed.

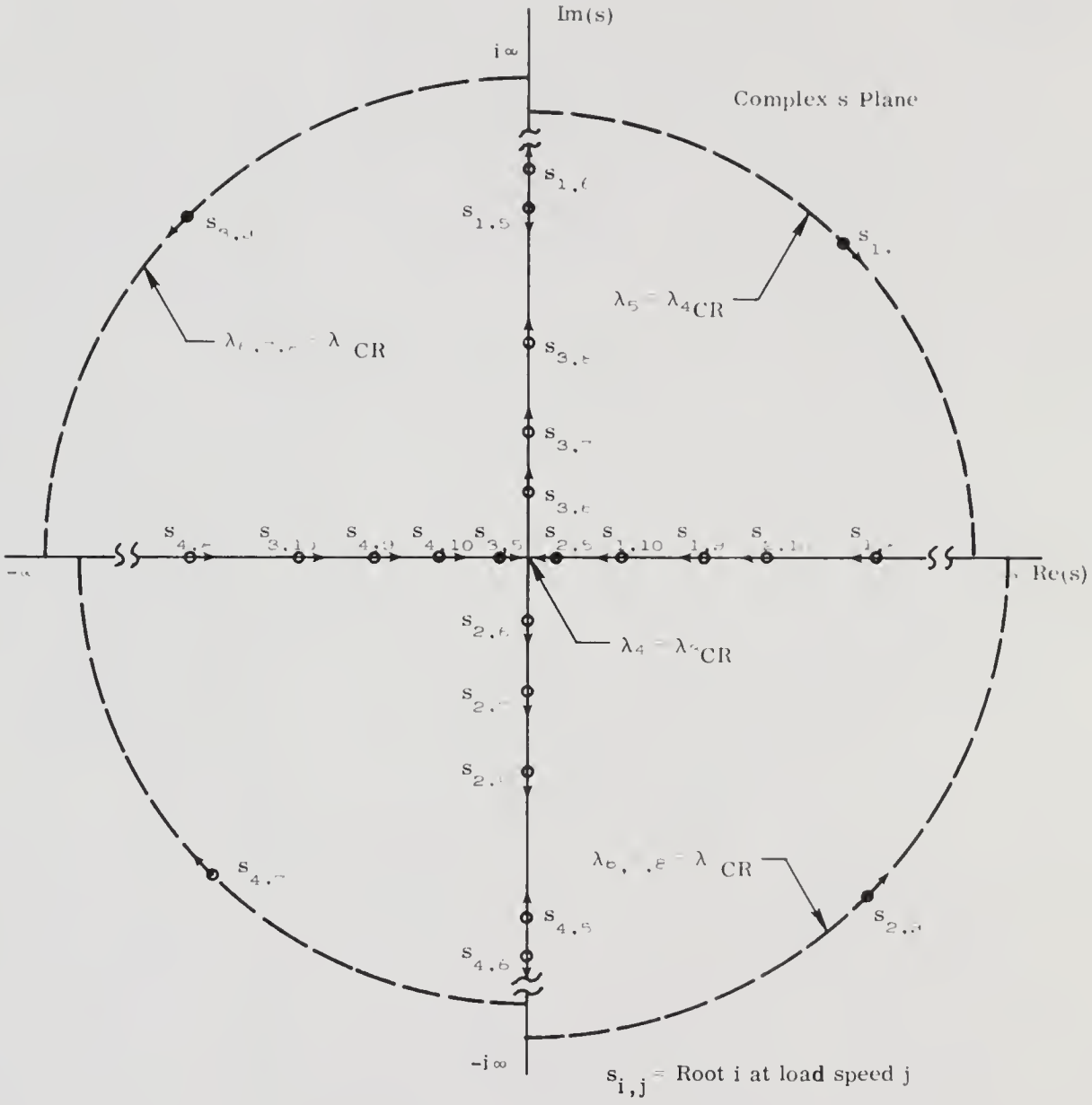

Figure 4.10. Path of the Roots of the Undamped Characteristic Equation for Increasing Load Speed (Beginning in Region V)

When this load speed goes to zero, the critical small deflection buckling load has been reached. From Equation (4-15) this load is seen to be approximately

$$F = -G \tag{4-22}$$

This corresponds to the second critical load for engineering materials with a more realistic value for shear modulus.

If prestress is not included, Region I disappears as shown by comparing Figures 4.2 and 4.3. Decreasing the tangential modulus drastically or increasing the normal modulus results in the same effect as shown by Figures 4.4 and 4.6. Circumferential prestress has essentially no effect on the critical load speeds but axial prestress has a pronounced effect as shown by Figures 4.7 and 4.8.

It is instructive to make a comparison of these results with those obtained in Reference (2). Three critical velocities were derived there, which are given as

$$V_{CR_1}^2 = \frac{Eh}{\rho_o R\,[3(1-\mu^2)]^{\frac{1}{2}}} - \frac{Eh^2\mu^2}{6\rho_o R^2(1-\mu^2)} \tag{4-23}$$

$$V_{CR_2}^2 = \frac{E}{\rho_o(1-\mu^2)} \tag{4-24}$$

$$V_{CR_3}^2 = \frac{E}{\rho_o} \tag{4-25}$$

for an isotropic material. Since, in the nomenclature used in the present work,

$$\lambda^2 = \frac{V^2\rho_o R(1-\mu^2)}{Eh} \tag{4-26}$$

The corresponding expressions in terms of λ^2 are

$$\lambda_{CR_1}^2 = \sqrt{\frac{1-\mu^2}{3}} - \frac{\mu^2}{6}\,\frac{h}{R} \tag{4-27}$$

$$\lambda_{CR_2}^2 = \frac{R}{h} \tag{4-28}$$

$$\lambda_{CR_3}^2 = \frac{R}{h}(1-\mu^2) \tag{4-29}$$

Now taking $\mu = .3$ it is found that

$$\lambda^2_{CR_1} = 0.55075 - 0.15\frac{h}{R} \tag{4-30}$$

$$\lambda^2_{CR_2} = \frac{R}{h} \tag{4-31}$$

$$\lambda^2_{CR_3} = 0.91\frac{R}{h}$$

From Figure 4.3 (which is a plot of λ_i^2 versus $\frac{h}{R}$ for an isotropic material with $\mu = .3$) for the case of zero axial and circumferential initial stress, $\lambda^2_{CR_1}$, $\lambda^2_{CR_2}$, and $\lambda^2_{CR_3}$ from Reference 2 agree extremely well with λ_2^2, $\lambda^2_{5,6,7,8}$, and λ_4^2 respectively. The two velocities, λ_1 and λ_3, arise in the present results because of initial prestress considerations and shear deformation, respectively, which were not included in the referenced results. λ_2 corresponds to the dilitational wave speed, λ_3 corresponds to the shear wave speed, λ_4 corresponds to the bar wave speed, and $\lambda_{5,6,7,8}$ corresponds to the plate wave speed.

CHAPTER V

SOLUTION FOR DISPLACEMENTS

General Solution

Transformed Displacements

From Equations (3-8) the transformed displacements can be written as

$$\frac{\overline{U}(s)}{q_o} = \frac{1 - e^{isd}}{s^2} \frac{c'_5 s^2 + c'_6}{\overline{D}(s)}$$

$$\frac{\overline{W}(s)}{q_o} = \frac{1 - e^{isd}}{is} \frac{c'_7 s^2 + c'_8}{\overline{D}(s)}$$

$$\frac{\overline{\psi}(s)}{q_o} = -(1 - e^{isd}) \frac{c'_9}{\overline{D}(s)} \qquad (5\text{-}1)$$

where

$$c'_5 = f_7(e_3 + e_1)$$

$$c'_6 = e_3 e_1$$

$$c'_7 = f_7(f_1 + e_4 \lambda^2)$$

$$c'_8 = e_3(f_o - r_1 \lambda^2)$$

$$c'_9 = e_1 f_7 + e_3(f_o - r_1 \lambda^2)$$

$$f_7 = D_1 - I_o \lambda^2 \qquad (5\text{-}2)$$

Inverse Transformation of the Rotation

Using the inverse transformation given by Equation (3-2) the rotation is defined as

$$\frac{\psi(\phi)}{q_o} = -\frac{c'_\vartheta}{2\pi} \int_{-\infty}^{\infty} \frac{(1 - e^{isd})}{\overline{D}(s)} e^{i\phi s} \, ds \tag{5-3}$$

By partial fraction expansion this can be put in the form*

$$\frac{\psi(\phi)}{q_o} = -\frac{c_\vartheta}{2\pi} \int_{-\infty}^{\infty} (1 - e^{isd}) e^{i\phi s} \sum_{k=1}^{4} \left(\frac{\alpha_k}{s - s_k} \right) ds \tag{5-4}$$

where

$$\alpha_k = \frac{1}{\left\{ \frac{d}{ds} \left[\overline{D}(s) \right] \right\}_{s=s_k}} = \frac{1}{\prod_{m=1}^{4} (s_k - s_m)} \qquad m \neq k$$

$$c_\vartheta = \frac{c'_\vartheta}{c_4} \tag{5-5}$$

Defining

$$F_k(\phi) = -\frac{c_\vartheta \, \alpha_k}{2\pi} \int_{-\infty}^{\infty} \frac{(1 - e^{isd})}{s - s_k} e^{i\phi s} \, ds \tag{5-6}$$

then

$$\frac{\psi(\phi)}{q_o} = \sum_{k=1}^{4} F_k(\phi) \tag{5-7}$$

*See Appendix F for the derivation of a sample partial fraction expansion expression.

Letting

$$f_k(s) = \frac{1 - e^{isd}}{s - s_k} e^{i\phi s} \tag{5-8}$$

the integral to be evaluated is

$$\int_{-\infty}^{\infty} f_k(s)\, ds$$

where $f_k(s)$ is an analytic function except at the simple pole $s = s_k$. Defining the complex root in general to be

$$s_k = a_k + i\, b_k ,$$

the Cauchy integral theorem is used to evaluate this integral.

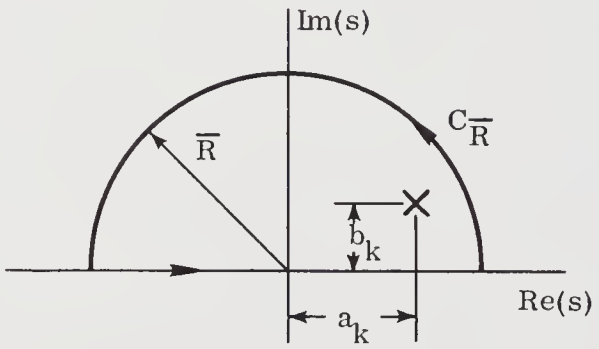

Figure 5.1. Contour Integration Path for Evaluating Rotation Integral

Assuming first that $b_k > 0$ the Cauchy integral theorem gives

$$\oint_C f_k(s)\, ds = 2\pi\, i\, \Sigma \text{ Residues} \tag{5-9}$$

The integral around the closed path shown in Figure 5.1 is

$$\oint_C f_k(s)\,ds = \int_{C_{\overline{R}}} f_k(s)\,ds + \int_{-\overline{R}}^{\overline{R}} f_k(s)\,ds \qquad (5\text{-}10)$$

From Reference (12) it is shown that if $f(s) \to 0$ uniformly as $\overline{R} \to \infty$ then

$$\lim_{\overline{R}\to\infty} \int_{C_{\overline{R}}} f(s)\, e^{i\phi s}\,ds = 0, \qquad (\phi > 0)$$

Therefore the first integral on the right in Equation (5-10) goes to zero as $\overline{R} \to \infty$ and

$$\oint_C f_k(s)\,ds = \int_{-\infty}^{\infty} f_k(s)\,ds = 2\pi i \operatorname{Res}(s_k)$$

$$= 2\pi i\, e^{i\phi(a_k + i b_k)}, \qquad \phi > 0$$

$$+ 2\pi i \left[- e^{i d(a_k + i b_k)} \right] e^{i\phi(a_k + i b_k)}, \qquad \phi + d > 0$$

Therefore

$$F_k = - i c_\ominus \alpha_k \left[e^{-b_k \phi + i a_k \phi} H(\phi) - e^{-b_k(d+\phi) + i a_k (d+\phi)} H(d+\phi) \right] \qquad (5\text{-}11)$$

where

$b_k > 0$

H = Heaviside step function.

Similarly, when $b_k < 0$ the integration path is in the lower half plane and the result is

$$F_k = i c_\ominus \alpha_k \left\{ e^{-b_k \phi + i a_k \phi} H(-\phi) - e^{-b_k(d+\phi) + i a_k (d+\phi)} H[-(d+\phi)] \right\},$$

$$b_k < 0 \qquad (5\text{-}12)$$

The general expression for F_k can be written in the form

$$F_k = -i\,\mathrm{sgn}(b_k)\, c_9\, \alpha_k \left\{ e^{-b_k \phi + i a_k \phi} H[\mathrm{sgn}(b_k)\phi] - e^{-b_k(d+\phi) + i a_k (d+\phi)} H[\mathrm{sgn}(b_k)(d+\phi)] \right\} \tag{5-13}$$

where H is the Heaviside step function and

$$\mathrm{sgn}(b_k) = \begin{cases} 1, & b_k > 0 \\ -1, & b_k < 0 \end{cases} \tag{5-14}$$

The rotation is given by Equation (5-7).

$$\frac{\psi(\phi)}{q_o} = \sum_{k=1}^{4} F_k(\phi)$$

Inverse Transformation of the Radial Deflection

The radial deflection is obtained by inverting $\overline{W}$ to give

$$\frac{W(\phi)}{q_o} = \frac{1}{2\pi i} \int_{-\infty}^{\infty} \frac{1 - e^{isd}}{s} \frac{c'_7 s^2 + c'_8}{\overline{D}(s)} e^{i\phi s}\, ds \tag{5-15}$$

The term $(c'_7 s^2 + c'_8)/\overline{D}(s)$ can be expanded in partial fractions to give

$$\frac{W(\phi)}{q_o} = \frac{1}{2\pi i} \int_{-\infty}^{\infty} \frac{1 - e^{isd}}{s} \left(\sum_{k=1}^{4} \frac{\beta_k}{s - s_k} \right) e^{i\phi s}\, ds \tag{5-16}$$

where

$$\beta_k = \frac{c_7 s_k^2 + c_8}{\prod_{m=1}^{4} (s_k - s_m)}, \qquad k \neq m$$

$$c_7 = \frac{c'_7}{c_4}, \qquad c_8 = \frac{c'_8}{c_4} \tag{5-17}$$

*See Appendix E for this expansion.

Defining

$$ {}_{w}F_{k}(\phi) = \frac{\beta_k}{2\pi i} \int_{-\infty}^{\infty} \frac{(1 - e^{isd})}{s(s - s_k)} e^{i\phi s} \, ds \tag{5-18} $$

The deflection is then given by the sum

$$ \frac{W(\phi)}{q_o} = \sum_{k=1}^{4} {}_{w}F_{k}(\phi) \tag{5-19} $$

By contour integration in the upper and lower half planes, the integral in Equation (5-18) can be evaluated. Breaking the integral into two parts gives

$$ {}_{w}F_{k}(\phi) = \frac{\beta_k}{2\pi i} \left[\int_{-\infty}^{\infty} \frac{e^{i\phi s}}{s(s - s_k)} \, ds - \int_{-\infty}^{\infty} \frac{e^{i(\phi+d)s}}{s(s - s_k)} \, ds \right] \tag{5-20} $$

The contour shown in Figure 5.2 is used to evaluate these integrals for $\phi > 0$, $b_k > 0$.

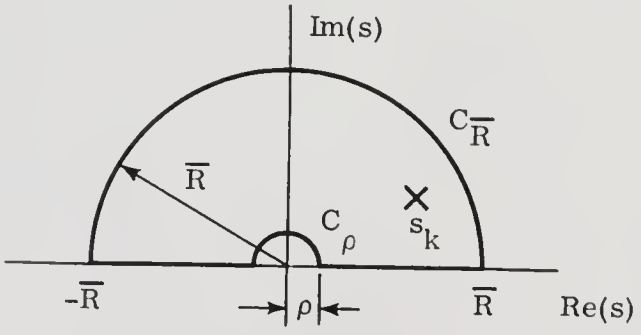

Figure 5.2. Integration Contour for Radial Deflection for $\phi > 0$, $b_k > 0$

From Cauchy's integral theorem

$$ \oint_C {}_{w}f_{k}(s) \, ds = \int_{C_{\overline{R}}} {}_{w}f_{k}(s) \, ds + \int_{-R}^{-\rho} {}_{w}f_{k}(s) \, ds + \int_{C_\rho} {}_{w}f_{k}(s) \, ds $$

$$ + \int_{\rho}^{\overline{R}} {}_{w}f_{k}(s) \, ds = 2\pi i \, \Sigma \, \text{Res} $$

From Jordan's Lemma (12) it can be seen that the integral on contour $C_{\bar{R}} \to 0$ as $\bar{R} \to \infty$, i.e.,

$$\lim_{\bar{R}\to\infty} \int_{C_{\bar{R}}} \frac{e^{i\phi s}}{s(s - s_k)}\, ds \;\to\; 0, \qquad \phi > 0$$

and

$$\lim_{\bar{R}\to\infty} \int_{C_{\bar{R}}} \frac{e^{i(\phi+d)s}}{s(s - s_k)}\, ds \;\to\; 0, \qquad \phi+d > 0$$

Also

$$\lim_{\substack{\rho\to 0 \\ \bar{R}\to\infty}} \left[\int_{-\bar{R}}^{-\rho} w\, f_k(s)\, ds + \int_{\rho}^{\bar{R}} w\, f_k(s)\, ds \right] = P \int_{-\infty}^{\infty} w\, f_k(s)\, ds$$

which is the Cauchy principal value of the improper integral. If the integral exists, then this is the correct value for the integral and the symbol P can be dropped. Therefore

$$\int_{-\infty}^{\infty} \frac{e^{i\phi s}}{s(s - s_k)}\, ds + \lim_{\rho\to 0} \int_{C_\rho} \frac{e^{i\phi s}}{s(s - s_k)}\, ds = 2\pi i\, \mathrm{Res}(s_k), \qquad \phi > 0 \quad (5\text{-}21)$$

The second integral in Equation (5-21) can be evaluated as

$$\lim_{\rho\to 0} \int_{C_\rho} \frac{e^{i\phi s}}{s(s - s_k)}\, ds = \alpha\, i\, \mathrm{Res}(0)$$

Since the integration is clockwise

$$\alpha = -\pi$$

and

$$\mathrm{Res}(0) = \left(\frac{e^{i\phi s}}{s - s_k} \right)_{s=0} = -\frac{1}{s_k}$$

so

$$\lim_{\rho \to 0} \int_{C_\rho} \frac{e^{i\phi s}}{s(s - s_k)}\, ds = \frac{\pi i}{s_k}$$

Integral (5-21) now may be written

$$\int_{-\infty}^{\infty} \frac{e^{i\phi s}}{s(s - s_k)}\, ds = -\frac{\pi i}{s_k} + \frac{2\pi i\, e^{i\phi s_k}}{s_k} \tag{5-22}$$

where

$\phi > 0$

$b_k > 0$

Similarly

$$\int_{-\infty}^{\infty} \frac{e^{i(\phi+d)s}}{s(s - s_k)}\, ds = -\frac{\pi i}{s_k} + \frac{2\pi i\, e^{i(\phi+d)}}{s_k} \tag{5-23}$$

where

$\phi + d > 0$

$b_k > 0$

Now the case is investigated where $b_k > 0$, $\phi < 0$. The contour shown below is used for this case.

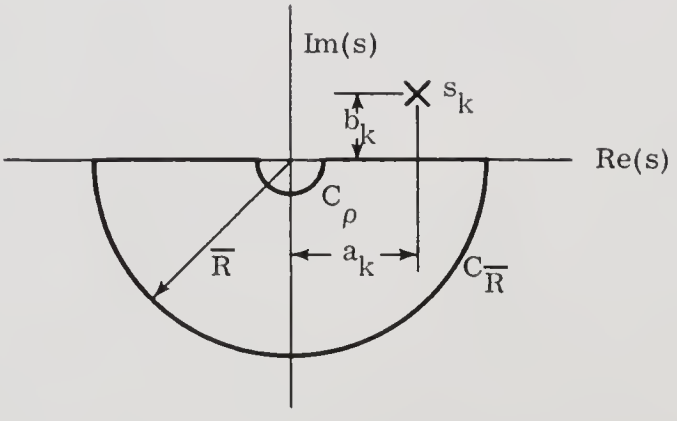

Figure 5.3. Integration Contour for Evaluating Radial Deflection for $\phi < 0$, $b_k > 0$

The integrals have the values

$$\int_{\infty}^{-\infty} \frac{e^{i\phi s}}{s(s - s_k)}\, ds + \lim_{\rho \to 0} \int_{C_\rho} \frac{e^{i\phi s}}{s(s - s_k)}\, ds = 0, \qquad \phi < 0$$

or

$$\int_{-\infty}^{\infty} \frac{e^{i\phi s}}{s(s - s_k)}\, ds = -\pi i \, \mathrm{Res}(0) = \frac{\pi i}{s_k}, \qquad \begin{matrix} \phi < 0 \\ b_k > 0 \end{matrix} \tag{5-24}$$

Similarly

$$\int_{-\infty}^{\infty} \frac{e^{i(\phi+d)s}}{s(s - s_k)}\, ds = \frac{\pi i}{s_k}, \qquad \begin{matrix} \phi + d < 0 \\ b_k > 0 \end{matrix} \tag{5-25}$$

Equations (5-22), (5-23), (5-24), and (5-25) can be combined to give the solution for ${}_wF_k(\phi)$ when $b_k > 0$ as

$$\begin{aligned} {}_wF_k(\phi) = \frac{\beta_k}{2\pi i} \Bigg\{ & \left(-\frac{\pi i}{s_k} + \frac{2\pi i}{s_k} e^{i\phi s_k} \right) H(\phi) + \frac{\pi i}{s_k} H(-\phi) \\ & - \left[\left(-\frac{\pi i}{s_k} + \frac{2\pi i}{s_k} e^{i(\phi+d)s_k} \right) H(\phi+d) + \frac{\pi i}{s_k} H(-\phi-d) \right] \Bigg\}, \qquad b_k > 0 \end{aligned}$$

or finally

$$\begin{aligned} {}_wF_k(\phi) = \frac{\beta_k}{s_k} \Bigg\{ & \left(-\frac{1}{2} + e^{i\phi s_k} \right) H(\phi) + \frac{1}{2} H(-\phi) \\ & - \left[\left(-\frac{1}{2} + e^{i(\phi+d)s_k} \right) H(\phi+d) + \frac{1}{2} H(-\phi-d) \right] \Bigg\} \end{aligned} \tag{5-26}$$

where $b_k > 0$.

The case where $b_k < 0$ is now investigated. Integrating in the lower half plane it is found that

$$\int_{\infty}^{-\infty} \frac{e^{i\phi s}}{s(s - s_k)}\, ds + \int_{C_\rho} \frac{e^{i\phi s}}{s(s - s_k)}\, ds = 2\pi i \frac{e^{i\phi s_k}}{s_k}, \qquad \begin{matrix}\phi < 0 \\ b_k < 0\end{matrix}$$

or

$$\int_{-\infty}^{\infty} \frac{e^{i\phi s}}{s(s - s_k)}\, ds = -2\pi i \frac{e^{i\phi s_k}}{s_k} + \frac{\pi i}{s_k}, \qquad \begin{matrix}\phi < 0 \\ b_k < 0\end{matrix}$$

It is evident, therefore, that the general expression for ${}_w F_k(\phi)$ can be written in the form

$$\begin{aligned} {}_w F_k(\phi) = \frac{\mathrm{sgn}(b_k)\,\beta_k}{s_k} \Bigg[& \left(-\frac{1}{2} + e^{i\phi s_k} \right) H[\mathrm{sgn}(b_k)\phi] + \frac{H[-\mathrm{sgn}(b_k)\phi]}{2} \\ & - \left\{ \left[-\frac{1}{2} + e^{i(\phi+d)s_k} \right] H[\mathrm{sgn}(b_k)(\phi+d)] \right. \\ & \left. + \frac{1}{2} H[-\mathrm{sgn}(b_k)(\phi+d)] \right\} \Bigg] \end{aligned} \tag{5-27}$$

Inverse Transformation of the Axial Deflection

The axial deflection in the s-plane can be written as

$$\frac{\overline{U}(s)}{q_o} = c'_5 \frac{(1 - e^{isd})}{\overline{D}(s)} + c'_6 \frac{(1 - e^{isd})}{s^2\, \overline{D}(s)} \tag{5-28}$$

From Equation (5-1) it can be seen that the first term in Equation (5-28) can be written in terms of $\overline{\psi}$. Thus

$$\frac{U(\phi)}{q_o} = -\frac{c'_5}{c'_9} \frac{\psi(\phi)}{q_o} + \frac{c'_6}{2\pi} \int_{-\infty}^{\infty} \frac{(1 - e^{isd})}{s^2\, \overline{D}(s)}\, e^{i\phi s}\, ds \tag{5-29}$$

The integral in Equation (5-29) can be written as

$$\frac{c_6}{2\pi} \int_{-\infty}^{\infty} \frac{(1 - e^{isd})}{s^2} e^{is\phi} \sum_{k=1}^{4} \left(\frac{\alpha_k}{s - s_k} \right) ds$$

where

$$c_6 = \frac{c'_6}{c_4}$$

Now defining

$$u F_k(\phi) = \frac{c_6 \alpha_k}{2\pi} \int_{-\infty}^{\infty} \frac{(1 - e^{isd}) e^{i\phi s}}{s^2(s - s_k)} ds \qquad (5\text{-}30)$$

then

$$\frac{U(\phi)}{q_o} = - \frac{c_5}{c_9} \frac{\psi(\phi)}{q_o} + \sum_{k=1}^{4} u F_k(\phi) \qquad (5\text{-}31)$$

The integrand in Equation (5-30) can be written in two parts as

$$u F_k(\phi) = \frac{c_6 \alpha_k}{2\pi} \left[\int_{-\infty}^{\infty} \frac{e^{i\phi s}}{s^2(s - s_k)} ds - \int_{-\infty}^{\infty} \frac{e^{i(\phi+d)s}}{s^2(s - s_k)} ds \right] \qquad (5\text{-}32)$$

The contours shown in Figures 5.2 and 5.3 are used to evaluate the integrals in Equation (5-32) for the case $b_k > 0$. Define

$$u f_k(s) = \frac{e^{i\phi s}}{s^2(s - s_k)}, \qquad u f'_k(s) = \frac{e^{i(\phi+d)s}}{s^2(s - s_k)}$$

By a procedure completely analogous to that just described for the radial deflection, the results can be written

$$\int_{-\infty}^{\infty} \frac{e^{i\phi s}}{s^2(s - s_k)} ds = \pi i \, \mathrm{Res}(0) + 2\pi i \, \mathrm{Res}[u f_k(s_k)], \qquad \phi > 0, \; b_k > 0 \qquad (5\text{-}33)$$

$$\int_{-\infty}^{\infty} \frac{e^{i(\phi+d)s}}{s^2(s - s_k)}\, ds = \pi i \,\mathrm{Res}'(0) + 2\pi i \,\mathrm{Res}[{}_u f_k'(s_k)], \qquad \begin{matrix}\phi+d > 0 \\ b_k > 0\end{matrix} \tag{5-34}$$

where

$$\mathrm{Res}[{}_u f_k(s_k)] = \frac{e^{-b_k \phi + i a_k \phi}}{(a_k + i b_k)^2} \tag{5-35}$$

$$\mathrm{Res}[{}_u f_k'(s_k)] = \frac{e^{-b_k(\phi+d) + i a_k(\phi+d)}}{(a_k + i b_k)^2} \tag{5-36}$$

To find the residue of the functions at $s = 0$ they are expanded in a Laurent series about the point $s = 0$.

$$\frac{e^{i\phi s}}{s^2} = \frac{1}{s^2} + \frac{i\phi}{s} - \frac{\phi^2}{2!} - \frac{i\phi^3 s}{3!} + \cdots$$

$$\frac{1}{s - s_k} = -\frac{1}{s_k}\left(1 + \frac{s}{s_k} + \frac{s^2}{s_k^2} + \cdots\right)$$

$$\frac{e^{i\phi s}}{s^2(s - s_k)} = -\frac{1}{s_k}\left(\frac{1}{s^2} + \frac{i\phi + \frac{1}{s_k}}{s} + \frac{1}{s_k^2} + \frac{i\phi}{s_k} - \frac{\phi^2}{2!} + \cdots\right)$$

The residues can be evaluated as

$$\mathrm{Res}(0) = -\frac{1}{s_k^2} - i\frac{\phi}{s_k} \tag{5-37}$$

$$\mathrm{Res}'(0) = -\frac{1}{s_k^2} - i\frac{\phi + d}{s_k} \tag{5-38}$$

so that

$$\int_{-\infty}^{\infty} \frac{e^{i\phi s}}{s^2(s - s_k)}\, ds = -\frac{\pi i}{s_k}\left(\frac{1}{s_k} + i\phi\right) + 2\pi i \frac{e^{i\phi s_k}}{s_k^2}, \qquad \begin{matrix} b_k > 0 \\ \phi > 0 \end{matrix}$$

$$\int_{-\infty}^{\infty} \frac{e^{i(\phi+d)s}}{s^2(s - s_k)}\, ds = -\frac{\pi i}{s_k}\left[\frac{1}{s_k} + i(\phi+d)\right] + 2\pi i \frac{e^{i(\phi+d)s_k}}{s_k^2}, \qquad \begin{matrix} b_k > 0 \\ d + \phi > 0 \end{matrix}$$

Integrating in the lower half plane for $\phi < 0$, Equation (5-30) can now be written in the form

$$\begin{aligned} {}_u F_k(\phi) = i \frac{c_6 \alpha_k}{s_k} \Bigg\{ & \left[-\frac{1}{2}\left(\frac{1}{s_k} + i\phi\right) + \frac{e^{i\phi s_k}}{s_k} \right] H(\phi) \\ & - \left[-\frac{1}{2}\left(\frac{1}{s_k} + i(\phi+d)\right) + \frac{e^{i(\phi+d)s_k}}{s_k} \right] H(\phi+d) \\ & + \frac{1}{2}\left(\frac{1 + i\phi s_k}{s_k}\right) H(-\phi) \\ & - \frac{1}{2}\left(\frac{1 + i(\phi+d) s_k}{s_k}\right) H(-\phi-d) \Bigg\}, \qquad b_k > 0 \end{aligned} \tag{5-39}$$

Performing the integrations for $b_k < 0$, the final result can be written as

$$\begin{aligned} {}_u F_k(\phi) = \frac{\mathrm{sgn}(b_k)\, i\, c_6 \alpha_k}{s_k^2} \Bigg\{ & \left[-\frac{1}{2}(1 + i\phi s_k) + e^{i\phi s_k} \right] \\ & \times H[\mathrm{sgn}(b_k)\phi] + \frac{1}{2}(1 + i\phi s_k)\, H[-\mathrm{sgn}(b_k)\phi] \\ & - \Bigg[\left\{ -\frac{1}{2}[1 + i(\phi+d)s_k] + e^{i(\phi+d)s_k} \right\} H[\mathrm{sgn}(b_k)(\phi+d)] \\ & + \frac{1}{2}[1 + i(\phi+d)s_k]\, H[-\mathrm{sgn}(b_k)(\phi+d)] \Bigg] \Bigg\} \end{aligned} \tag{5-40}$$

The solutions given by Equations (5-7), (5-19), and (5-31) with the corresponding F_k functions (5-13), (5-27), and (5-40) are substituted into the governing equations of motion in Appendix G to show that the solutions satisfy the differential equations.

Summary of Deflection Expressions

The following expressions summarize the solution for the deflections.

$$\frac{\psi(\phi)}{q_o} = \sum_{k=1}^{4} F_k(\phi) \tag{5-41a}$$

$$\frac{W(\phi)}{q_o} = \sum_{k=1}^{4} {}_wF_k(\phi) \tag{5-41b}$$

$$\frac{U(\phi)}{q_o} = -\frac{c_5}{c_9}\frac{\psi(\phi)}{q_o} + \sum_{k=1}^{4} {}_uF_k(\phi) \tag{5-41c}$$

where

$$F_k(\phi) = -\operatorname{sgn}(b_k)\, i\, c_9\, \alpha_k \left\{ e^{i s_k \phi} H[\operatorname{sgn}(b_k)\phi] - e^{i s_k(\phi+d)} H[\operatorname{sgn}(b_k)(\phi+d)] \right\} \tag{5-41d}$$

$$\begin{aligned} {}_wF_k(\phi) = \frac{\operatorname{sgn}(b_k)\,\beta_k}{s_k} \Bigg[& \left(-\frac{1}{2} + e^{i s_k \phi} \right) H[\operatorname{sgn}(b_k)\phi] + \frac{1}{2} H[-\operatorname{sgn}(b_k)\phi] \\ & - \left\{ \left[-\frac{1}{2} + e^{i s_k(\phi+d)} \right] H[\operatorname{sgn}(b_k)(\phi+d)] \right. \\ & \left. + \frac{1}{2} H[-\operatorname{sgn}(b_k)(\phi+d)] \right\} \Bigg] \end{aligned} \tag{5-41e}$$

$$
{}_{u}F_{k}(\phi) = \frac{\mathrm{sgn}(b_k)\, i\, c_6\, \alpha_k}{s_k^2} \left\{ \left[-\frac{1}{2}(1 + i s_k \phi) + e^{i\phi s_k} \right] H[\mathrm{sgn}(b_k)\phi] \right.
$$

$$
+ \frac{1}{2}(1 + i s_k \phi)\, H[-\mathrm{sgn}(b_k)\phi]
$$

$$
- \left[\left\{ -\frac{1}{2}\,[1 + i s_k(\phi+d)] + e^{i s_k(\phi+d)} \right\} H[\mathrm{sgn}(b_k)(\phi+d)] \right.
$$

$$
\left. \left. + \frac{1}{2}\,[1 + i s_k(\phi+d)]\, H[-\mathrm{sgn}(b_k)(\phi+d)] \right] \right\} \qquad (5\text{-}41f)
$$

$$
\mathrm{sgn}(b_k) = \begin{cases} 1, & b_k > 0 \\ -1, & b_k < 0 \end{cases}
$$

$$
H(y) = \begin{cases} 0, & y < 0 \\ 1, & y > 1 \end{cases}
$$

$$
\alpha_k = \frac{1}{\prod_{m=1}^{4} (s_k - s_m)}, \qquad \beta_k = \frac{c_7 s_k^2 + c_8}{\prod_{m=1}^{4} (s_k - s_m)}, \qquad k \neq m
$$

$s_k = a_k + i\, b_k$ $(k = 1, \ldots, 4)$ are the roots of the characteristic equation

$$
\overline{D}(s) = c_4 s^4 + i c_3 s^3 + c_2 s^2 + i c_1 s + c_0 = 0
$$

and the coefficients are defined as

$$c = f_1 + e_4\lambda^2$$

$$c_0 = e_3(f_8 e_0 - e_1^2)$$

$$c_1 = -\epsilon\lambda e_3 f_8$$

$$c_2 = f_7(e_0 c - e_1 e_2) + e_3 f_8(f_2 - r\lambda^2)$$

$$c_3 = -\epsilon\lambda f_7 c$$

$$c_4 = (f_3 - r\lambda^2) f_7 c$$

$$c'_5 = f_7(e_3 + e_1)$$

$$c'_6 = e_1 e_3$$

$$c'_7 = f_7(f_1 + e_4\lambda^2)$$

$$c'_8 = e_3 f_8$$

$$c'_9 = e_1 f_7 + c'_8$$

$$e_0 = E_0 + Pr_0 \qquad f_0 = 1 + F$$

$$e_1 = E_1 - P \qquad f_1 = 1 + F - D_1$$

$$e_2 = E_1 - P + 2(G + Pr_0) \qquad f_2 = F - Pr_0$$

$$e_3 = G + Pr_0 \qquad f_3 = G + F$$

$$e_4 = I_0 - r_1 \qquad f_4 = D_1 r_1 + I_0 f_0$$

$$e_5 = e_0 f_1 - e_1 e_2 \qquad f_5 = r_1 f_2 + r f_0$$

$$e_6 = e_0 f_0 - e_1^2 \qquad f_6 = e_4 D_1 - I_0 f_1$$

$$f_7 = D_1 - I_0\lambda^2$$

$$f_8 = f_0 - r_1\lambda^2$$

(5-42)

The derivatives of the deflections are

$$\frac{\psi'(\phi)}{q_o} = \sum_{k=1}^{4} F'_k(\phi)$$

$$\frac{W'(\phi)}{q_o} = \sum_{k=1}^{4} {}_wF'_k(\phi)$$

$$\frac{U'(\phi)}{q_o} = -\frac{c_5}{c_9}\frac{\psi'(\phi)}{q_o} + \sum_{k=1}^{4} {}_uF'_k(\phi) \qquad (5\text{-}43)$$

where

$$F'_k(\phi) = i\, s_k\, F_k(\phi)$$

$${}_wF'_k(\phi) = -\frac{\beta_k}{c_9\,\alpha_k} F_k(\phi) = -\frac{c_7 s_k^2 + c_8}{c_9} F_k(\phi)$$

$${}_uF'_k(\phi) = -\frac{c_6\,\alpha_k}{\beta_k} {}_wF_k(\phi) = -\frac{c_6}{c_7 s_k^2 + c_8} {}_wF_k(\phi) \qquad (5\text{-}44)$$

$$\phi,\ \phi+d \neq 0$$

Solution for No External Damping

For the case of no external damping, the solutions as given in Equation (5-41) are not directly applicable. It will be noticed that the forms of the solutions are dependent upon the signs of the imaginary parts of the complex roots. Figures 4.2 through 4.8 show that there are regions in which there are only real roots of the Characteristic Equation with no damping, thus causing a problem of non-uniqueness of the solutions.

Following the method of Achenbach and Sun (13) the undamped solution will be obtained uniquely by assuming the undamped solution is the limit of the damped solution as the damping approaches zero. In this manner the sgn functions in the

F_k functions for Equation (5-41) can be determined. Figure 5.4 provides an example of the behavior of a set of roots as the damping, ϵ, approaches zero. This figure shows the type of the four roots (s_{ij} = root i with damping ϵ_j) for heavy damping to be two complex and two imaginary, root 1 being very near the origin. As the damping is decreased, the imaginary roots approach one another and finally meet and separate which gives four complex roots. Meanwhile the other complex roots are also approaching the real axis. This establishes the correct sign for the imaginary part of each root in the limit as $\epsilon \to 0$ and the roots all approach the real axis.

Form of the Radial Deflection in Region IV

The roots are all real, having the form $\pm a_1$, $\pm a_2$. From Equation (5-41b), the radial deflection expression (when the proper signs are established) in Region IV becomes

$$\frac{W}{q_o} = \left[\frac{\beta_1}{a_1} - \frac{\beta_2}{a_1} + \frac{\beta_3}{a_2} - \frac{\beta_4}{a_2}\right][H(\phi+d) - H(\phi)]$$

$$- \frac{\beta_1}{a_1}\left[e^{i a_1 \phi} H(-\phi) - e^{i a_1(\phi+d)} H(-\phi-d)\right]$$

$$+ \frac{\beta_2}{a_1}\left[e^{-i a_1 \phi} H(-\phi) - e^{-i a_1(\phi+d)} H(-\phi-d)\right]$$

$$+ \frac{\beta_3}{a_2}\left[e^{i a_2 \phi} H(\phi) - e^{i a_2(\phi+d)} H(\phi+d)\right]$$

$$- \frac{\beta_4}{a_2}\left[e^{-i a_2 \phi} H(\phi) - e^{-i a_2(\phi+d)} H(\phi+d)\right] \qquad (5\text{-}45)$$

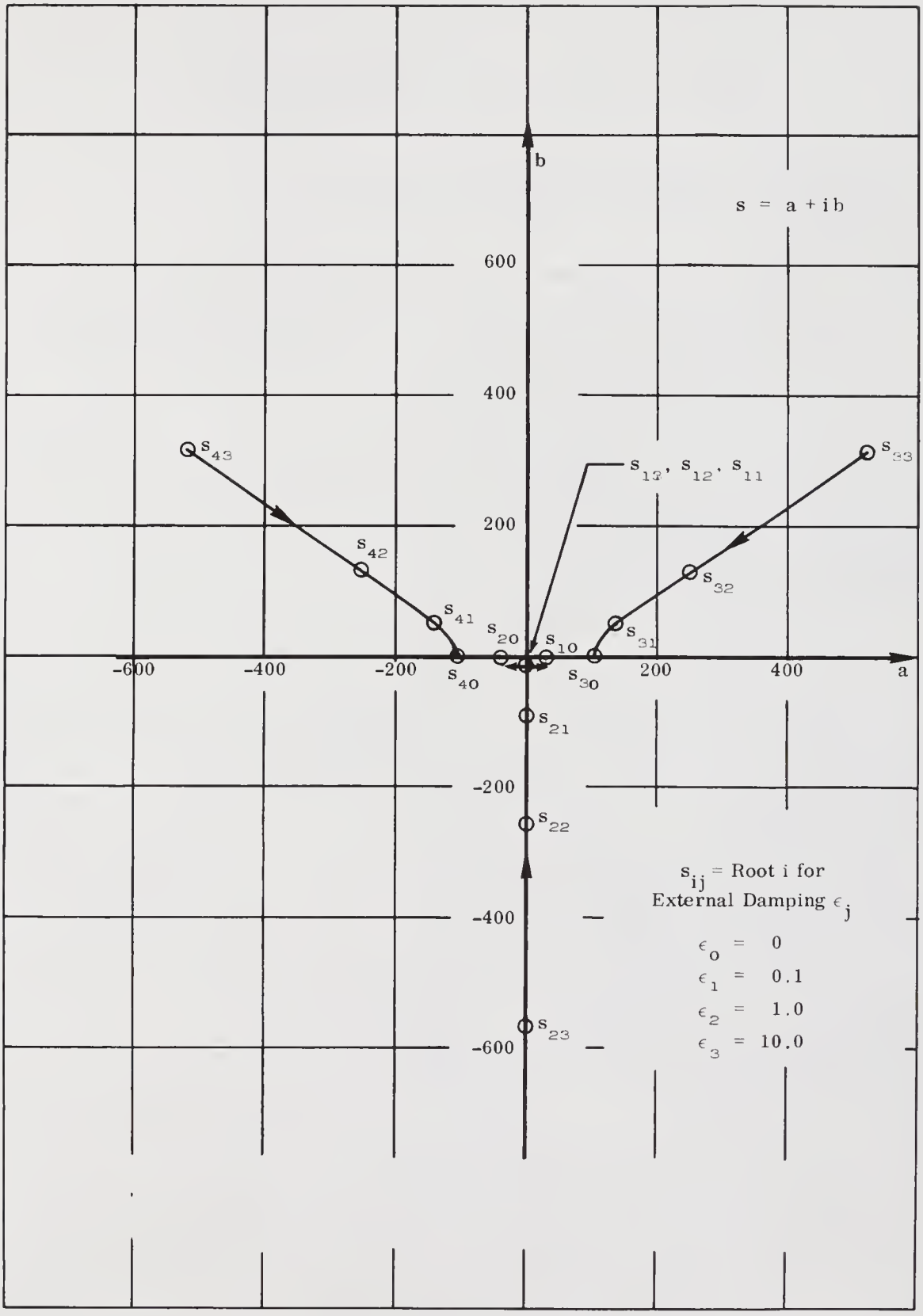

Figure 5.4. Loci of the Roots of the Characteristic Equation as the Damping Approaches Zero

Expanding the β_i coefficients gives

$$\beta_1 = -\beta_2 = \frac{c_7 a_1^2 + c_8}{2a_1(a_1^2 - a_2^2)}$$

$$\beta_3 = -\beta_4 = -\frac{c_7 a_2^2 + c_8}{2a_2(a_1^2 - a_2^2)} \qquad (5\text{-}46)$$

Substituting expressions (5-46) into (5-45) gives

$$\frac{W}{q_o} = -\frac{c_7 a_1^2 + c_8}{2a_1^2(a_1^2 - a_2^2)} \left\{ \left(e^{i a_1 \phi} + e^{-i a_1 \phi} \right) H(-\phi) - \left[e^{i a_1 (\phi+d)} + e^{-i a_1 (\phi+d)} \right] H(-\phi-d) \right\}$$

$$- \frac{c_7 a_2^2 + c_8}{2a_2^2(a_1^2 - a_2^2)} \left\{ \left(e^{i a_2 \phi} + e^{-i a_2 \phi} \right) H(\phi) - \left[e^{i a_2 (\phi+d)} + e^{-i a_2 (\phi+d)} \right] H(\phi+d) \right\}$$

$$- \frac{c_8}{a_1^2 a_2^2} [H(\phi+d) - H(\phi)]$$

or

$$\frac{W}{q_o} = -\frac{c_8}{a_1^2 a_2^2} [H(\phi+d) - H(\phi)] - \frac{c_7 a_1^2 + c_8}{a_1^2(a_1^2 - a_2^2)} \times \left[\cos(a_1 \phi)\, H(-\phi) - \cos[a_1(\phi+d)]\, H(-\phi-d) \right]$$

$$- \frac{c_7 a_2^2 + c_8}{a_2^2(a_1^2 - a_2^2)} \left[\cos(a_2 \phi)\, H(\phi) - \cos[a_2(\phi+d)]\, H(\phi+d) \right] \qquad (5\text{-}47)$$

Therefore, for the three distinct regions of the cylinder, the solutions are:

Solution behind the load ($\phi < -d$)

$$\frac{W}{q_o} = - \frac{c_7 a_1^2 + c_8}{a_1^2(a_1^2 - a_2^2)} \left\{ \cos(a_1 \phi) - \cos[a_1(\phi+d)] \right\} \tag{5-48}$$

Solution under load ($-d < \phi < 0$)

$$\frac{W}{q_o} = - \frac{c_8}{a_1^2 a_2^2} - \frac{c_7 a_1^2 + c_8}{a_1^2(a_1^2 - a_2^2)} \cos(a_1 \phi) + \frac{c_7 a_2^2 + c_8}{a_2^2(a_1^2 - a_2^2)} \cos[a_2(\phi+d)] \tag{5-49}$$

Solution ahead of load ($\phi > 0$)

$$\frac{W}{q_o} = - \frac{c_7 a_2^2 + c_8}{a_2^2(a_1^2 - a_2^2)} \left\{ \cos(a_2 \phi) - \cos[a_2(\phi+d)] \right\} \tag{5-50}$$

Form of the Radial Deflection in Region VII

As in Region IV, the roots are $\pm a_1$, $\pm a_2$. However, there can be no deflection ahead of the load in this region because the load speed is greater than any of the wave speeds in the material. This zero displacement comes about mathematically because the roots all approach the real axis from the negative imaginary direction. The solution for this region has the form

$$\begin{aligned} \frac{W}{q_o} = & - \frac{c_8}{a_1^2 a_2^2} [H(-\phi) - H(-\phi-d)] - \frac{c_7 a_1^2 + c_8}{a_1^2(a_1^2 - a_2^2)} \\ & \times \left\{ \cos(a_1 \phi) H(-\phi) - \cos[a_1(\phi+d)] H(-\phi-d) \right\} \\ & + \frac{c_7 a_2^2 + c_8}{a_2^2(a_1^2 - a_2^2)} \left\{ \cos(a_2 \phi) H(-\phi) - \cos[a_2(\phi+d)] H(=\phi-d) \right\} \end{aligned} \tag{5-51}$$

Form of the Radial Deflection in Region V

The roots in this region have the form $\pm a$, $\pm i\,b$. The radial deflection in this region is given by the expression

$$\frac{W}{q_o} = \frac{c_8}{a^2 b^2}\,[H(-\phi) - H(-\phi-d)]$$

$$- \frac{c_7 a^2 + c_8}{a^2(a^2+b^2)}\left[\cos(a\phi)H(-\phi) - \cos[a(\phi+d)]\,H(-\phi-d)\right]$$

$$+ \frac{c_7 b^2 + c_8}{2b^2(a^2+b^2)}\left[e^{-b\phi}\,H(\phi) - e^{b\phi}\,H(-\phi) - e^{-b(\phi+d)}\,H(\phi+d)\right.$$

$$\left. + e^{b(\phi+d)}\,H(-\phi-d)\right] \qquad (5\text{-}52)$$

Form of the Radial Deflection in Region VI

In this region the roots are all imaginary, of the form $\pm i\,b_1$, $\pm i\,b_2$. This gives an exponentially decaying solution as in Regions I and III. The radial deflection expression is given below.

$$\frac{W}{q_o} = -\frac{c_8}{b_1^2 b_2^2}\,[H(\phi+d) - H(\phi)]$$

$$+ \frac{c_8 - c_7 b_1^2}{2b_1^2(b_1^2 - b_2^2)}\left[e^{-b_1\phi}\,H(\phi) - e^{b_1\phi}\,H(-\phi) - e^{-b_1(\phi+d)}\,H(\phi+d)\right.$$

$$\left. + e^{b_1(\phi+d)}\,H(-\phi-d)\right]$$

$$+ \frac{c_8 - c_7 b_2^2}{2b_2^2(b_1^2 - b_2^2)}\left[e^{b_2\phi}\,H(-\phi) - e^{-b_2\phi}\,H(\phi) - e^{b_2(\phi+d)}\,H(-\phi-d)\right.$$

$$\left. + e^{-b_2(\phi+d)}\,H(\phi+d)\right] \qquad (5\text{-}53)$$

Comparison of Solution with Other Results

As a comparison of the results of this analysis with another theory, the static problem of a distributed pressure load on an isotropic shell was considered as shown in Figure 5.5.

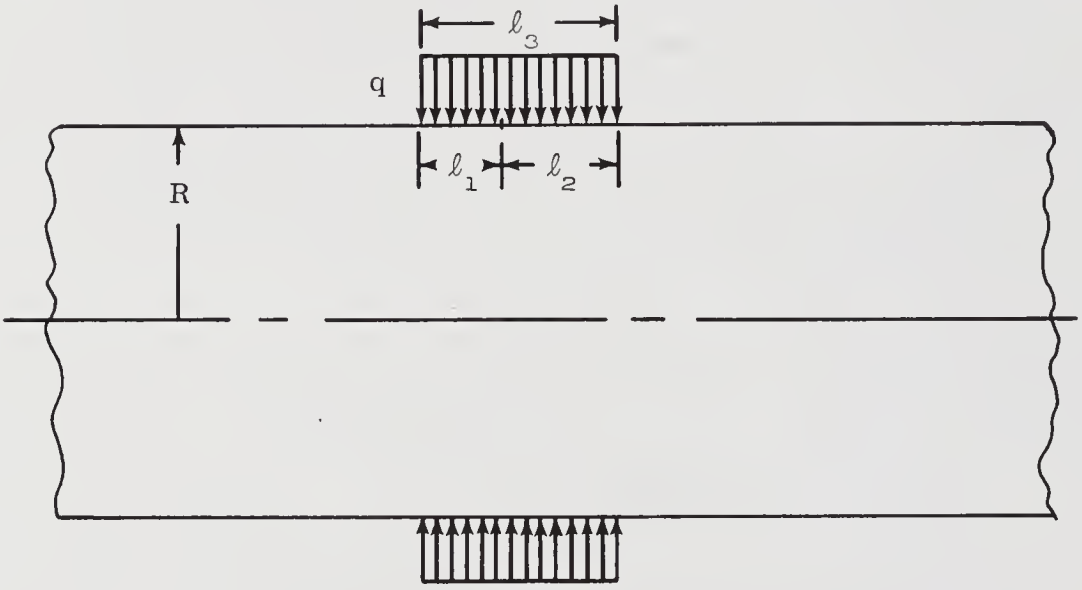

Figure 5.5 Static Load Problem

For the static problem shown above the roots of the characteristic equation, excluding prestress, are complex. The solution for the region under the load as given by the present theory can be reduced to

$$\frac{W}{q_o} = K_1\left(2 - e^{-a L_2}\cos a L_2 - e^{-a L_1}\cos a L_1\right) + K_2\left(e^{-a L_2}\sin a L_2 + e^{-a L_1}\sin a L_1\right) \qquad (5\text{-}54)$$

where

$$L_2 = \frac{\ell_2}{R}, \qquad L_1 = \frac{\ell_1}{R}$$

This problem is solved by Timoshenko (14) and the deflection given by his theory, when put in a compatible form, becomes

$$\frac{W}{q_o} = K_1' \left(2 - e^{-\beta \ell_2} \cos \beta \ell_2 - e^{-\beta \ell_1} \cos \beta \ell_1 \right) \qquad (5\text{-}55)$$

The second term appearing in Equation (5-54) is missing from Equation (5-55). This additional term arises because of the inclusion of shear deflection which was not present in the Timoshenko theory. A comparison of the results of these deflection expressions is made in Figure 5.7.

Numerical Results

A computer program was developed for the calculation of the displacements and stresses determined in this research. The general expressions given by Equations (5-41) were programmed for the displacement solutions and the stress calculations are discussed in Chapter VI. A flow diagram of the computer program is shown in Figure 5.6. The details of the program can be found in Appendix H. It is written in Fortran for time share computer application.

Comparison of Results with Other Solutions for a Static Load

The radial deflection for a static distributed load on a cylindrical shell is given in Reference (14). As a check on the solution this static problem was solved using the present results and the comparison is shown in Figure 5.7. The results agree very well. The effect of variation in the thickness-to-radius is also illustrated in Figure 5.7. The rotation and axial deflection are shown for this static problem in Figure 5.8. In addition to showing the form of the displacements for the static load, Figures 5.7 and 5.8 serve as a basis against which the dynamic displacements can be compared. The deflections are symmetric about $\phi = -0.5$ for the static load.

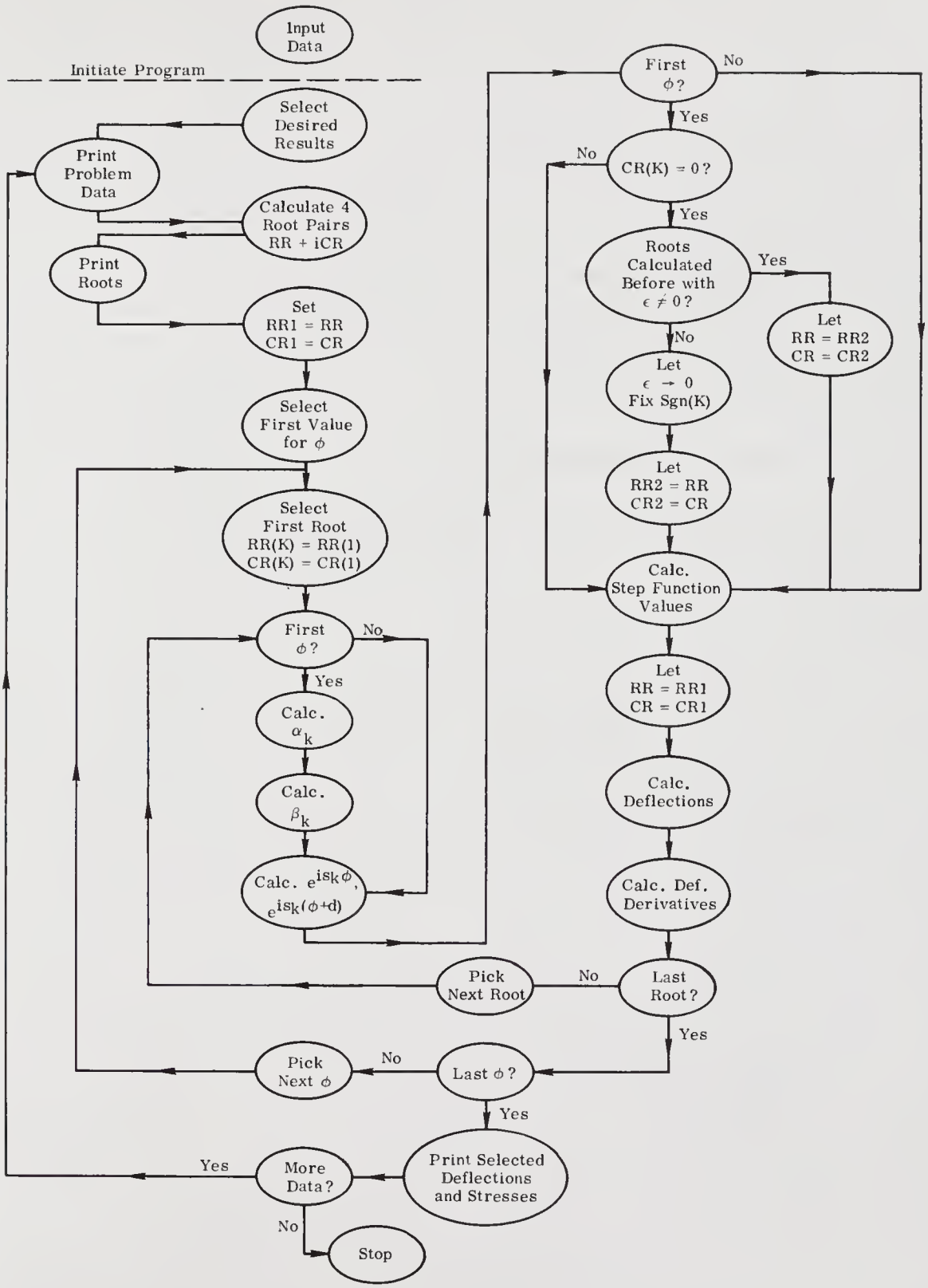

Figure 5.6. Flow Diagram for Computer Program for Deflection and Stress Calculations

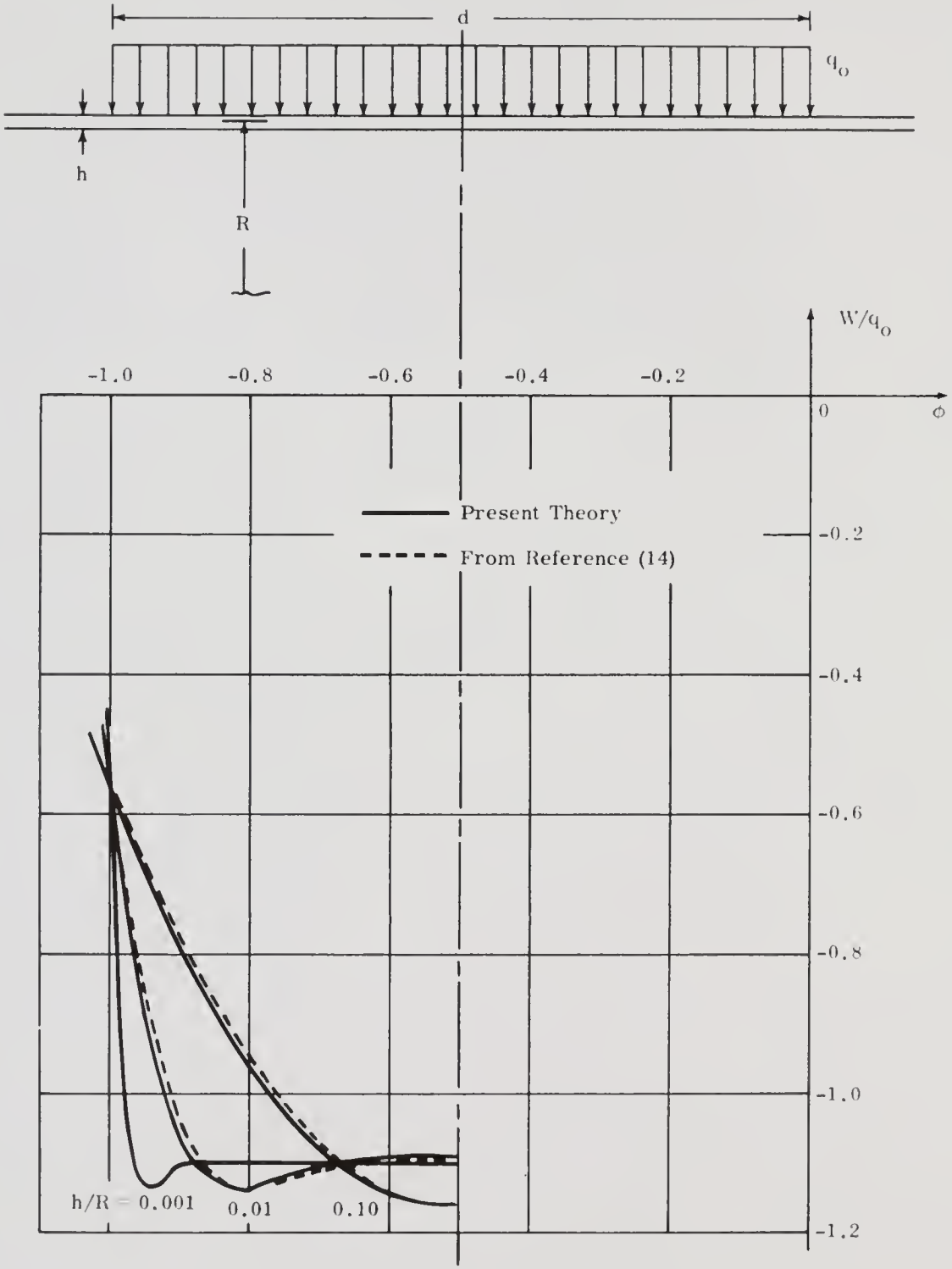

Figure 5.7. Radial Deflection for Static Load on an Isotropic Shell ($\mu = 0.3$)

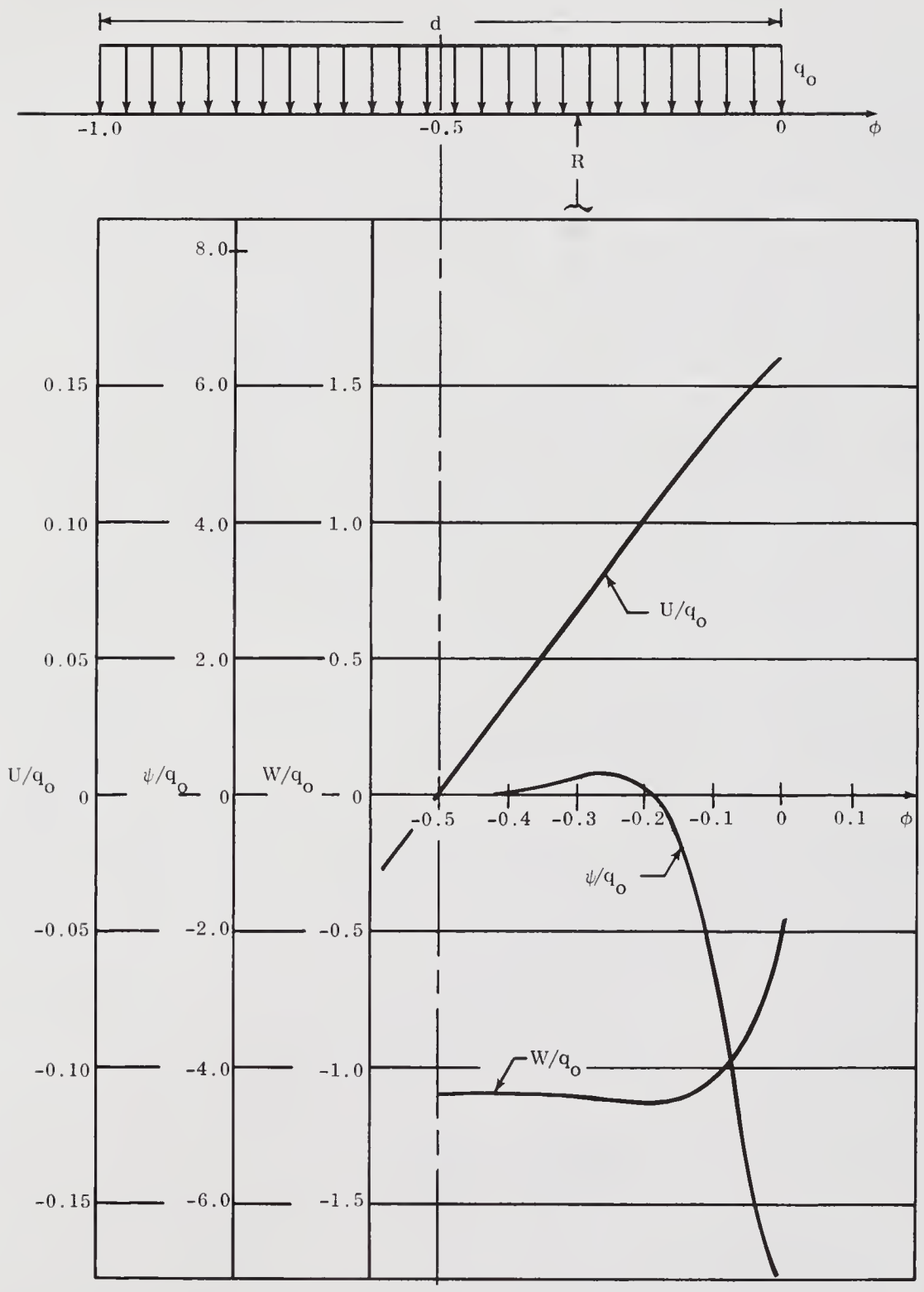

Figure 5.8. Displacements for a Static Load on an Isotropic Shell ($\mu = 0.3$, $h/R = 0.01$)

Summary of Deflection Response for Shells under Various Load Velocities

A summary of some of the types of deflection patterns assumed by a shell for increasing load speed is shown in Figure 5.9. For the particular properties used for this example, the various regions (root types) associated with each waveform can be found by inspection of Figures 4.2 through 4.8. For example, for no damping, positive prestress corresponding to internal pressure, $h/R = 0.001$ and the material properties given in Figure 5.9 (properties are those corresponding to an isotropic shell as shown in Appendix I), Figure 4.2 can be used to associate load speed with root type.

Following the vertical line of $h/R = 0.001$, it is evident that $\lambda^2 = 1$ lies in Region I where the roots are all imaginary. This gives a critically damped exponentially decaying solution as shown by Equation (5-53) and is shown in Figure 5.9(a). As the load speed increases Region II is entered where the roots are complex. This is the form of the static load problem roots, and if no prestress existed Region II would extend from zero load speed up to the first critical, which is at λ_2. The solution for $\lambda^2 = 2$ is shown in Figure 5.9(b), and is exponentially decaying.

The response becomes sinusoidal after crossing $\lambda = \lambda_2$. At a load speed just greater than λ_2 the deflection response has a very short period. A small amplitude wave train precedes the load and a large amplitude wave follows it. As the load speed increases the sine wave period increases as shown in Figure 5.9(d) for $\lambda^2 = 30$. These sinusoidal deflection patterns are in Region IV where the roots of the Characteristic Equation are all real. The mathematical expression for W/q_o is given by Equation (5-47). Crossing λ_3 into Region V, the roots are real and imaginary. Equation (5-52) gives the radial deflection, and Figure 5.9(e) shows the response to be a long period sine function for $\lambda^2 = 500$.

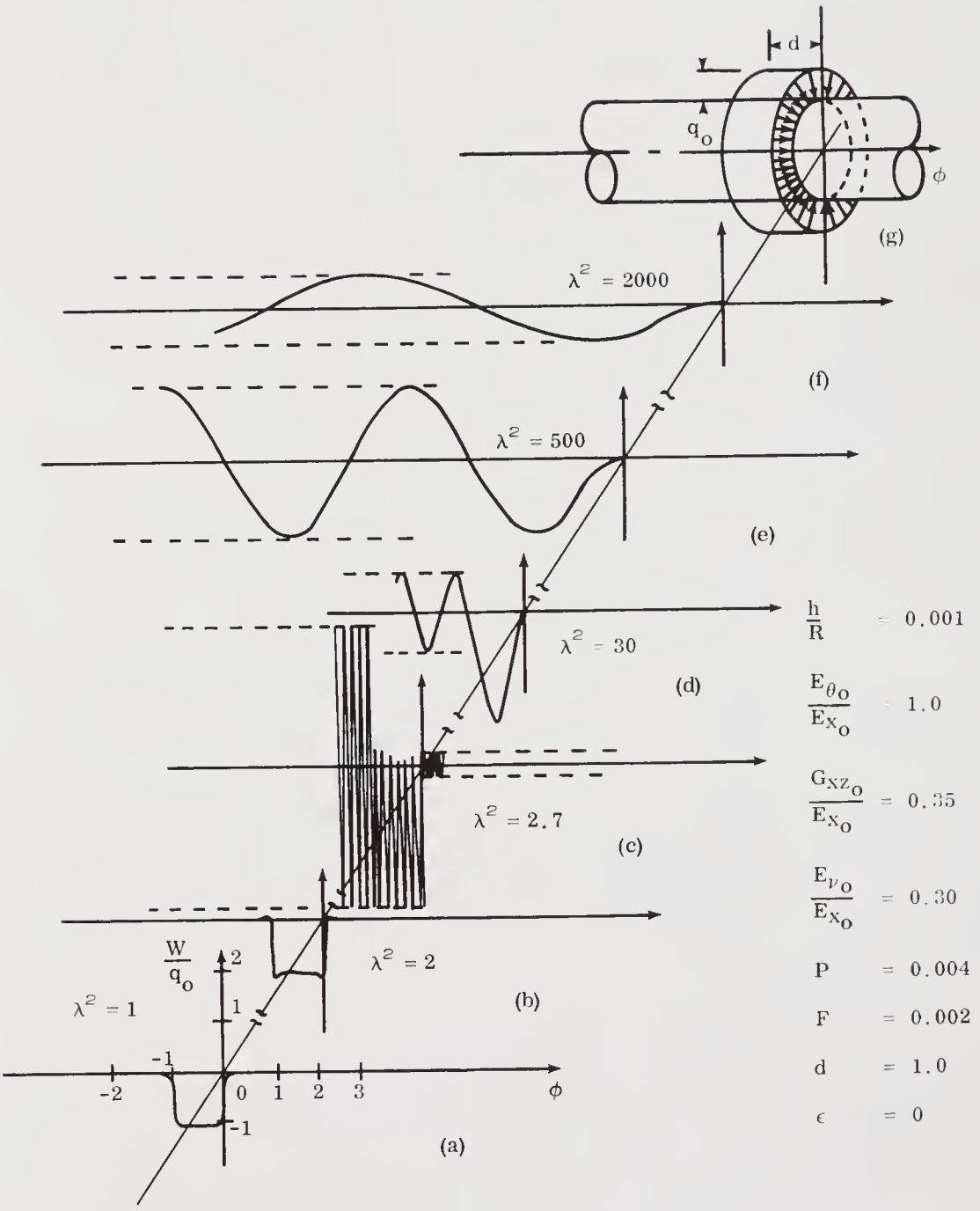

Figure 5.9. Radial Deflection Shape for Various Load Velocities

Jumping to Region VII brings a longer period sinusoidal oscillation as illustrated by Figure 5.9(f) and the response in this region, where the roots are again all real, was discussed previously. The radial deflection is given by Equation (5-51).

Because Region VI covers such a limited range in velocity the response was not included in the summary but is discussed later.

Region II Response

A study of the response of an isotropic shell at a load speed below the first critical was made to determine the effect of external damping. These results are shown in Figure 5.10 where the damping ranges from very light to very heavy. Of course, when damping is introduced the root form is no longer the same as that of Region II.

Region IV Response

The short period sinusoidal response of the radial deflection at $\lambda^2 = 2.7$ is shown in Figure 5.11. As the radial damping is increased this response is changed drastically as shown in Figure 5.12. The response for a damped system, which was in Region IV with $\epsilon = 0$, approaches closely that of the Region II behavior. Figure 5.13 shows the radial response at $\lambda^2 = 5$ and 10. The maximum amplitude remains constant as the period of the wave increases for greater load velocities.

Damping Effect on Regions V and VII Response

The effect of damping on the wave forms for $\lambda^2 = 500$ and 2000 is shown in Figures 5.14 and 5.15. The amplitudes of the sinusoidal deflection response are initially decreased, and, as the damping becomes greater, the response becomes critically damped and the deflection approaches zero with an increase in distance from the load.

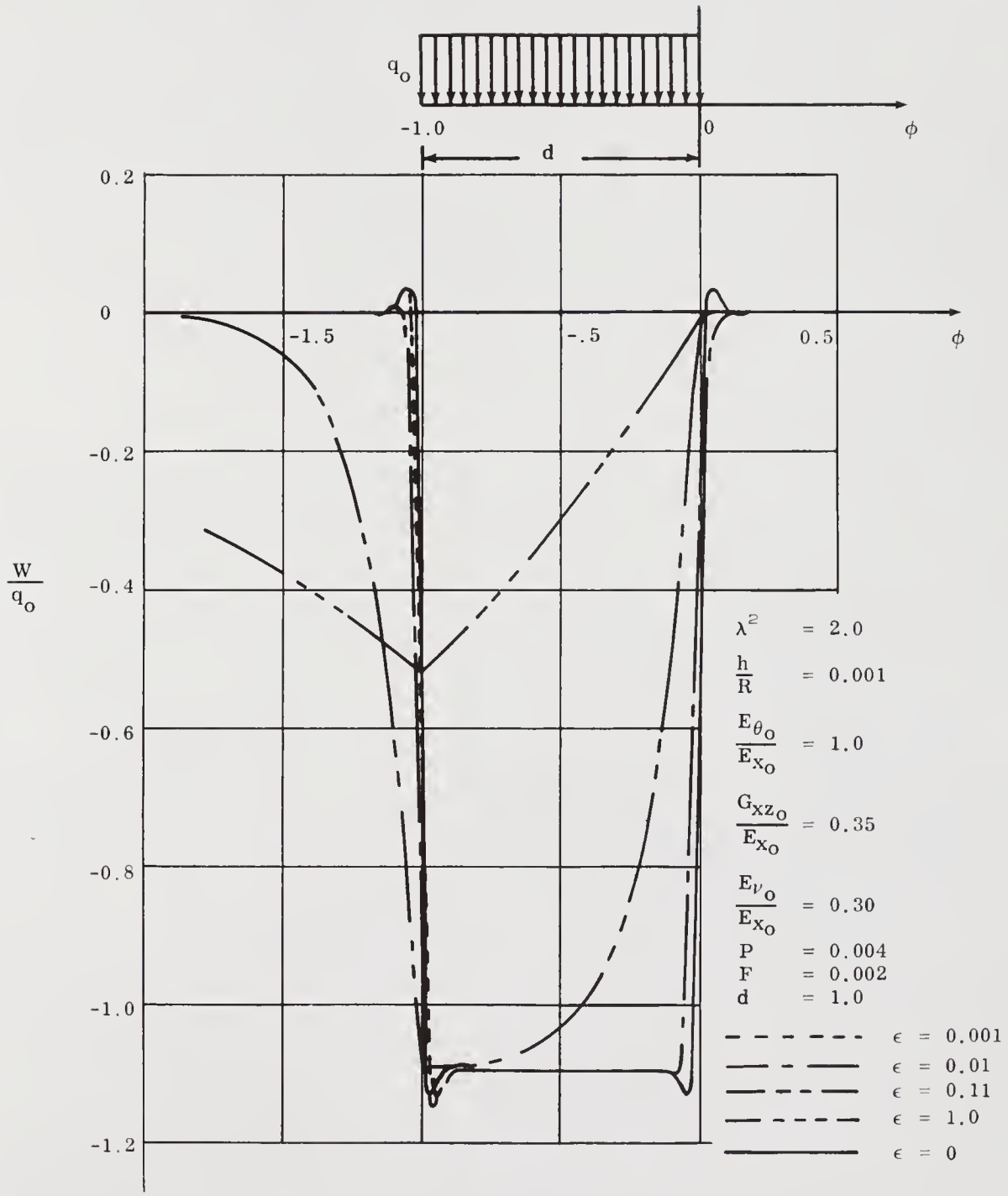

Figure 5.10. Radial Deflection Response for Variations in Radial Damping ($\lambda^2 = 2.0$)

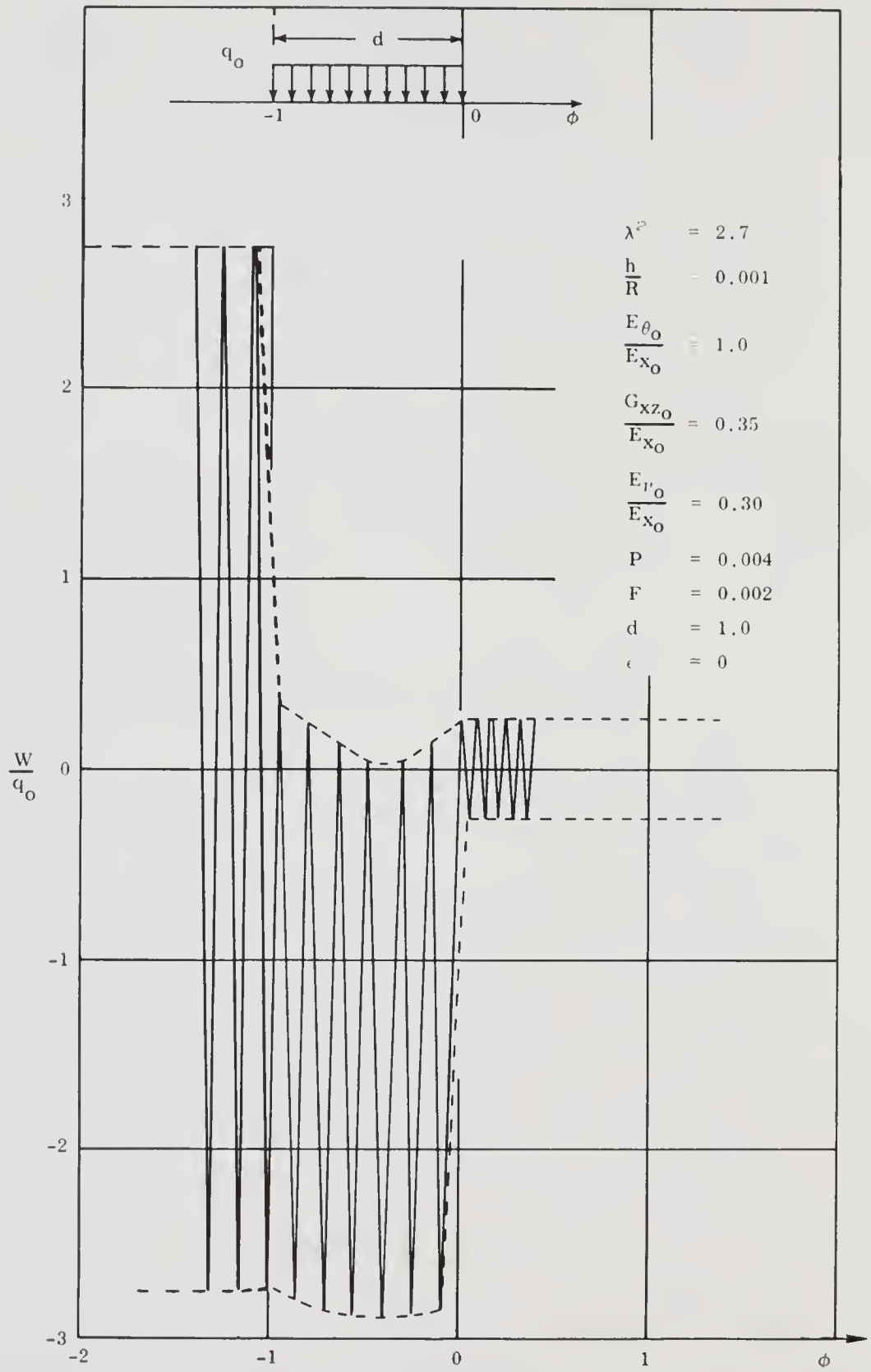

Figure 5.11. Radial Deflection Pattern Immediately Above the First Critical Load Speed

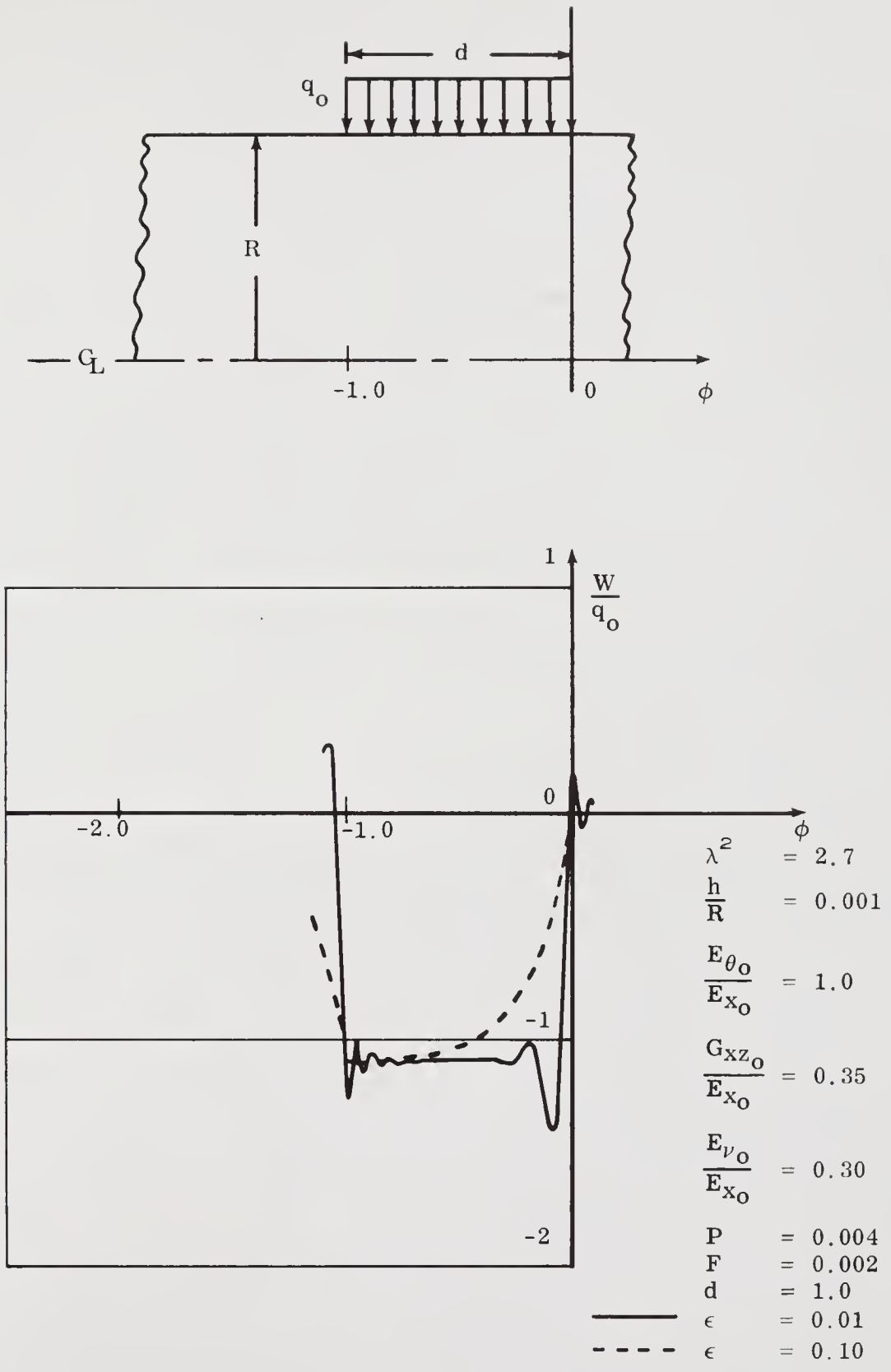

Figure 5.12. Change in the Radial Deflection Pattern with Increasing Damping ($\lambda^2 = 2.7$)

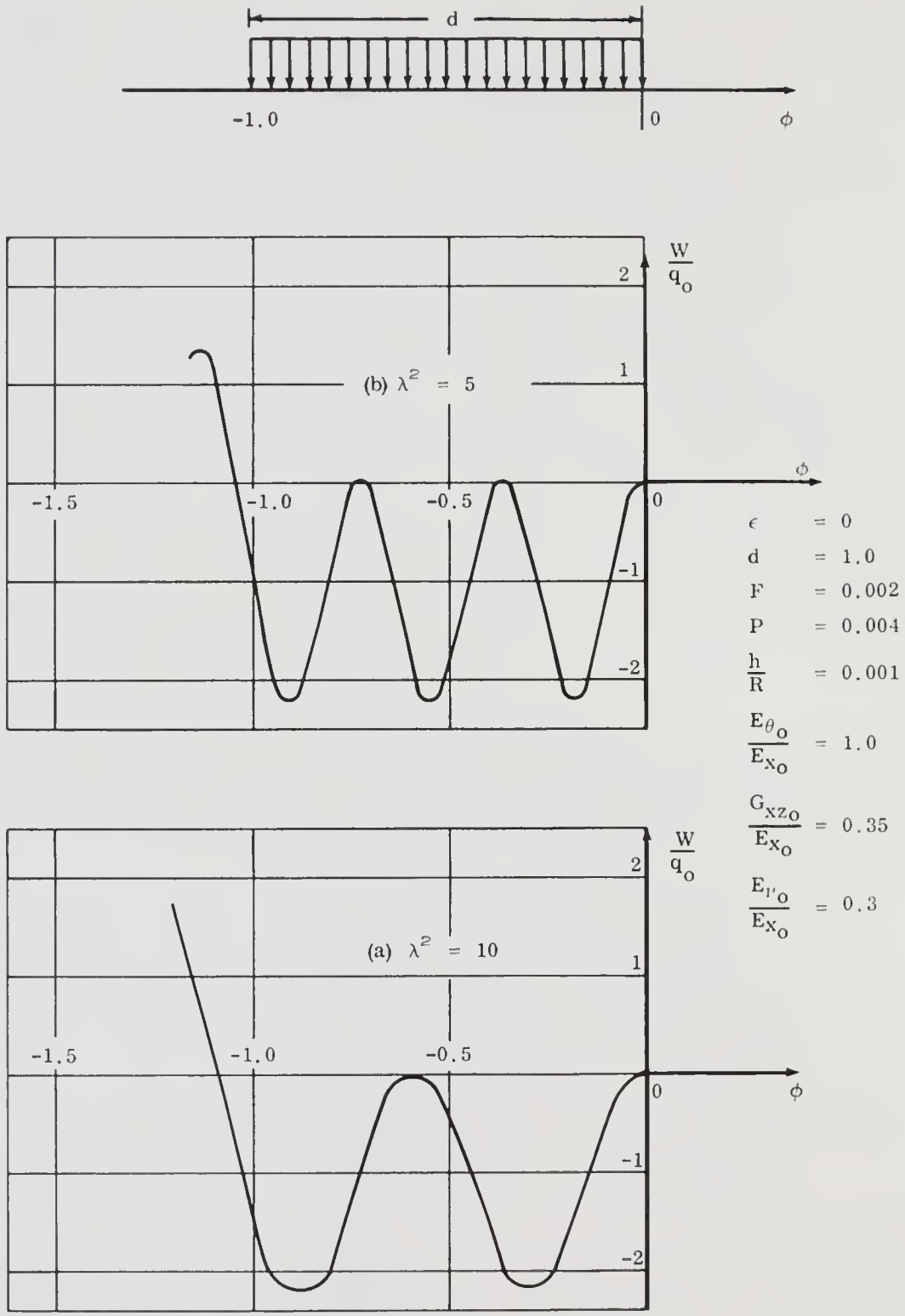

Figure 5.13. Deflection Wave Form at $\lambda^2 = 5$ and 10

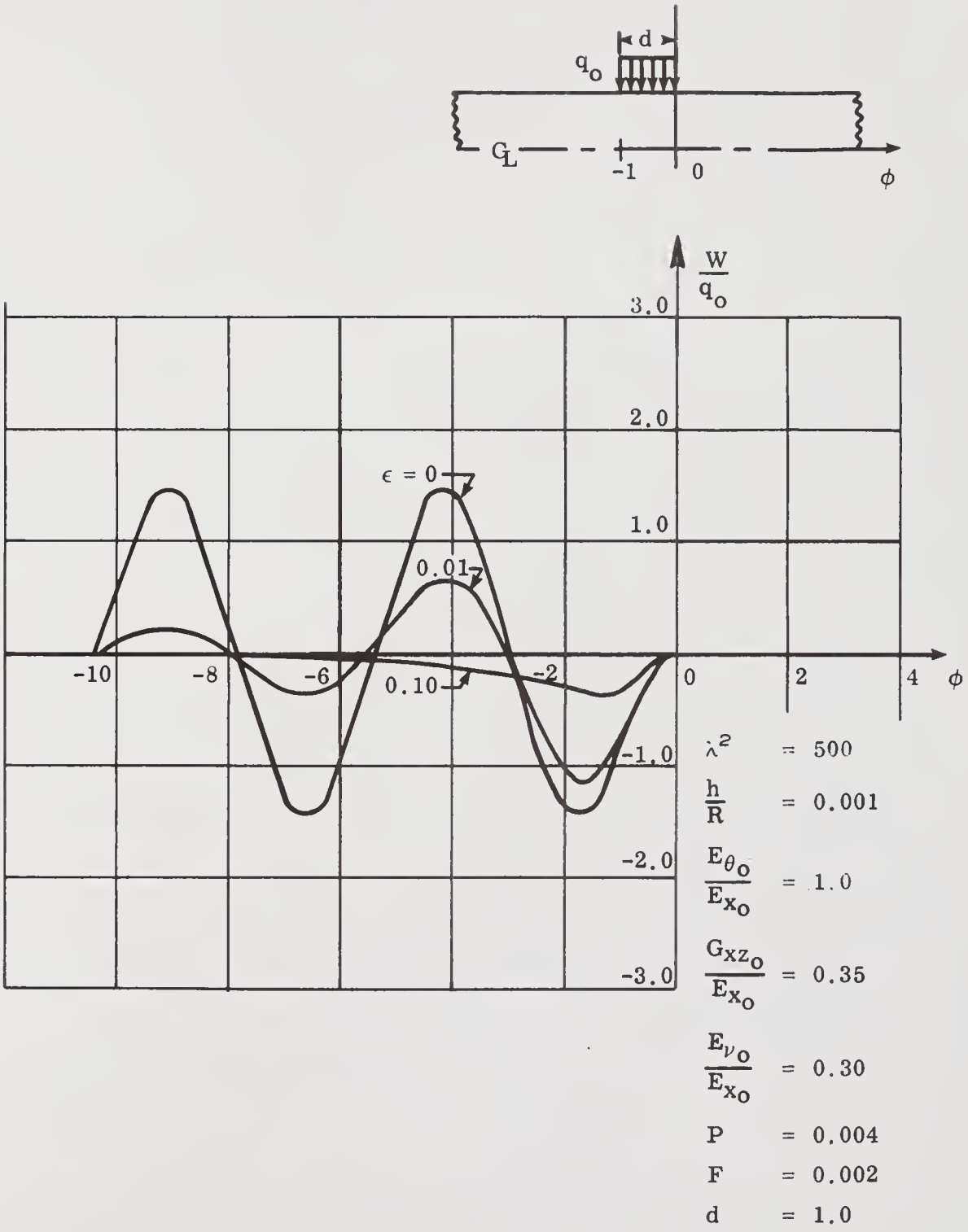

Figure 5.14. Effect of Damping for $\lambda^2 = 500$

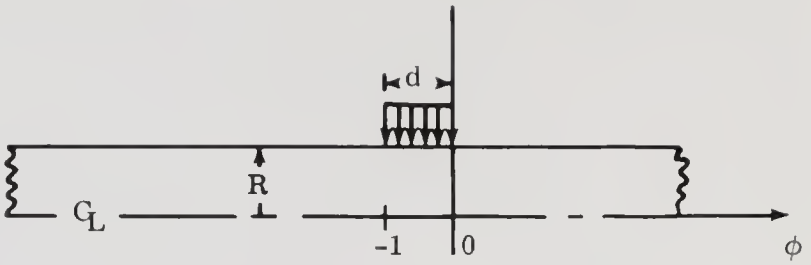

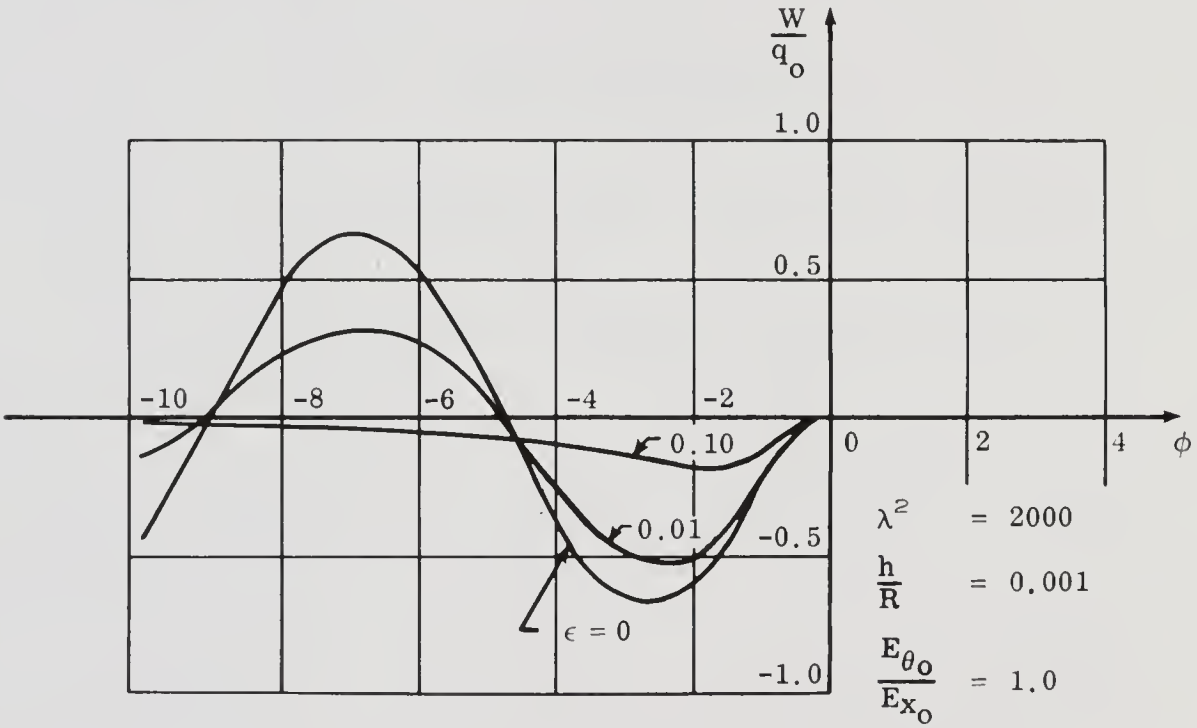

$\lambda^2 = 2000$

$\frac{h}{R} = 0.001$

$\frac{E_{\theta_o}}{E_{x_o}} = 1.0$

$\frac{G_{xz_o}}{E_{x_o}} = 0.35$

$\frac{E_{\nu_o}}{E_{x_o}} = 0.30$

$P = 0\ 004$

$F = 0.002$

$d = 1.0$

Figure 5.15. Effect of Damping for $\lambda^2 = 2000$

Region VI Response

This region has a deflection pattern which is almost totally axial. Three critical velocities have been crossed to get into this velocity range which correspond to the longitudinal, shear, and bar wave speeds. Therefore, there can be no bending effect transmitted. The behavior is like an axial compression on a membrane which expands radially, as shown by Figure 5.16. The effect of prestress is observable in this figure. The maximum deflection is increased by about 20 percent when going from external hydrostatic pressure to internal hydrostatic pressure.

This axial mode of deflection also appears in other velocity ranges. For instance, the broken lines in Figure 5.16 show the behavior at $\lambda^2 = 1001$. This is the range between $\lambda^2 = 1000$ and $\lambda^2 = 1002$ where the roots are real and imaginary. Another example is shown in Figure 5.22 where E_{θ_o}/E_{x_o} is less than 0.08 and this occurs in Region VIII as shown in Figure 4.4.

Deflection Behavior in the Vicinity of λ^2_{1CR}

The first (lowest) critical load speed occurs at $\lambda^2_{1CR} = \lambda^2_2 = 2.552$. Figure 5.17 illustrates the unbounded response of the deflection as that speed is approached. The effect of damping on the maximum deflection is also illustrated. There are four other critical velocities as discussed in Chapter IV.

Effect of Prestress on λ^2_{1CR}

The effect of the axial prestress on the location of the first critical load speed is shown in Figure 5.18. This effect is also observable in Figure 4.8, since the first critical load speed is at λ^2_2. The circumferential prestress does not have a significant effect on load speed, as shown in Figure 4.7.

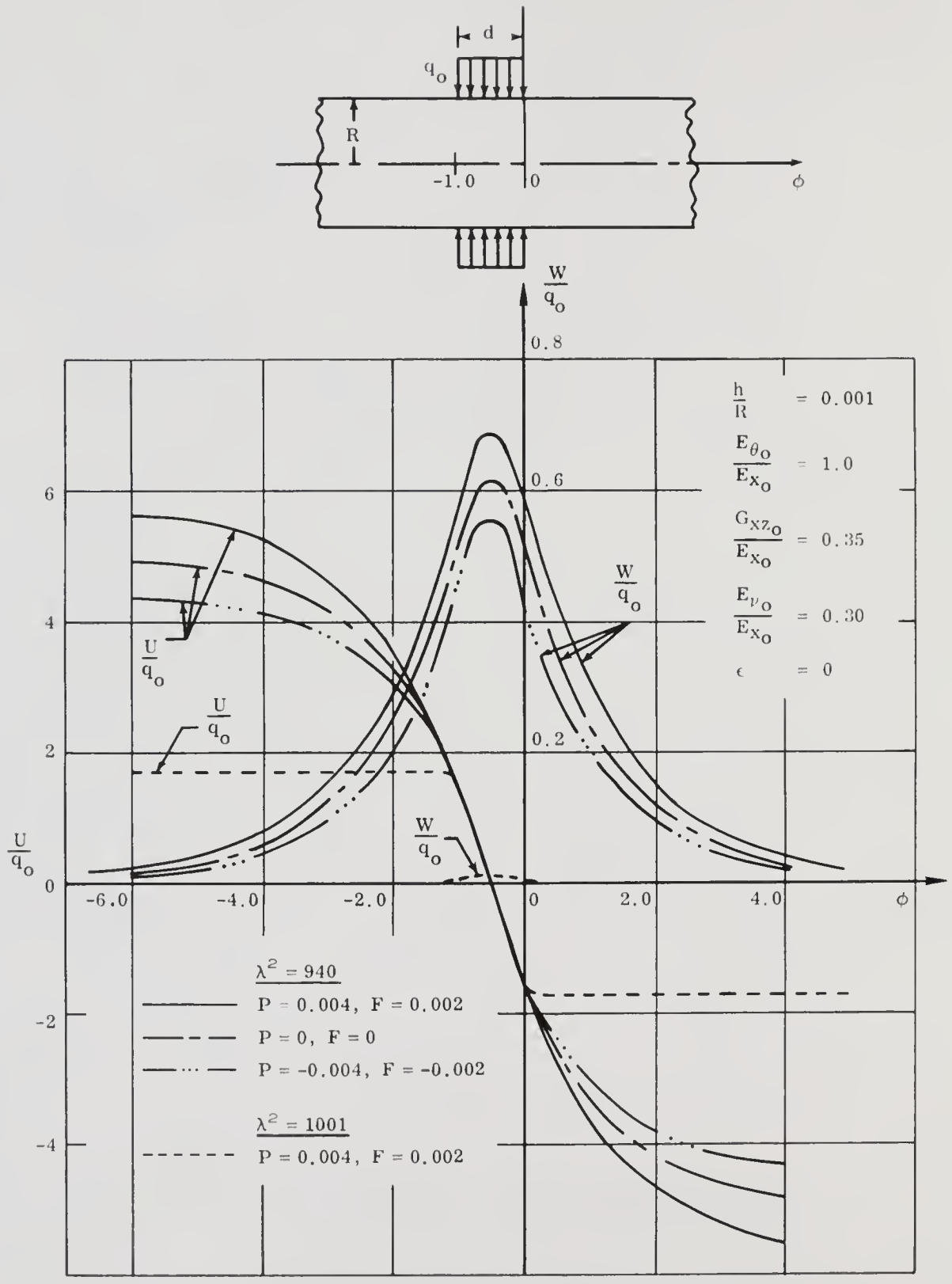

Figure 5.16. Deflection Response for Variations in Circumferential and Axial Prestress

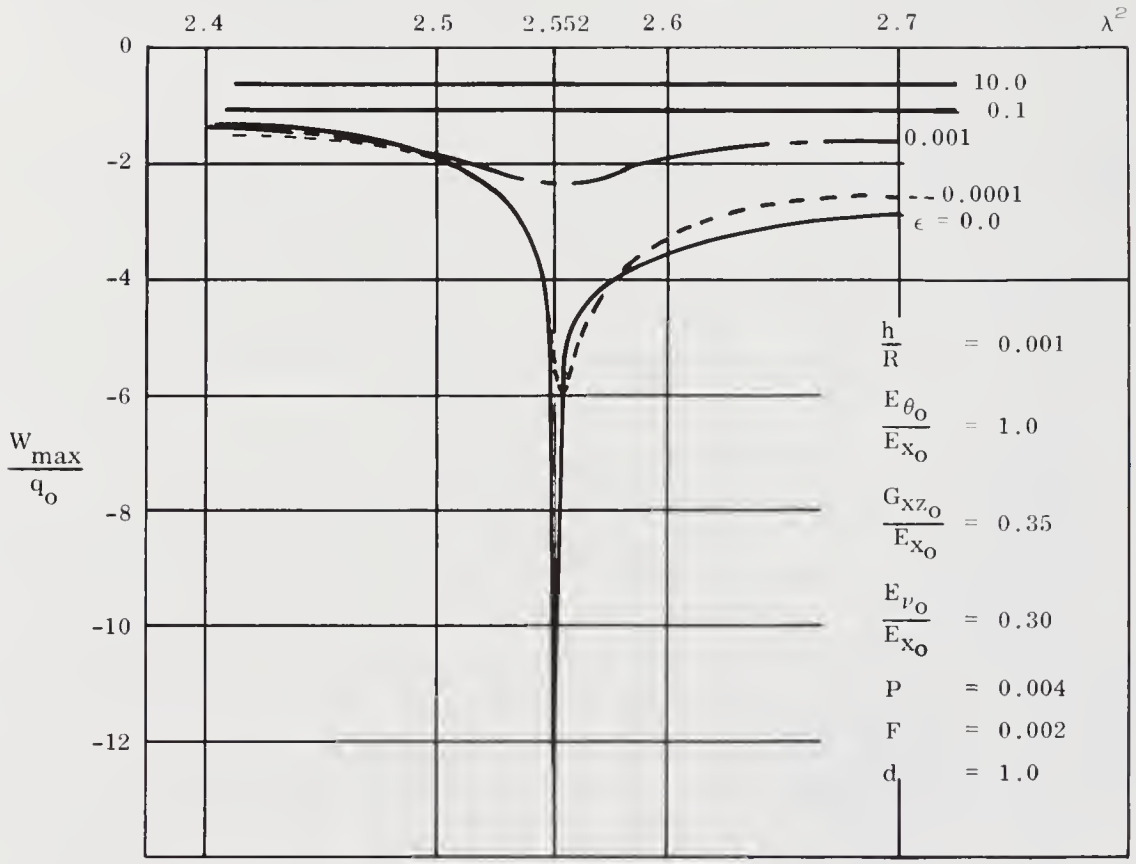

Figure 5.17. Maximum Radial Deflection in the Vicinity of the First Critical Load Speed

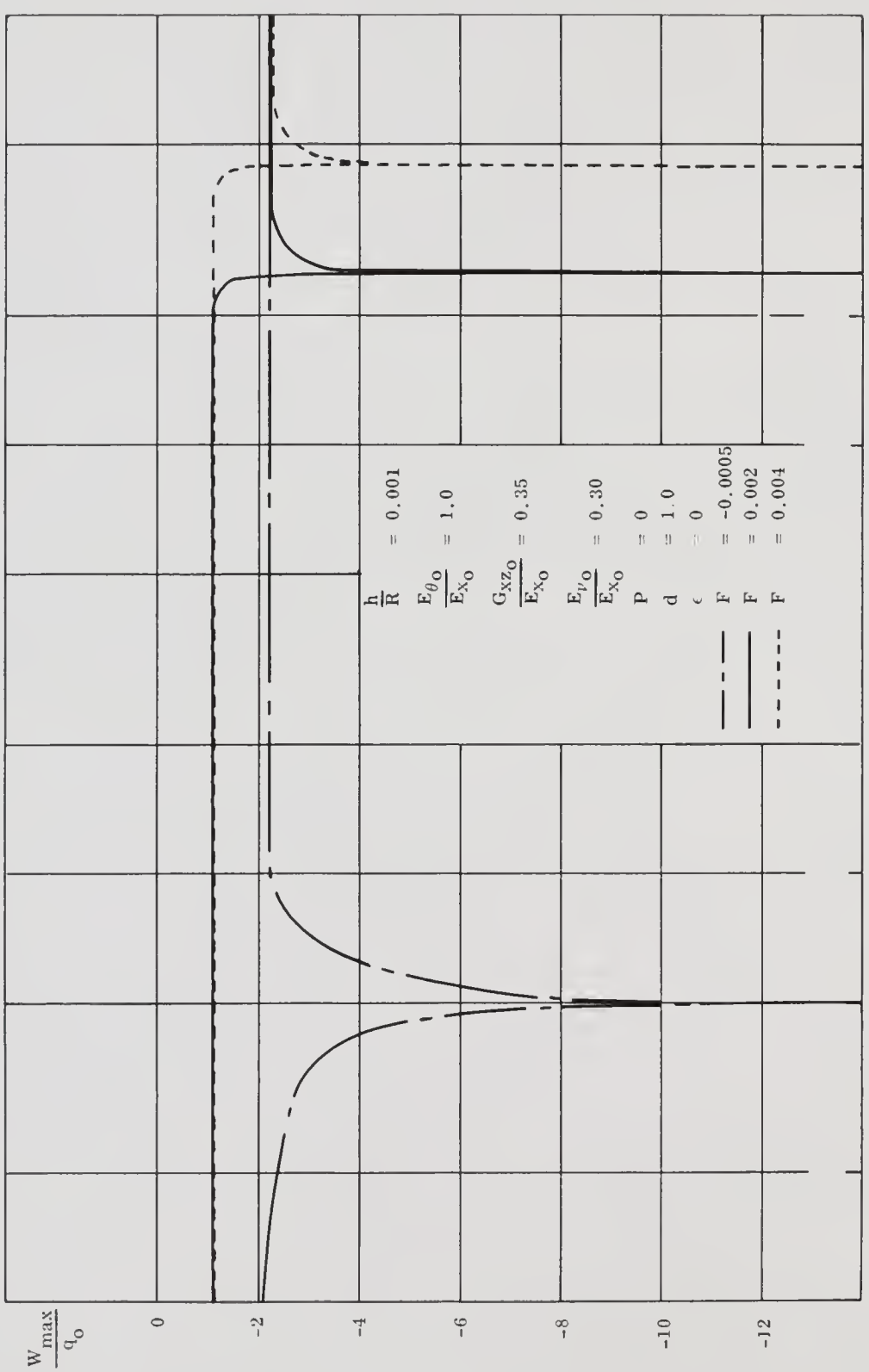

Figure 5.18. Effect of the Axial Prestress on the First Critical Load Speed

Superposition of Step Loads

The effect on the radial deflection can be observed in Figure 5.19(a)-(f) where the load length was varied from 0.1 to 5.0. By superposing various combinations of step loads it is possible to approximate any shape of load desired. As an example of this type of application, the radial deflection response from a symmetric sine wave type load and a sharp edged pressure front was determined. The results of these calculations are presented in Figures 5.20 and 5.21, respectively.

Study of Material Properties Variations

A look at the effect of decreasing the E_{θ_o}/E_{x_o} ratio is summarized in Figure 5.22. Starting in Region IV, as can be seen in Figure 4.4, the ratio is decreased from 1.0 (as for an isotropic material) to 0.04. As the ratio is lowered, the maximum deflection gets large rapidly, and becomes unbounded as $\lambda_4^2 = \lambda_{3CR}^2$ is approached. After crossing λ_{3CR}^2 into Region VIII, the strength in the circumferential direction is of course very low and the material is of little interest for engineering applications.

The same type of response as in Figure 5.22 will be obtained by increasing E_{ν_o}/E_{x_o} significantly. This can be observed by inspecting Figure 4.6. For other types of material property variations, the general response can be pinpointed by observing the type of roots at the particular location through the use of Figures 4.2 through 4.8 and using the numerical results presented here showing similar calculations of deflections.

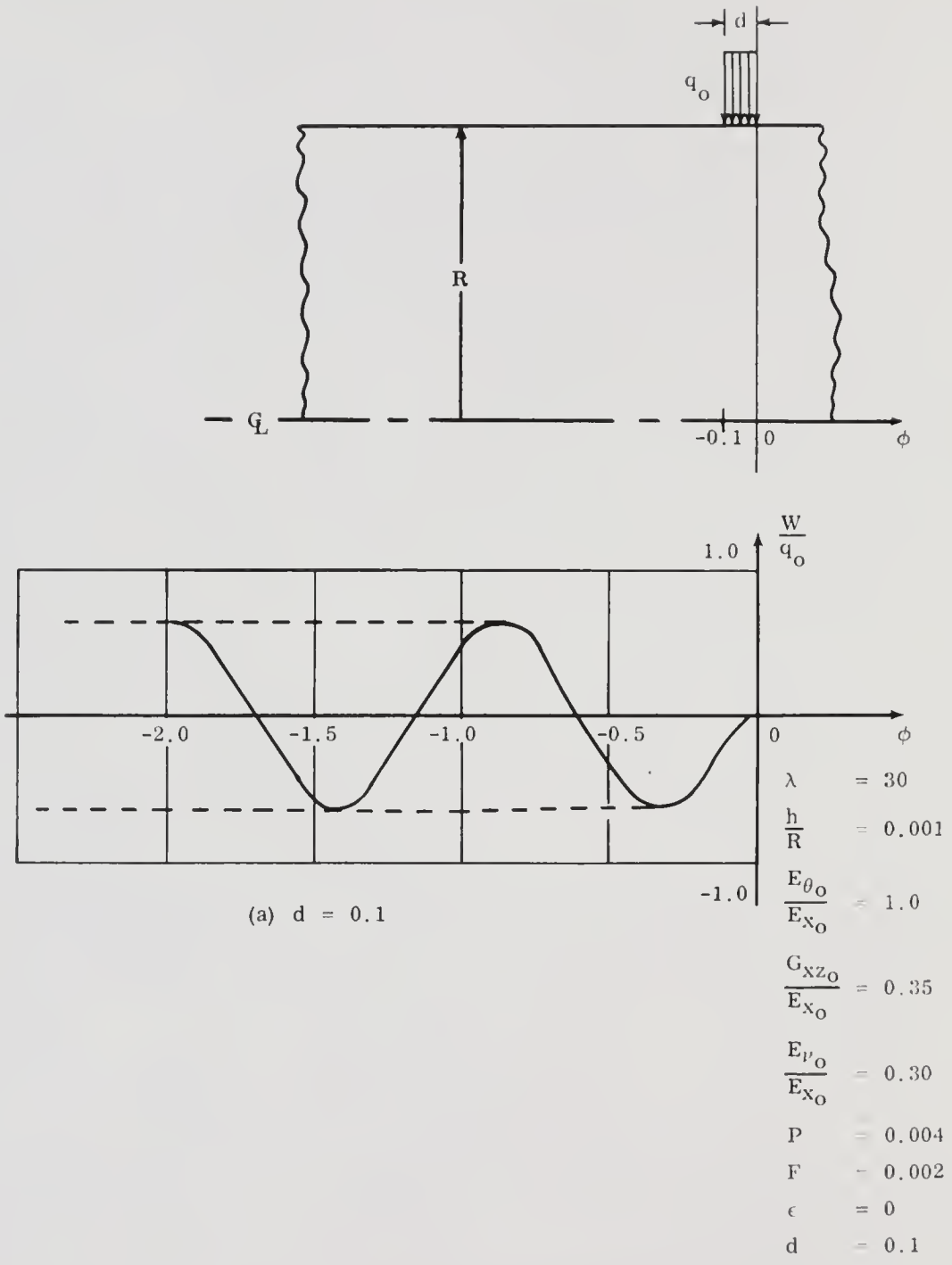

(a) d = 0.1

Figure 5.19(a). Variation of Pressure Pulse Length, d, at $\lambda^2 = 30$

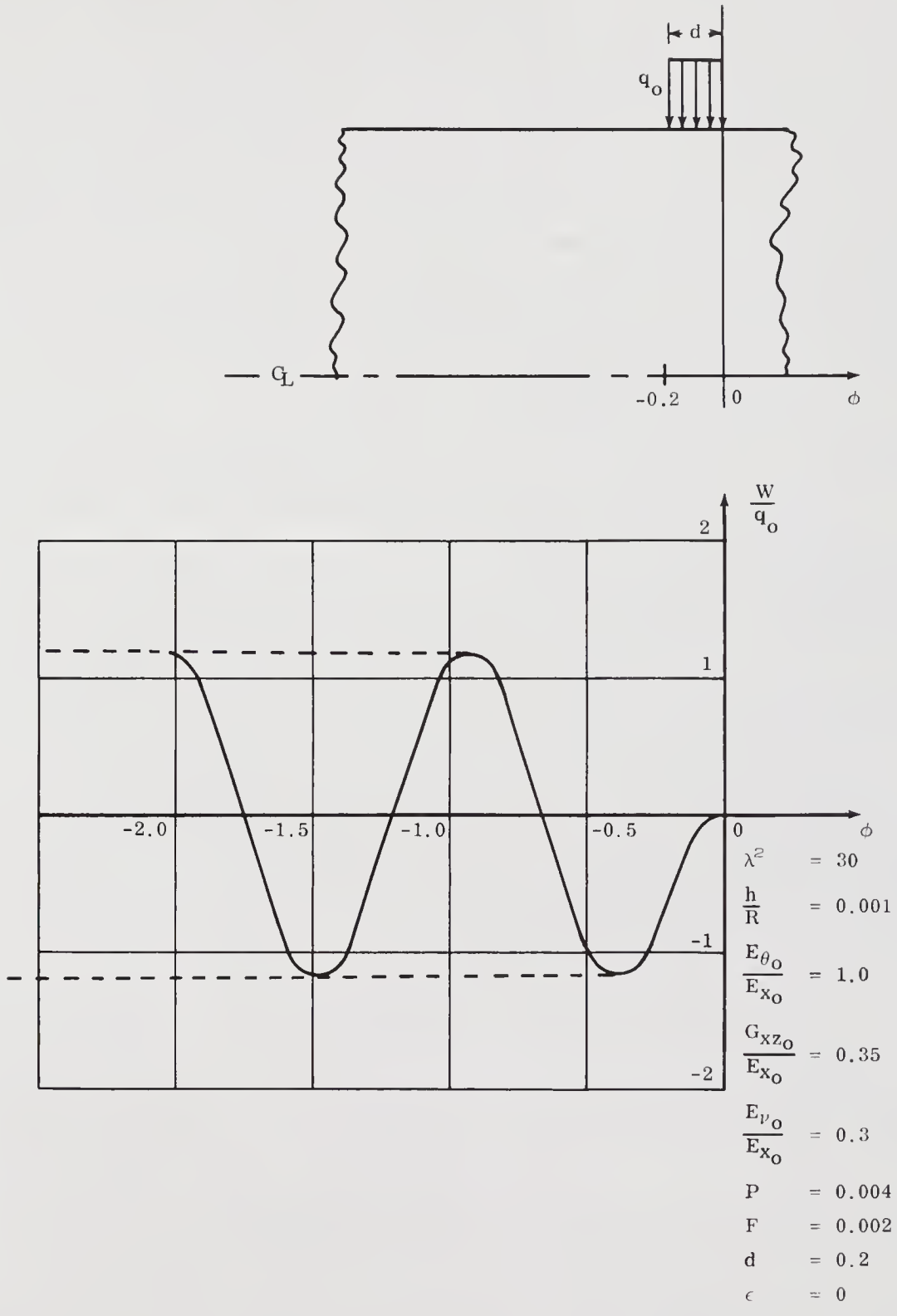

Figure 5.19(b). (d = 0.2)

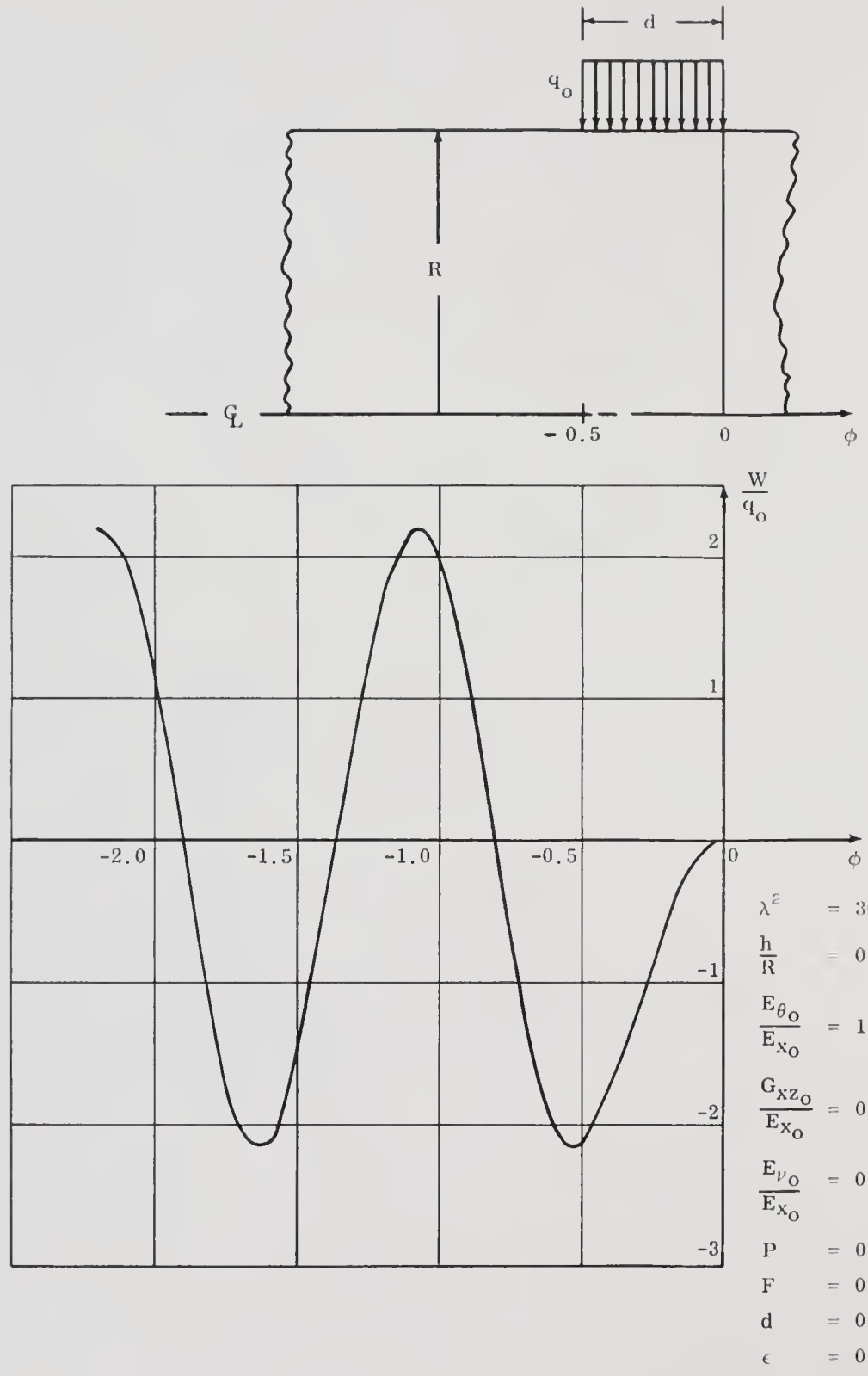

Figure 5.19(c). (d = 0.5)

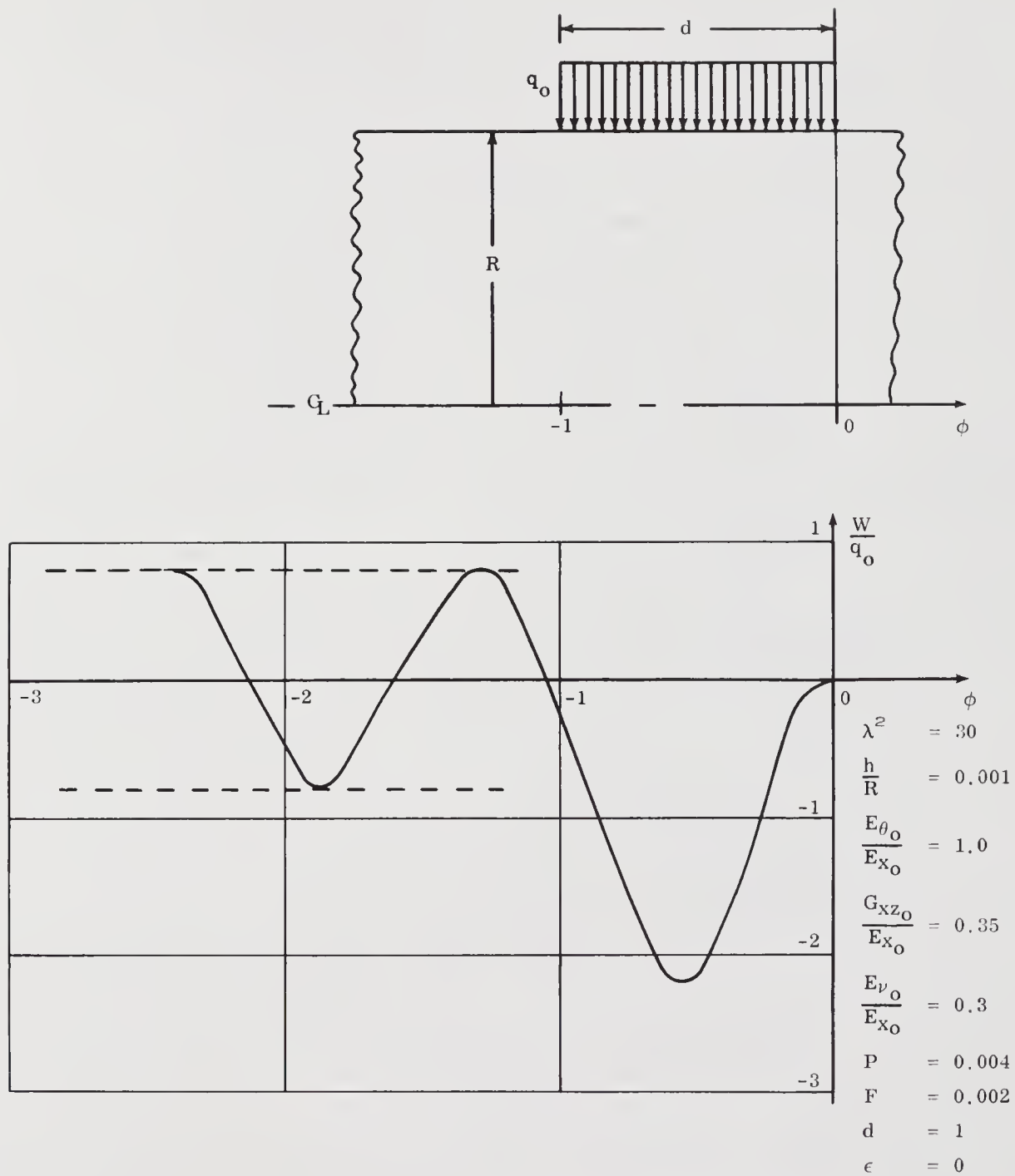

Figure 5.19(d). (d = 1.0)

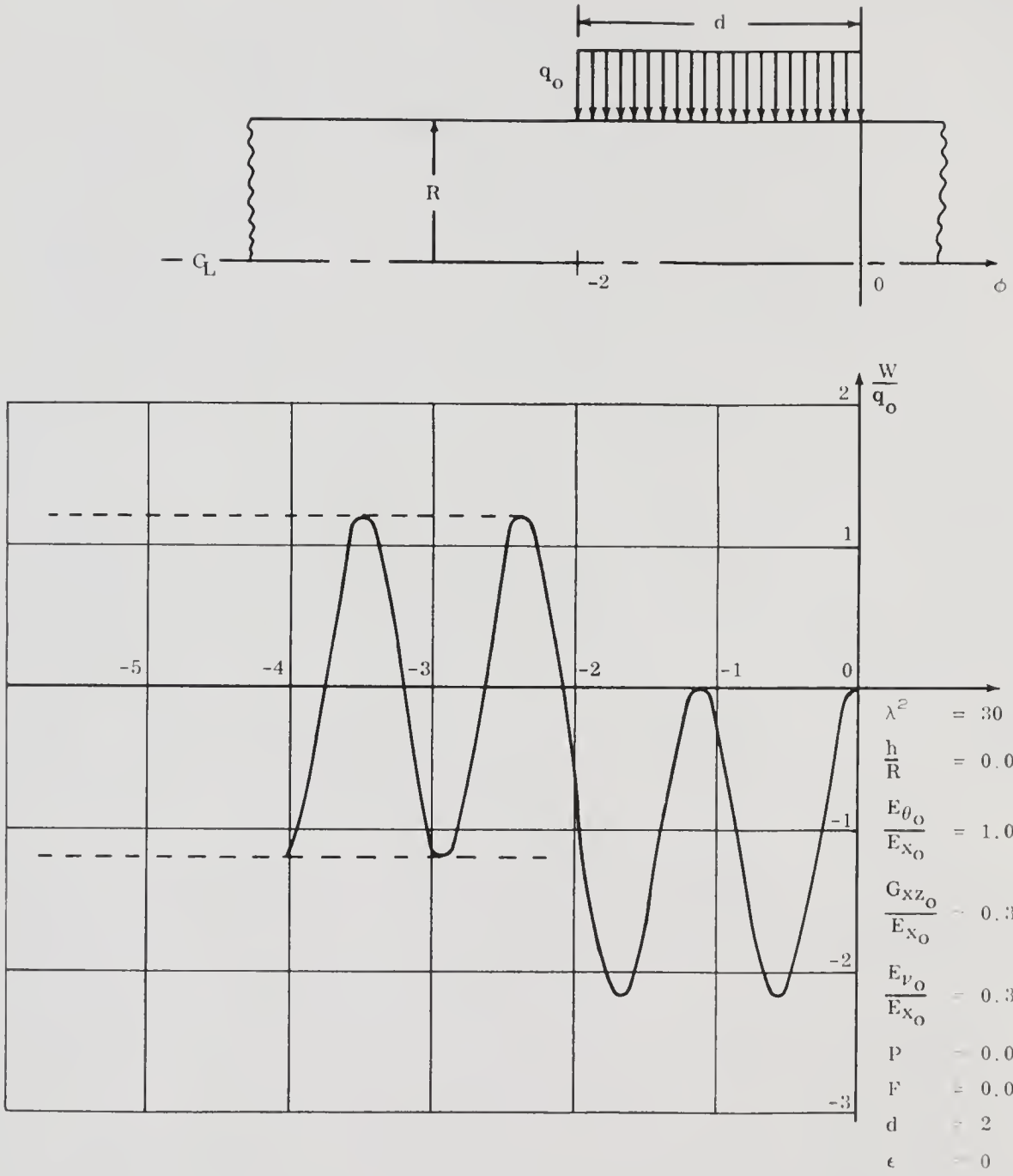

Figure 5.19(e). (d = 2.0)

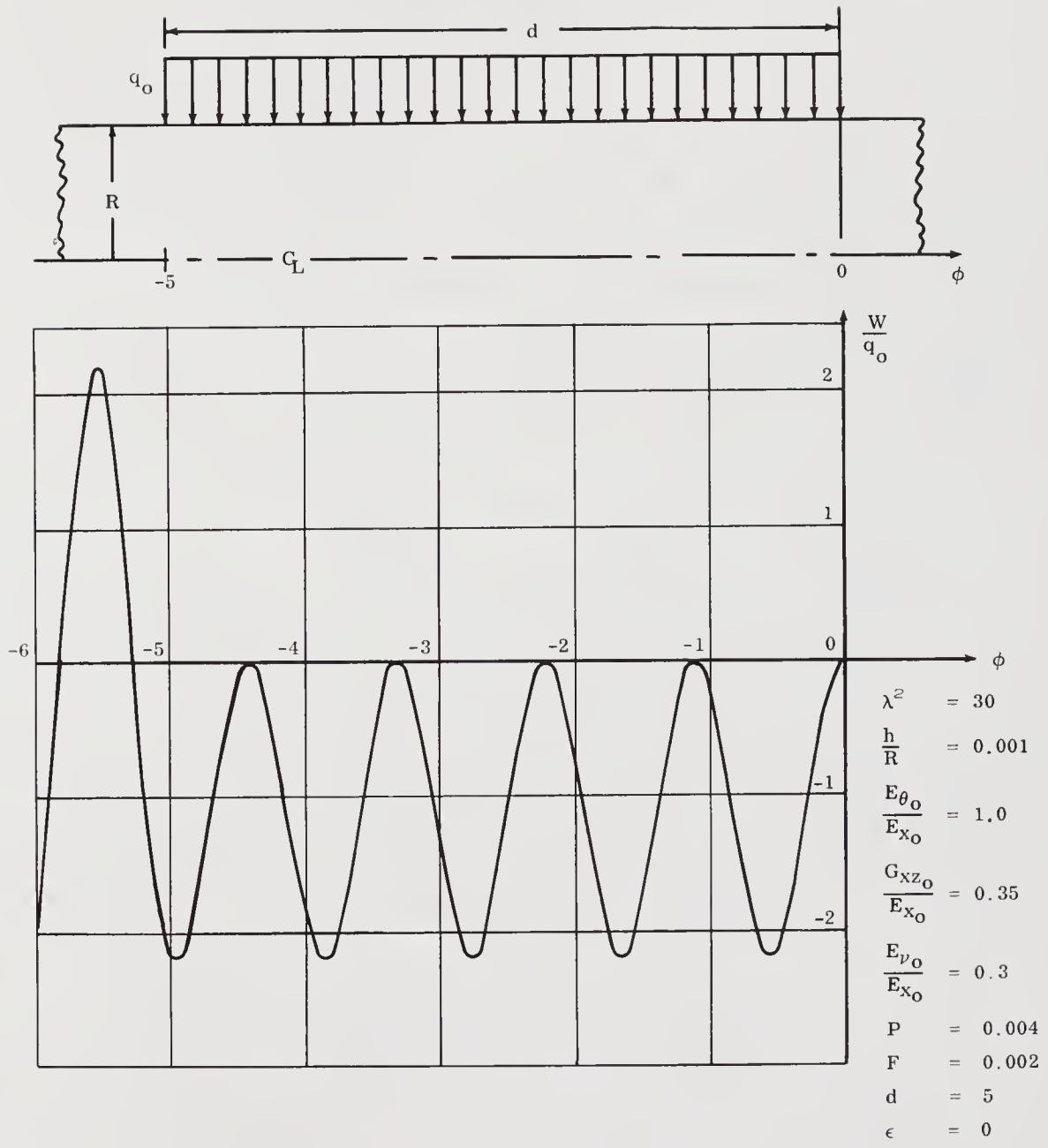

Figure 5.19(f). (d = 5.0)

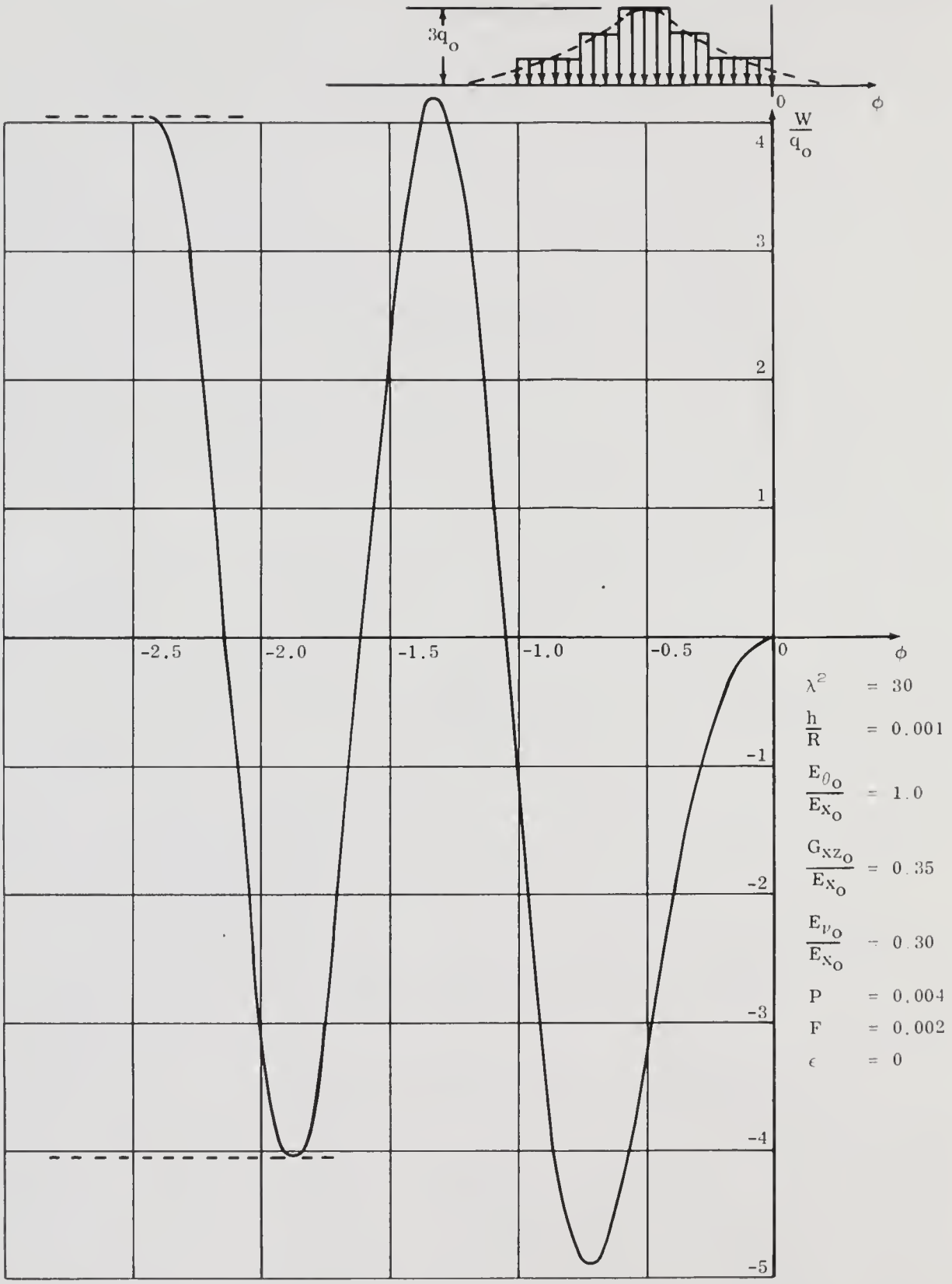

Figure 5.20. Response from a Smooth Sine Wave Type Pressure Pulse Using Superposition

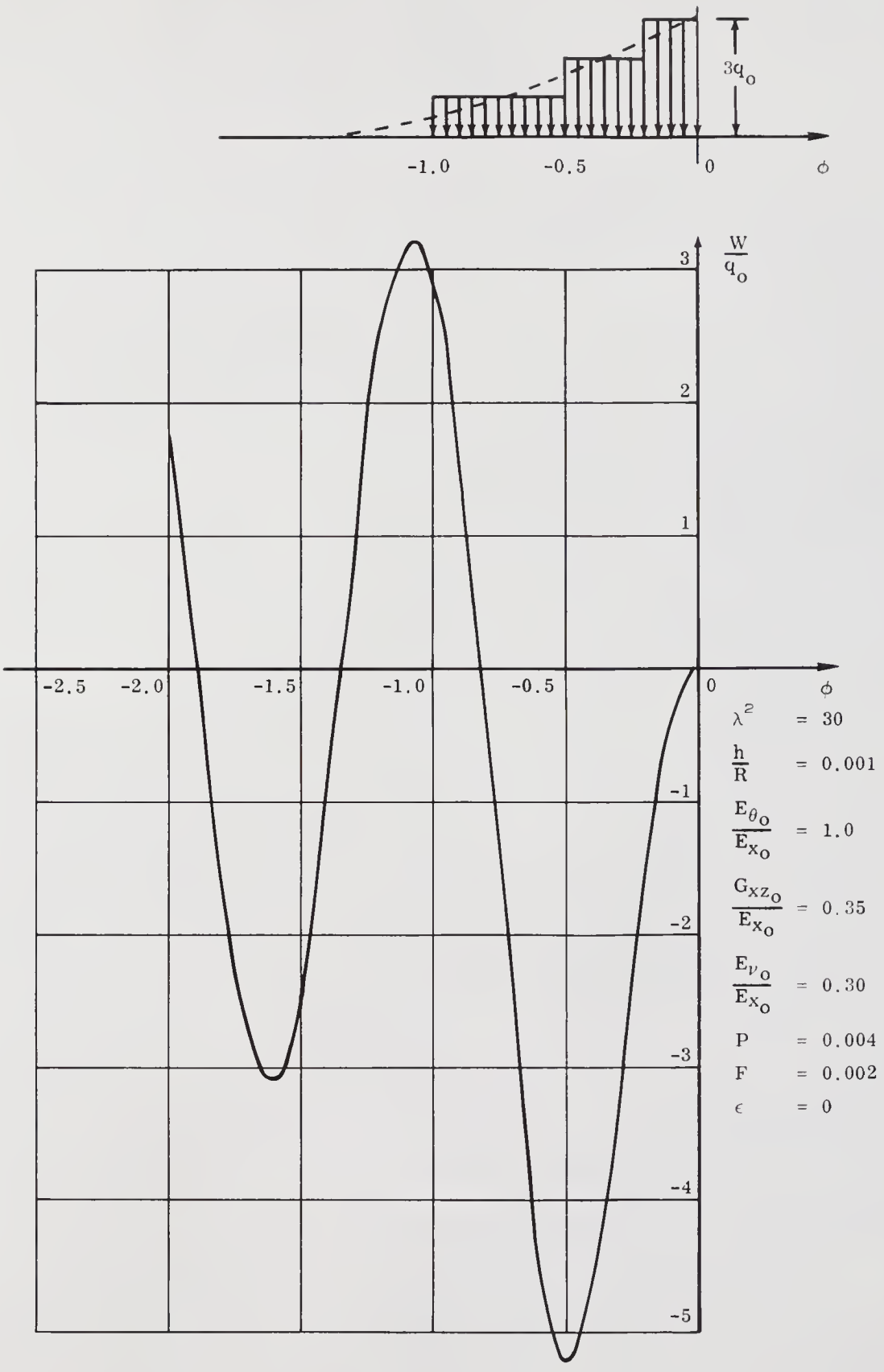

Figure 5.21. Response from a Sharp Pressure Front Using Superposition

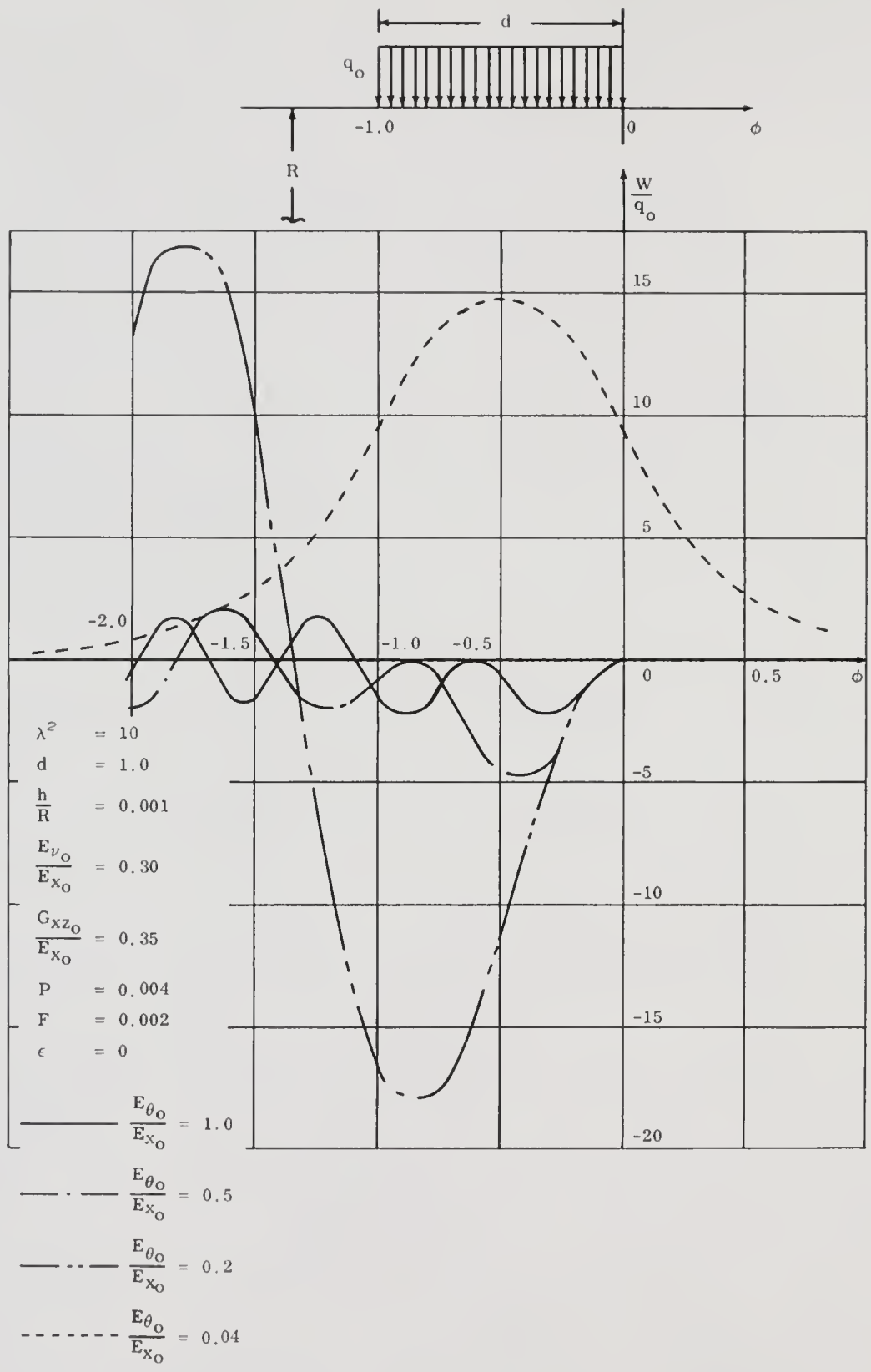

Figure 5.22. Radial Deflection Response for Variations in the Circumferential Modulus

CHAPTER VI

STRESSES

Development of Stress Equations

For the axisymmetric loading the stress and moment resultants become

$$N_x = E_x \frac{\partial u}{\partial x} + \frac{D_x}{R} \frac{\partial \psi}{\partial x} + E_\nu \frac{w}{R} \tag{6-1}$$

$$N_\theta = \left(E_\theta + \frac{D_\theta}{R^2} \right) \frac{w}{R} + E_\nu \frac{\partial u}{\partial x} \tag{6-2}$$

$$M_x = \frac{D_x}{R} \frac{\partial u}{\partial x} + D_x \frac{\partial \psi}{\partial x} \tag{6-3}$$

$$M_\theta = - \frac{D_\theta}{R} \frac{w}{R} + D_\nu \frac{\partial \psi}{\partial x} \tag{6-4}$$

$$Q_x = G_x \left(\psi + \frac{\partial w}{\partial x} \right) \tag{6-5}$$

Assuming the bending stress is linear across the thickness of the shell, the stresses can be put in the nondimensional form

$$\frac{N_x}{E_x} = \frac{dU}{d\phi} + D_1 \frac{d\psi}{d\phi} + E_1 W = \frac{\sigma_{x_m}}{E_{x_o}} \tag{6-6}$$

$$\frac{N_\theta}{E_x} = E_o W + E_1 \frac{dU}{d\phi} = \frac{\sigma_{\theta_m}}{E_{x_o}} \tag{6-7}$$

$$\frac{R M_x}{D_x} = \frac{dU}{d\phi} + \frac{d\psi}{d\phi} = 2 \frac{R}{h} \frac{\sigma_{x_b}}{E_{x_o}} \tag{6-8}$$

$$\frac{E_{\theta_o} R M_\theta}{E_{x_o} D_\theta} = - \frac{E_{\theta_o}}{E_{x_o}} W + E_1 \frac{d\psi}{d\phi} = 2 \frac{R}{h} \frac{\sigma_{\theta_b}}{E_{x_o}} \tag{6-9}$$

$$\frac{G Q_x}{G_x} = G \left(\psi + \frac{dW}{d\phi} \right) = \frac{\sigma_{xz}}{E_{x_o}} \tag{6-10}$$

The stresses are therefore

$$\frac{\sigma_{x_m}}{E_{x_o} q_o} = E_1 \frac{W(\phi)}{q_o} + D_1 \frac{\psi'(\phi)}{q_o} + \frac{U'(\phi)}{q_o} \tag{6-11}$$

$$\frac{\sigma_{\theta_m}}{E_{x_o} q_o} = E_o \frac{W(\phi)}{q_o} + E_1 \frac{U'(\phi)}{q_o} \tag{6-12}$$

$$\frac{\sigma_{x_b}}{E_{x_o} q_o} = \frac{1}{2} \frac{h}{R} \left(\frac{U'(\phi)}{q_o} + \frac{\psi'(\phi)}{q_o} \right) \tag{6-13}$$

$$\frac{\sigma_{\theta_b}}{E_{x_o} q_o} = \frac{1}{2} \frac{h}{R} \left(E_1 \frac{\psi'(\phi)}{q_o} - \frac{E_{\theta_o}}{E_{x_o}} \frac{W(\phi)}{q_o} \right) \tag{6-14}$$

$$\frac{\sigma_{x_z}}{E_{x_o} q_o} = G \left(\frac{\psi(\phi)}{q_o} + \frac{W'(\phi)}{q_o} \right) \tag{6-15}$$

The stresses at the outer and inner surfaces of the shell are now determined.

$$\frac{(\sigma_x)_{outer}}{q_o E_{x_o}} = \frac{\sigma_{x_m}}{q_o E_{x_o}} + \frac{\sigma_{x_b}}{q_o E_{x_o}} \tag{6-16}$$

$$\frac{(\sigma_\theta)_{outer}}{q_o E_{x_o}} = \frac{\sigma_{\theta_m}}{q_o E_{x_o}} + \frac{\sigma_{\theta_b}}{q_o E_{x_o}} \tag{6-17}$$

$$\frac{(\sigma_x)_{inner}}{q_o E x_o} = \frac{\sigma x_m}{q_o E x_o} - \frac{\sigma x_b}{q_o E x_o} \tag{6-18}$$

$$\frac{(\sigma_\theta)_{inner}}{q_o E x_o} = \frac{\sigma \theta_m}{q_o E x_o} - \frac{\sigma \theta_b}{q_o E x_o} \tag{6-19}$$

Both the individual stresses given by Equations (6-11) - (6-15) and (6-16 - (6-19) are calculated by the computer program which is outlined in Figure 5.6. The program listing is given in Appendix H.

There are various relationships which exist between parameters used in this research. Some of these relationships are collected in Appendix I for reference purposes, for use in obtaining the dimensional form of stresses and deflections.

Numerical Results

For an isotropic shell under a static ring load, P, the second derivative of the radial deflection is given in Reference (14) as

$$\frac{d^2 w}{dx^2} = 2\beta^2 \frac{P}{8\beta^3 D} e^{-\beta x} (\sin \beta x - \cos \beta x) \tag{6-20}$$

The solution for the static problem shown in Figure 5.5 can be obtained by replacing P by q dx and integrating so that

$$\frac{d^2 w}{dx^2} = \int_0^{\ell_2} 2\beta^2 \frac{q\, dx}{8\beta^3 D} e^{-\beta x} (\sin \beta x - \cos \beta x) + \int_0^{\ell_1} 2\beta^2 \frac{q\, dx}{8\beta^3 D} e^{-\beta x} (\sin \beta x - \cos \beta x) \tag{6-21}$$

The moment, M_x, in Reference (14) is assumed to be

$$M_x = - D \frac{d^2 w}{dx^2} \tag{6-22}$$

Combining Equations (6-21) and (6-22) and assuming a linear stress distribution through the thickness, the bending stress is determined.

$$\frac{\sigma_{x_b}}{q_o E_{x_o}} = \frac{3}{2\sqrt{3(1 - \mu^2)}} \left(e^{-\beta \ell_2} \sin \beta \ell_2 + e^{-\beta \ell_1} \sin \beta \ell_1 \right) \tag{6-23}$$

where

$$\beta^4 = \frac{3(1 - \mu^2)}{R^2 h^2} \tag{6-24}$$

The stress given by Equation (6-23) is shown in Figure 6.1 in comparison with the results derived in this work. The results given by (6-23) are good for thin shells and get worse as the shell becomes thicker. The axial and tangential surface stresses are shown in Figure 6.2 for the static load problem. The computer program developed can be used to calculate the individual stresses and/or the surface stresses as desired.

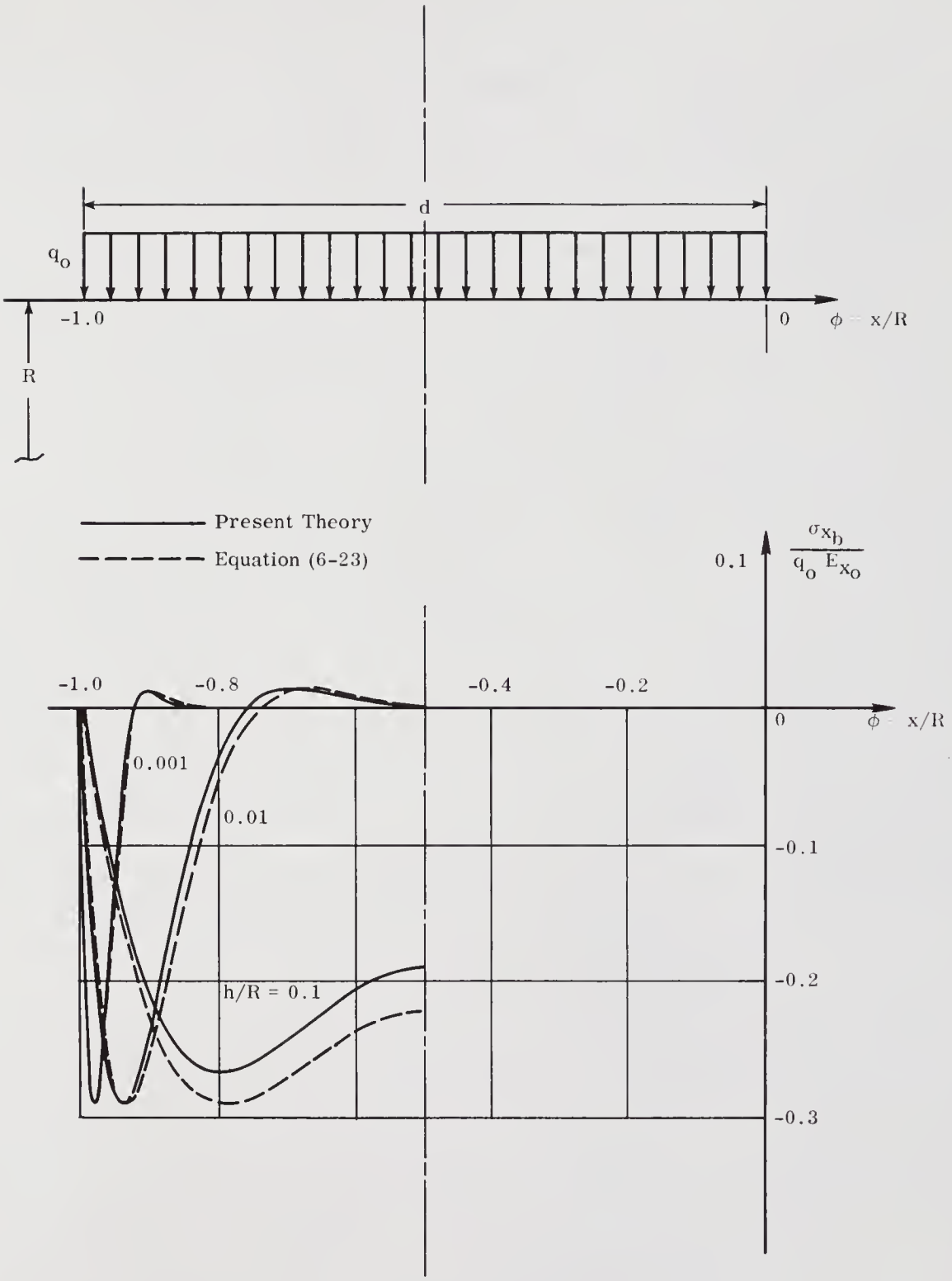

Figure 6.1. Bending Stress in an Isotropic Shell Under a Static Load ($\mu = 0.3$, $d = 1$)

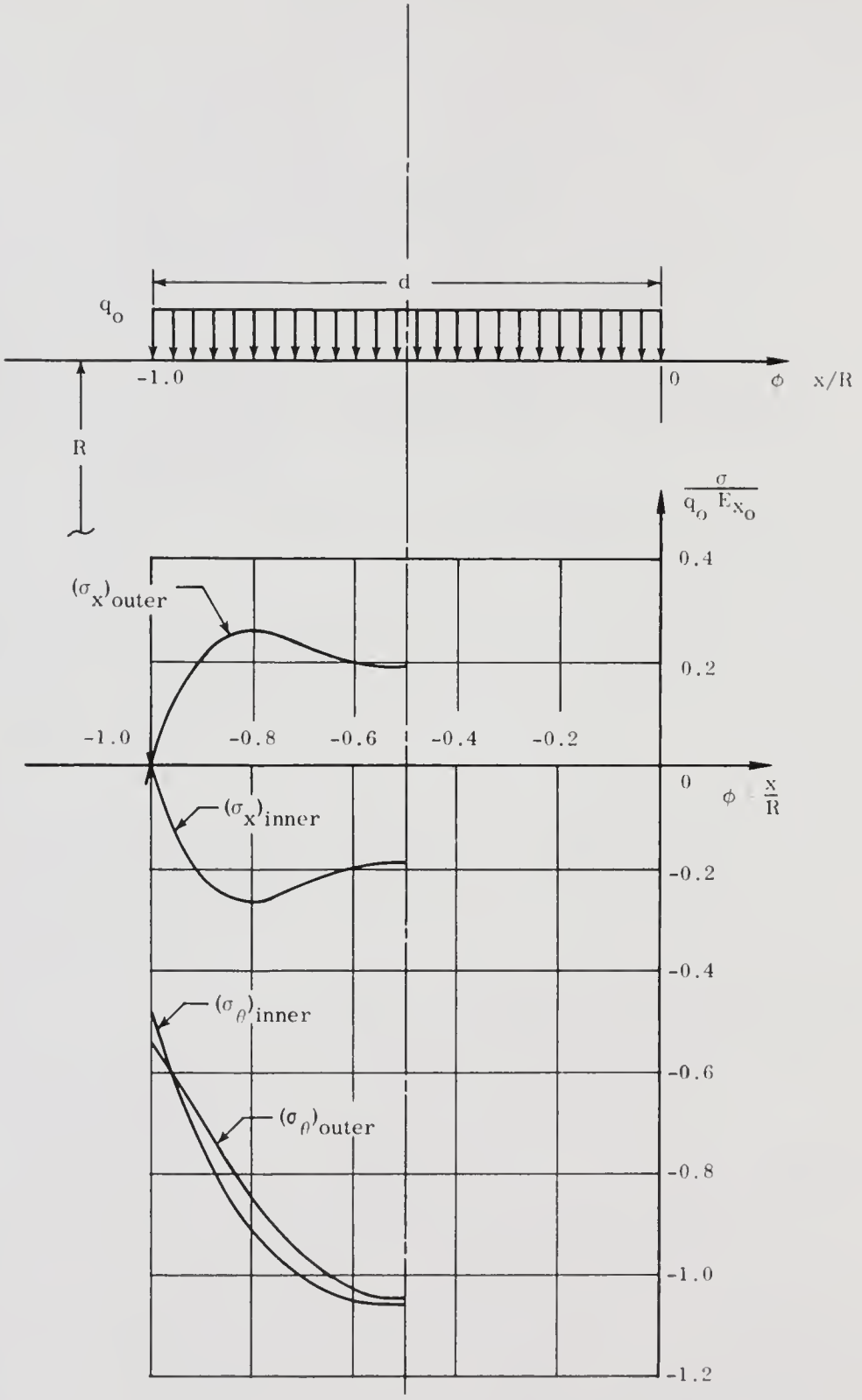

Figure 6.2. Surface Stresses in an Isotropic Shell Under a Static Load (μ = 0.3, h/R = 0.1)

CHAPTER VII

CONCLUDING REMARKS

Conclusions

An analysis has been made of an orthotropic infinite circular cylinder subjected to an axisymmetric discontinuous pressure loading of finite length moving in the axial direction with a constant velocity. Fourier transforms were used to solve for the steady state solution and proved to be very useful for this type of application. The problem of nonuniqueness-of-solution arose for the case of an undamped cylinder. This was handled by taking the undamped solution as the limit of the damped solution when the damping approached zero.

Investigation of the higher load speeds showed that there are five critical load speeds, the two highest being very close together and corresponding approximately to the plate wave speed. Lowering of the tangential modulus ratio was found to cause a rapid increase in deflections. An increase of speed above the bar wave speed was found to cause a mode of deflection which is mainly axial in nature as opposed to the low speed bending type deflection pattern. The method of superposition was used to demonstrate the adaptability of the results to other forms of loads.

Although the shell theory used was linear, small deflection theory, the results are useful for loads in the range for which most structures are designed. The general response picture can be obtained from the results presented here and the location of the critical load speeds observed. The computer program developed here can be used to investigate in detail particular problems of interest. Because of the increasing frequency of applications of cylindrical shells

in dynamic loading conditions in military, government, and industrial programs, the critical load speed environment should be considered in the design requirements. Programs utilizing thin walled launching tubes for launching missiles are a specific example of such applications.

Suggestions for Future Work

For large deflections the theory used in this analysis becomes invalid. A natural extension of this work would be the investigation of the stability through use of large deflection theory. Also the increased use of composite materials for structural applications makes the inclusion of anisotropic material a worthwhile endeavor. In this analysis the axial and circumferential prestress were considered. Another parameter which may prove to have a significant effect is that of torsional prestress.

The computer program developed for the calculation of stresses and deflections in the shell is by no means efficiently programmed. Extensive use would warrant an investigation to reduce run time.

APPENDIX A

FOURIER TRANSFORM OF THE FORCING FUNCTION

Let I_f denote the transform of the pressure function given on the right hand side of Equation (2-34b); the integral to be evaluated is

$$I_f = \int_{-\infty}^{\infty} q_o \left[H(-R\phi) - H(-R\phi - Vt_o)\right] e^{-is\phi}\, d\phi \tag{A-1}$$

or

$$I_f = q_o \int_{-\infty}^{\infty} \left[H(-\phi) - H(-\phi - d)\right] e^{-is\phi}\, d\phi \tag{A-2}$$

where

$$d = \frac{Vt_o}{R} \tag{A-3}$$

$$H(-\phi) = \begin{cases} 0, & \phi > 0 \\ 1, & \phi < 0 \end{cases} \tag{A-4}$$

$$H(-\phi - d) = \begin{cases} 0, & \phi + d > 0 \\ 1, & \phi + d < 0 \end{cases} \tag{A-5}$$

Integral (A-2) therefore can be broken up into two integrals.

$$I_f = q_o \left[\int_{-\infty}^{0} e^{-is\phi} d\phi - \int_{-\infty}^{-d} e^{-is\phi} d\phi \right] \tag{A-6}$$

Furthermore, the second integral can be written

$$\int_{-\infty}^{-d} e^{-is\phi} d\phi = \int_{-\infty}^{0} e^{-is\phi} d\phi - \int_{-d}^{0} e^{-is\phi} d\phi \qquad \text{(A-7)}$$

Therefore,

$$I_f = q_o \int_{-d}^{0} e^{-is\phi} d\phi = \frac{q_o}{-is} \left[e^{-is\phi} \right]_{-d}^{0}$$

$$I_f = \frac{q_o}{-is} (1 - e^{isd}) = \frac{q_o}{is} (e^{isd} - 1) \qquad \text{(A-8)}$$

Equation (A-8) gives the transform of the pressure loading.

APPENDIX B

SOLUTION OF EQUATIONS FOR THE TRANSFORMED DEFLECTIONS

From Equation (3-7) the set of equations to be solved is

$$\begin{bmatrix} (1+F-r_1\lambda^2)s^2 & -i(E_1-P)s & (D_1-I_0\lambda^2)s^2 \\ i(E_1-P)s & (G+F-r\lambda^2)s^2-i\epsilon\lambda s+E_0+Pr_0 & -i(G+Pr_0)s \\ (D_1-I_0\lambda^2)s^2 & i(G+Pr_0)s & (D_1-I_0\lambda^2)s^2+G+Pr_0 \end{bmatrix} \begin{bmatrix} \overline{U}(s) \\ \overline{W}(s) \\ \overline{\psi}(s) \end{bmatrix} = \begin{bmatrix} 0 \\ \frac{q_0}{is}(1-e^{isd}) \\ 0 \end{bmatrix} \tag{B-1}$$

First, the determinant of the coefficients, denoted as Δ, will be determined.

$$\Delta = \begin{vmatrix} 1+F-r_1\lambda^2 & -i(E_1-P)s & (D_1-I_0\lambda^2)s^2 \\ i(E_1-P)s & (G+F-r\lambda^2)s^2-i\epsilon\lambda s+E_0+Pr_0 & -i(G+Pr_0)s \\ (D_1-I_0\lambda^2)s^2 & i(G+Pr_0)s & (D_1-I_0\lambda^2)s^2+G+Pr_0 \end{vmatrix} \tag{B-2}$$

Expanding this determinant gives

$$\begin{aligned} \Delta = {} & (1+F-r_1\lambda^2)s^2\Big\{(G+F-r\lambda^2)(D_1-I_0\lambda^2)s^4 - i\epsilon\lambda(D_1-I_0\lambda^2)s^3 \\ & + \Big[(D_1-I_0\lambda^2)(E_0+Pr_0)+(G+F-r\lambda^2)(G+Pr_0)\Big]s^2 \\ & - i\epsilon\lambda(G+Pr_0)s+(E_0+Pr_0)(G+Pr_0)\Big\} \\ & - 2(E_1-P)(G+Pr_0)(D_1-I_0\lambda^2)s^4 - (D_1-I_0\lambda^2)^2(G+F-r\lambda^2)s^6 \\ & + i\epsilon\lambda(D_1-I_0\lambda^2)^2s^5 - (E_0+Pr_0)(D_1-I_0\lambda^2)^2s^4 - (1+F-r_1\lambda^2)(G+Pr_0)^2s^4 \\ & - (D_1-I_0\lambda^2)(E_1-P)^2s^4 - (G+Pr_0)(E_1-P)^2s^2 \end{aligned} \tag{B-3}$$

Collecting coefficients on powers of s gives the expression for the determinant in the form

$$\begin{aligned}\Delta = {} & (G + F - r\lambda^2)(D_1 - I_0\lambda^2)\left[(1 + F - r_1\lambda^2) - (D_1 - I_0\lambda^2)\right] s^6 \\ & + i\epsilon\lambda(D_1 - I_0\lambda^2)\left[(D_1 - I_0\lambda^2) - (1 + F - r_1\lambda^2)\right] s^5 \\ & + \Big\{(E_0 + Pr_0)(D_1 - I_0\lambda^2)\left[(1 + F - r_1\lambda^2) - (D_1 - I_0\lambda^2)\right] \\ & + (1 + F - r_1\lambda^2)(G + Pr_0)\left[(G + F - r\lambda^2) - (G + Pr_0)\right] \\ & - (D_1 - I_0\lambda^2)\left[(E_1 - P)^2 + 2(E_1 - P)(G + Pr_0)\right]\Big\} s^4 \\ & - i\epsilon\lambda(1 + F - r_1\lambda^2)(G + Pr_0)s^3 \\ & + (G + Pr_0)\left[(1 + F - r_1\lambda^2)(E + Pr_0) - (E_1 - P)^2\right] s^2 \end{aligned} \tag{B-4}$$

Solving for $\overline{U}(s)$ using Cramer's rule gives

$$\overline{U}(s) = \frac{1}{\Delta}\begin{vmatrix} 0 & -i(E_1 - P)s & (D_1 - I_0\lambda^2)s^2 \\ -\frac{q_0}{is}(e^{isd} - 1) & (G + F - r\lambda^2)s^2 - i\epsilon\lambda s + E_0 + Pr_0 & -i(G + Pr_0)s \\ 0 & i(G + Pr_0)s & (D_1 - I_0\lambda^2)s^2 + (G + Pr_0) \end{vmatrix} \tag{B-5}$$

or, after expanding the determinant,

$$\begin{aligned}\overline{U}(s) = \frac{1}{\Delta}\Big[& -q_0(e^{isd} - 1)\Big\{\Big[(G + Pr_0)(D_1 - I_0\lambda^2) \\ & + (E_1 - P)(D_1 - I_0\lambda^2)\Big] s^2 \\ & + (E_1 - P)(G + Pr_0)\Big\}\Big] \end{aligned} \tag{B-6}$$

Defining the coefficients in Δ as

$$c_o = (G + Pr_o)\left[(1 + F - r_1\lambda^2)(E_o + Pr_o) - (E_1 - P)^2\right]$$

$$c_1 = -\epsilon\lambda(G + Pr_o)(1 + F - r_1\lambda^2)$$

$$c_2 = (D_1 - I_o\lambda^2)\left\{(E_o + Pr_o)c - (E_1 - P)\left[(E_1 - P) + 2(G + Pr_o)\right]\right\}$$

$$+ (G + Pr_o)(1 + F - r_1\lambda^2)(F - Pr_o - r\lambda^2)$$

$$c_3 = -\epsilon\lambda(D_1 - I_o\lambda^2)c$$

$$c_4 = (G + F - r\lambda^2)(D_1 - I_o\lambda^2)c$$

$$c = 1 + F - D_1 - r_1\lambda^2 + I_o\lambda^2 \qquad \text{(B-7)}$$

then

$$\Delta = s^2\,\overline{D}(s) \qquad \text{(B-8)}$$

where

$$\overline{D}(s) = c_4 s^4 + ic_3 s^3 + c_2 s^2 + ic_1 s + c_o \qquad \text{(B-9)}$$

Using this nomenclature Equation (B-6) can be written

$$\frac{\overline{U}(s)}{q_o} = \frac{1 - e^{isd}}{\Delta}\left[(D_1 - I_o\lambda^2)(G + Pr_o + E_1 - P)s^2\right.$$

$$\left. + (G + Pr_o)(E_1 - P)\right] \qquad \text{(B-10)}$$

Now $\overline{W}(s)$ is determined. Using Cramer's rule again, the transformed radial deflection is given by

$$\overline{W}(s) = \frac{1}{\Delta}\begin{vmatrix} (1+F-r_1\lambda^2)s^2 & 0 & (D_1 - I_o\lambda^2)s^2 \\ i(E_1 - P)s & \frac{q_o}{is}(1 - e^{isd}) & -i(G+Pr_o)s \\ (D_1 - I_o\lambda^2)s^2 & 0 & (D_1 - I_o\lambda^2)s^2 + (G+Pr_o) \end{vmatrix} \qquad \text{(B-11)}$$

Expanding the determinant gives

$$\overline{W}(s) = \frac{1}{\Delta}\frac{q_o}{is}(1 - e^{isd})\Big[(1 + F - r_1\lambda^2)(D_1 - I_o\lambda^2)s^4 + (1 + F - r_1\lambda^2)(G + Pr_o)s^2 - (D_1 - I_o\lambda^2)^2 s^4\Big] \quad \text{(B-12)}$$

or

$$\frac{\overline{W}(s)}{q_o} = \frac{(1 - e^{isd})}{is\overline{D}(s)}\Big[(D_1 - I_o\lambda^2)\epsilon s^2 + (1 + F - r_1\lambda^2)(G + Pr_o)\Big] \quad \text{(B-13)}$$

Finally, the rotation expression is determined as

$$\overline{\psi}(s) = \frac{1}{\Delta}\begin{vmatrix} (1+F-r_1\lambda^2)s^2 & -i(E_1-P)s & 0 \\ i(E_1-P)s & (G+F-r\lambda^2)s^2 - i\epsilon\lambda s + E_o + Pr_o & \frac{q_o}{is}(1-e^{isd}) \\ (D_1-I_o\lambda^2)s^2 & i(G+Pr_o)s & 0 \end{vmatrix} \quad \text{(B-14)}$$

or

$$\overline{\psi}(s) = -\frac{q_o(1 - e^{isd})}{\Delta}\Big[(E_1 - P)(D_1 - I_o\lambda^2) + (G + Pr_o)(1 + F - r_1\lambda^2)\Big]s^2 \quad \text{(B-15)}$$

$$\frac{\overline{\psi}(s)}{q_o} = -\frac{(1 - e^{isd})}{\overline{D}(s)}\Big[(E_1 - P)(D_1 - I_o\lambda^2) + (G + Pr_o)(1 + F - r_1\lambda^2)\Big] \quad \text{(B-16)}$$

APPENDIX C

EVALUATION OF THE DISCRIMINANT OF A FOURTH ORDER POLYNOMIAL

The discriminant of an n^{th} order polynomial

$$a_o x^n + a_1 x^{n-1} + \ldots + a_{n-1} x + a_n = 0 \qquad \text{(C-1)}$$

is defined as (15)

$$\overline{\Delta} = a_o^{2n-2} \begin{vmatrix} S_o & S_1 & \ldots & S_{n-1} \\ S_1 & S_2 & \ldots & S_n \\ \vdots & \vdots & & \vdots \\ S_{n-1} & S_n & \ldots & S_{2n-2} \end{vmatrix} \qquad \text{(C-2)}$$

The preceding determinant is called Vandermonde's determinant and the elements of it are defined as

$$S_o = n \qquad \text{(C-3)}$$

$$S_k = \left(-\frac{1}{a_o}\right)^k \begin{vmatrix} a_1 & a_o & 0 & \ldots\ldots\ldots & 0 \\ 2a_2 & a_1 & a_o & 0 \quad \ldots & 0 \\ 3a_3 & a_2 & a_1 & a_o \quad \ldots & 0 \\ \vdots & \vdots & \vdots & \vdots & \vdots \\ ka_k & a_{k-1} & \ldots\ldots\ldots\ldots & & a_1 \end{vmatrix} \quad (k = 1, 2, \ldots, n) \qquad \text{(C-4)}$$

For a fourth order equation of the form

$$a_o x^4 + a_2 x^2 + a_4 = 0 \qquad \text{(C-5)}$$

the S_k's become

$$S_1 = \left(-\frac{1}{a_o}\right) a_1 = 0 \tag{C-6}$$

$$S_2 = \left(-\frac{1}{a_o}\right)^2 \begin{vmatrix} 0 & a_o \\ 2a_2 & 0 \end{vmatrix} = -\frac{2a_o a_2}{a_o^2} = -2\frac{a_2}{a_o} \tag{C-7}$$

$$S_3 = \left(-\frac{1}{a_o}\right)^3 \begin{vmatrix} 0 & a_o & 0 \\ 2a_2 & 0 & a_o \\ 0 & a_2 & 0 \end{vmatrix} = 0 \tag{C-8}$$

$$S_4 = \left(-\frac{1}{a_o}\right)^4 \begin{vmatrix} 0 & a_o & 0 & 0 \\ 2a_2 & 0 & a_o & 0 \\ 0 & a_2 & 0 & a_o \\ 4a_4 & 0 & a_2 & 0 \end{vmatrix} = -\frac{a_o}{a_o^4} \begin{vmatrix} 2a_2 & a_o & 0 \\ 0 & 0 & a_o \\ 4a_4 & a_2 & 0 \end{vmatrix} \tag{C-9}$$

or

$$S_4 = -\frac{1}{a_o^3}\left[4a_o^2 a_4 - 2a_o a_2^2\right] = -\frac{2}{a_o^2}(2a_o a_4 - a_2^2) \tag{C-10}$$

$$S_5 = \left(-\frac{1}{a_o}\right)^5 \begin{vmatrix} 0 & a_o & 0 & 0 & 0 \\ 2a_2 & 0 & a_o & 0 & 0 \\ 0 & a_2 & 0 & a_o & 0 \\ 4a_4 & 0 & a_2 & 0 & a_o \\ 0 & a_4 & 0 & a_2 & 0 \end{vmatrix} = \frac{1}{a_o^4} \begin{vmatrix} 2a_2 & a_o & 0 & 0 \\ 0 & 0 & a_o & 0 \\ 4a_4 & a_2 & 0 & a_o \\ 0 & 0 & a_2 & 0 \end{vmatrix} \tag{C-11}$$

or

$$S_5 = -\frac{1}{a_o^3}\begin{vmatrix} 2a_2 & a_o & 0 \\ 4a_4 & a_2 & a_o \\ 0 & 0 & 0 \end{vmatrix} = \frac{1}{a_o^2}(0) = 0 \qquad \text{(C-12)}$$

$$S_6 = \frac{1}{a_o^6}\begin{vmatrix} 0 & a_o & 0 & 0 & 0 & 0 \\ 2a_2 & 0 & a_o & 0 & 0 & 0 \\ 0 & a_2 & 0 & a_o & 0 & 0 \\ 4a_4 & 0 & a_2 & 0 & a_o & 0 \\ 0 & a_4 & 0 & a_2 & 0 & a_o \\ 0 & 0 & a_4 & 0 & a_2 & 0 \end{vmatrix}$$

$$= -\frac{1}{a_o^5}\begin{vmatrix} 2a_2 & a_o & 0 & 0 & 0 \\ 0 & 0 & a_o & 0 & 0 \\ 4a_4 & a_2 & 0 & a_o & 0 \\ 0 & 0 & a_2 & 0 & a_o \\ 0 & a_4 & 0 & a_2 & 0 \end{vmatrix} = \frac{1}{a_o^4}\begin{vmatrix} 2a_2 & a_o & 0 & 0 \\ 4a_4 & a_2 & a_o & 0 \\ 0 & 0 & 0 & a_o \\ 0 & a_4 & a_2 & 0 \end{vmatrix}$$

$$= -\frac{1}{a_o^3}\begin{vmatrix} 2a_2 & a_o & 0 \\ 4a_4 & a_2 & a_o \\ 0 & a_4 & a_2 \end{vmatrix} = -\frac{1}{a_o^3}\left[2a_2(a_2^2 - a_o\, a_4) - a_o(4a_2\, a_4)\right]$$

$$S_6 = -\frac{2a_2}{a_o^3}\left[a_2^2 - 3a_o\, a_4\right] \qquad \text{(C-13)}$$

The discriminant can now be evaluated.

$$\overline{\Delta} = a_o^6 \begin{vmatrix} 4 & 0 & -2\frac{a_2}{a_o} & 0 \\ 0 & -2\frac{a_2}{a_o} & 0 & -\frac{2}{a_o^2}(2a_oa_4 - a_2^2) \\ -2\frac{a_2}{a_o} & 0 & -\frac{2}{a_o^2}(2a_oa_4 - a_2^2) & 0 \\ 0 & -\frac{2}{a_o^2}(2a_oa_4 - a_2^2) & 0 & -\frac{2a_2}{a_o^3}(a_2^2 - 3a_oa_4) \end{vmatrix} \tag{C-14}$$

Expanding the determinant about the last column gives

$$\overline{\Delta} = a_o^6 \left\{ -\frac{2}{a_o^2}(2a_oa_4 - a_2^2) \begin{vmatrix} 4 & 0 & -2\frac{a_2}{a_o} \\ -2\frac{a_2}{a_o} & 0 & -\frac{2}{a_o^2}(2a_oa_4 - a_2^2) \\ 0 & -\frac{2}{a_o^2}(2a_oa_4 - a_2^2) & 0 \end{vmatrix} \right. - \frac{2a_2}{a_o^3}(a_2^2 - 3a_oa_4) \left. \begin{vmatrix} 4 & 0 & -2\frac{a_2}{a_o} \\ 0 & -2\frac{a_2}{a_o} & 0 \\ -2\frac{a_2}{a_o} & 0 & -\frac{2}{a_o^2}(2a_oa_4 - a_2^2) \end{vmatrix} \right\} \tag{C-15}$$

Expanding this further gives

$$\overline{\Delta} = a_o^6 \left\{ -\frac{4}{a_o^4}(2a_oa_4 - a_2^2)\left[-\frac{8}{a_o^2}(2a_oa_4 - a_2^2) - 4\frac{a_2^2}{a_o^2} \right] + \frac{4a_2^2}{a_o^4}(a_2^2 - 3a_oa_4)\left[-\frac{8}{a_o^2}(2a_oa_4 - a_2^2) - 4\frac{a_2^2}{a_o^2} \right] \right\} \qquad \text{(C-16)}$$

$$\overline{\Delta} = -4\left(2a_oa_4 - a_2^2\right)^2 \left[-16a_oa_4 + 8a_2^2 - 4a_2^2\right]$$

$$+4a_2^2(a_2^2 - 3a_oa_4)\left(-16a_oa_4 + 8a_2^2 - 4a_2^2\right)$$

$$= 16(a_2^2 - 4a_oa_4)\left[-(2a_oa_4 - a_2^2)^2 + a_2^2(a_2^2 - 3a_oa_4)\right]$$

$$= 16(a_2^2 - 4a_oa_4)\left[-4a_o^2a_4^2 + 4a_oa_2^2a_4 - a_2^4 + a_2^4 - 3a_oa_2^2a_4\right]$$

$$= 16(a_2^2 - 4a_oa_4)\left(-4a_o^2a_4^2 + a_oa_2^2a_4\right)$$

$$= 16(a_2^2 - 4a_oa_4)\left(a_oa_4\right)\left(a_2^2 - 4a_oa_4\right)$$

Finally

$$\overline{\Delta} = 16a_oa_4(a_2^2 - 4a_oa_4)^2 \qquad \text{(C-17)}$$

APPENDIX D

DETERMINATION OF THE CRITICAL VELOCITY EQUATIONS

Equation (4-3) is the first expression satisfying the conditions for which repeated roots occur. It is repeated here for reference.

$$c_2^2 - 4c_0 c_4 = 0 \qquad \text{(D-1)}$$

With the definition of terms as given by Equation (D-2),

$$e_0 = E_0 + Pr_0 \qquad f_0 = 1 + F$$

$$e_1 = E_1 - P \qquad f_1 = 1 + F - D_1$$

$$e_2 = E_1 - P + 2(G + Pr_0) \qquad f_2 = F - Pr_0$$

$$e_3 = G + Pr_0 \qquad f_3 = G + F$$

$$e_4 = I_0 - r_1 \qquad f_4 = D_1 r_1 + I_0 f_0$$

$$e_5 = e_0 f_1 - e_1 e_2 \qquad f_5 = r_1 f_2 + r f_0$$

$$e_6 = e_0 f_0 - e_1^2 \qquad f_6 = e_4 D_1 - I_0 f_1$$

$$f_7 = D_1 - I_0 \lambda^2$$

$$f_8 = f_0 - r_1 \lambda^2$$

$$f_9 = D_1 e_4 - I_0 f_1 \qquad \text{(D-2)}$$

The coefficients in Equation (3-10) can be written in the following form.

$$
\begin{aligned}
c &= f_1 + e_4\lambda^2 \\
c_0 &= e_3(f_8 e_0 - e_1^2) \\
c_1 &= -\epsilon\lambda e_3 f_8 \\
c_2 &= f_7(e_0 c - e_1 e_2) + e_3 f_8 (f_2 - r\lambda^2) \\
c_3 &= -\epsilon\lambda f_7 c \\
c_4 &= (f_3 - r\lambda^2) f_7 c \\
c_5 &= f_7(e_3 + e_1) \\
c_6 &= e_1 e_3 \\
c_7 &= f_7(f_1 + e_4\lambda^2) \\
c_8 &= e_3 f_8 \\
c_9 &= e_1 f_7 + c_8
\end{aligned}
\qquad \text{(D-3)}
$$

The coefficients in Equation (D-3) are substituted into Equation (D-1) and terms are collected which multiply various powers of λ^2. Proceeding to this end, the first coefficient is c_2.

$$
\begin{aligned}
c_2 &= (D_1 - I_0\lambda^2)\,[e_0(f_1 + e_4\lambda^2) - e_1 e_2] + e_3(f_0 - r_1\lambda^2)(f_2 - r\lambda^2) \\
&= D_1 e_0 f_1 + D_1 e_0 e_4\lambda^2 - D_1 e_1 e_2 \\
&\qquad - I_0 e_0 f_1\lambda^2 \\
&\qquad + I_0 e_1 e_2\lambda^2 \qquad\qquad - I_0 e_0 e_4\lambda^4 \\
&\quad + e_3 f_0 f_2 - e_3(r_1 f_2 + r f_0)\lambda^2 \quad + e_3 r r_1\lambda^4
\end{aligned}
$$

$$c_2 = D_1(e_0f_1 - e_1e_2) + e_3f_0f_2$$

$$+ [D_1e_0e_4 + I_0(e_1e_2 - e_0f_1) - e_3(r_1f_2 + rf_0)]\lambda^2$$

$$+ (e_3rr_1 - I_0e_0e_4)\lambda^4$$

$$c_2 = D_1e_5 + e_3f_0f_2 + (D_1e_0e_4 - I_0e_5 - e_3f_5)\lambda^2 + (e_3rr_1 - I_0e_0e_4)\lambda^4$$

$$c_2 = e_7 + e_8\lambda^2 + e_9\lambda^4$$

where

$$e_7 = D_1e_5 + e_3f_0f_2$$

$$e_8 = D_1e_0e_4 - I_0e_5 - e_3f_5$$

$$e_9 = e_3rr_1 - I_0e_0e_4 \qquad \text{(D-4)}$$

Now this coefficient is squared

$$c_2^2 = e_7^2 + 2e_7e_8\lambda^2 + (e_8^2 + 2e_7e_9)\lambda^4 + 2e_8e_9\lambda^6 + e_9^2\lambda^8 \qquad \text{(D-5)}$$

$$c_0 = e_3[e_0(f_0 - r_1\lambda^2) - e_1^2]$$

$$= e_3(e_0f_0 - e_1^2) - e_3e_0r_1\lambda^2$$

$$= e_3(e_6 - e_0r_1\lambda^2) \qquad \text{(D-6)}$$

$$c_4 = (f_3 - r\lambda^2)(D_1 - I_0\lambda^2)(f_1 + e_4\lambda^2)$$

$$= (f_3 - r\lambda^2)[D_1f_1 + (D_1e_4 - I_0f_1)\lambda^2 - I_0e_4\lambda^4]$$

$$= f_3D_1f_1 + [f_3(D_1e_4 - I_0f_1) - rD_1f_1]\lambda^2$$

$$+ [r(I_0f_1 - D_1e_4) - f_3I_0e_4]\lambda^4 + rI_0e_4\lambda^6 \qquad \text{(D-7)}$$

Let

$$D_1 e_4 - I_o f_1 = f_9 \tag{D-8}$$

then

$$c_4 = f_3 D_1 f_1 + (f_3 f_9 - r D_1 f_1)\lambda^2 - (r f_9 + f_3 I_o e_4)\lambda^4 + r I_o e_4 \lambda^6$$

and

$$4c_o c_4 = 4e_3 \{(e_6 - e_o r_1 \lambda^2) c_4\}$$

$$= 4e_3 \{(e_6 f_3 D_1 f_1) + [e_6 (f_3 f_9 - r D_1 f_1) - e_o r_1 f_3 D_1 f_1]\lambda^2$$

$$- [e_6 (r f_9 + f_3 I_o e_4) + e_o r_1 (f_3 f_9 - r D_1 f_1)]\lambda^4$$

$$+ [e_6 r I_o e_4 + e_o r_1 (r f_9 + f_3 I_o e_4)]\lambda^6 - e_o r_1 r I_o e_4 \lambda^8 \}$$

Finally

$$4c_o c_4 = e_{10} + e_{11}\lambda^2 + e_{12}\lambda^4 + e_{13}\lambda^6 + e_{14}\lambda^8 \tag{D-9}$$

where

$$e_{10} = 4e_3 e_6 f_3 D_1 f_1$$

$$e_{11} = 4e_3 [e_6 (f_3 f_9 - r D_1 f_1) - e_o r_1 f_3 D_1 f_1]$$

$$e_{12} = -4e_3 [e_6 (r f_9 + f_3 I_o e_4) + e_o r_1 (f_3 f_9 - r D_1 f_1)]$$

$$e_{13} = 4e_3 [e_6 r I_o e_4 + e_o r_1 (r f_9 + f_3 I_o e_4)]$$

$$e_{14} = -4e_3 e_o r_1 r I_o e_4 \tag{D-10}$$

Equation (D-1) now becomes

$$C_8 \lambda^8 + C_6 \lambda^6 + C_4 \lambda^4 + C_2 \lambda^2 + C_o = 0 \tag{D-11}$$

where

$$C_8 = e_9^2 - e_{14}$$

$$C_6 = 2e_8 e_9 - e_{13}$$

$$C_4 = e_8^2 + 2e_7 e_9 - e_{12}$$

$$C_2 = 2e_7 e_8 - e_{11}$$

$$C_0 = e_7^2 - e_{10} \qquad \text{(D-12)}$$

If the axial and rotatory inertia are neglected

$$r_1 = 0$$

$$I_o = 0$$

$$e_4 = 0$$

$$f_6 = 0$$

$$f_4 = 0$$

$$f_5 = rf_o \qquad \text{(D-13)}$$

The coefficients in Equation (D-11) reduce to

$$C_6 = C_8 = 0$$

$$C_4 \rightarrow \overline{C}_4 = e_3[e_3 r^2 f_o^2] = e_3^2 r^2 f_o^2$$

$$\overline{C}_2 = 2\{D_1(-e_3 e_5 f_o r) + e_3[2e_6 r D_1 f_1 - e_3 f_o^2 f_2 r]\}$$

$$C_2 \rightarrow \overline{C}_2 = 2e_3[2e_6 r D_1 f_1 - f_o r(D_1 e_5 + e_3 f_o f_2)]$$

$$\overline{C}_o = C_o = (D_1 e_5 + e_3 f_o f_2)^2 - 4e_3 f_3 D_1 f_1 e_6 \qquad \text{(D-14)}$$

APPENDIX E

COMPUTER PROGRAM FOR SOLUTION OF LOAD VELOCITIES WHICH CAUSE REPEATED ROOTS IN THE UNDAMPED CHARACTERISTIC EQUATION

The program shown here is used for calculation of the location of the repeated roots of the undamped characteristic equation using the polynomials defined in Chapter IV. The program is written in Fortran for use on General Electric Company Mark II time sharing system. The only requirement for running the program is that a data file which is named "EMFILE" must be established which includes the data for the cases to be solved.

EMFILE is set up such that there are seven numbers in each line of the file, the first being the file line number; the next six are the dimensionless parameters h/R, E_{θ_o}/E_{x_o}, G_{xz_o}/E_{x_o}, E_{ν_o}/E_{x_o}, P, and F in that order. Starting the program will cause the eight roots for λ^2 to be calculated and printed. Also, the program automatically calculates the set of roots in which the axial and rotatory inertia are neglected. The following is a listing of the program.

VCRIT

```
100 DIMENSIØN A(5),RR(4),CR(4)
110 5 READ("EMFILE",2)DUMV,H,ETØEX,GXZØEX,E1U,P,F
120 2 FØRMAT(V)
130 N=4
140 IF(P-0)7,8,8
150 7 RØ=H/2;GØTØ 9
160 8 RO=-H/2
170 9 D1=(H)**2/12
180 XKX= 3.14159/(12.)↑.5
190 G=(XKX)↑2*GXZØEX
200 PRINT,"       H       ETHETA/EX  GXZ/EX     ENU/EX     P
210 &          F          G"
220
230 PRINT 10,H,ETØEX,GXZØEX,E1U,P,F,G
240 10 FØRMAT (7F10.5)
250 PRINT,"**********************************************
255 &*****************"
```

The above steps read the data from EMFILE and print the data used as a heading on the output.

```
260 PRINT,
270 EOU=ETØEX*(1+H↑2/12)
280 R=H
290 XIO=H↑3/12
300 R1=H
310 E0=EOU+P*R0
320 E1=E1U-P
330 E2=E1U-P+2*(G+P*R0)
340 E3=G+P*R0
350 15 E4=XIO-R1
360 F1=1+F-D1
370 F2=F-P*R0
380 F0=1+F
390 F3=G+F
400 E5=E0*F1-E1*E2
410 E6=E0*F0-E1*E1
420 F4=D1*R1+XIO*F0
430 F5=R1*F2+R*F0
440 F6=E4*D1-XIO*F1
450 F9=D1*E4-XIO*F1
460 E7=D1*E5+E3*F0*F2
470 E8=D1*E0*E4-XIO*E5-E3*F5
480 E9=E3*R*R1-XIO*E0*E4
490 E10=4*E3*E6*F3*D1*F1
500 E11=4*E3*(E6*(F3*F9-R*D1*F1)-E0*R1*F3*D1*F1)
510 E12=-4*E3*(E6*(R*F9+F3*XIO*E4)+E0*R1*(F3*F9-R*D1*F1))
520 E13=4*E3*(E6*R*XIO*E4+E0*R1*(R*F9+F3*XIO*E4))
```

```
530 E14=-4*E3*E0*R*R1*XI0*E4
540 C0=E7*E7-E10
550 C2=2*E7*E8-E11
560 C4=E8*E8+2*E7*E9-E12
570 C6=2*E8*E9-E13; C8=E9*E9-E14
580 C0P=F1*F3*D1
590 C2P=E4*F3*D1-F1*(R*D1+F3*XI0)
600 C4P=F1*R*XI0-E4*(R*D1+F3*XI0)
610 C6P=E4*XI0*R
620 PRINT 82
630 82 FORMAT(/"       C0              C2              C4
640 &           C6        C8" )
650 90 PRINT 20,C0,C2,C4,C6,C8
660 20 FORMAT(5E14.6//)
```

The above steps calculate the coefficients for the polynomials and print those for the fourth order polynomial.

```
670 A(1)=C0;A(2)=C2;A(3)=C4;A(4)=C6;A(5)=C8
680 CALL DOWNH(A,N,RR,CR)
690 PRINT,
700 PRINT,"                                REAL COMPONENT
705 &IMAGINARY COMPONENT"
710 DO 25 I=1,N
720 25 PRINT 50,I,RR(I),CR(I)
730 50 FORMAT (5H ROOT,I2,10X,1P2E20.7)
740 PRINT 60
750 60 FORMAT(/" THE RECONST. COEFF. OF THE POLYN. ARE:")
760 PRINT,
770 M=N+1
780 L=M+1
790 IF((-1)**N)110,100,100
800 100 PRINT 102
810 102 FORMAT(/"       C0              C2              C4
820 &           C6              C8")
```

The above steps solve for the roots of the fourth order polynomial and print the reconstructed coefficients as a check on the validity of the roots.

```
830 IF (M-5)67,73,73
840 67 DO 70 I=L,5
850 70 A(I)=0
860 73 PRINT 20,A(1),A(2),A(3),A(4),A(5)
870 PRINT,
880 PRINT 104
890 104 FORMAT("     COPRIME         C2PRIME         C4PRIME
895 &C6PRIME")
900 PRINT 66,COP,C2P,C4P,C6P
910 66 FORMAT(4E14.6//)
920 A(1)=COP;A(2)=C2P;A(3)=C4P;A(4)=C6P
930 75 N=N-1
940 IF(2-N)80,130,140
950 140 IF(-N)80,150,150
960 110 PRINT 112
970 112 FORMAT(/"     COPRIME         C2PRIME         C4PRIME
975 &C6PRIME")
980 IF(M-5)72,83,83
990 72 DO81 I=L,5
1000 81 A(I)=0
1010 83 PRINT 20,A(1),A(2),A(3),A(4),A(5)
1020 PRINT,
1030 GOTO 75
1040 130 VCR=E6/(E0*R1)
1050 PRINT 120,VCR
1060 PRINT 122
```

Lines 830 to 1060 direct the solution and printing of the other four roots for λ^2.

```
1070 122 FØRMAT(" NEGLECT. RØTAT. AND AX. INERTIA, THE
1080 & COEFF. & RØØTS ARE:"/)
1090 PRINT 99
1100 99 FØRMAT("                    **********************
1105 &********")
1110 IF(-XIO)30,40,40
1120 30 CONTINUE
1130 XIO=0
1140 R1=0
1150 GØTØ 15
1160 1 PRINT,
1170 150 PRINT,
1180 120 FØRMAT(" THE FINAL CRITICAL VELØCITY IS "E15.8//)
1190 PRINT 152
1200 152 FØRMAT(" THE FINAL CRIT. VEL. APPR. INFINITY"//)
1210 PRINT 160
1220 160 FØRMAT("---------------------------------------
1230 &-------------------------------"///)
1240
1250 40 GØTØ 5
1260 300 STØP
1270 END
```

This section of the program makes the simplification of neglecting axial and rotatory inertia and directs the solution for the corresponding roots.

APPENDIX F

PARTIAL FRACTION EXPANSION OF A FOURTH ORDER POLYNOMIAL

The characteristic equation $\overline{D}(s)$ can be factored as

$$\overline{D}(S) = c_4(s - s_1)(s - s_2)(s - s_3)(s - s_4) \tag{F-1}$$

so that

$$\frac{c'_5 s^2 + c'_6}{\overline{D}(s)} = \frac{c_5 s^2 + c_6}{(s - s_1)(s - s_2)(s - s_3)(s - s_4)} = \frac{A(s)}{B(s)} \tag{F-2}$$

Let

$$\frac{A(s)}{B(s)} = \frac{\beta_1}{s - s_1} + \frac{\beta_2}{s - s_2} + \frac{\beta_3}{s - s_3} + \frac{\beta_4}{s - s_4} \tag{F-3}$$

The coefficients β_k can be found (16) from the expression

$$\beta_k = \frac{A(s_k)}{B'(s_k)} \tag{F-4}$$

which means that A over the derivative of B is to be evaluated at $s = s_k$. This derivative is

$$B'(s) = \frac{d}{ds} B(s) = (s - s_1) \frac{d}{ds} [(s - s_2)(s - s_3)(s - s_4)] + (s - s_2)(s - s_3)(s - s_4) \tag{F-5}$$

Furthermore

$$\frac{d}{ds} [(s - s_2)(s - s_3)(s - s_4)] = (s - s_2) \frac{d}{ds} [(s - s_3)(s - s_4)] + (s - s_3)(s - s_4)$$

and

$$\frac{d}{ds} [(s - s_3)(s - s_4)] = (s - s_3) + (s - s_4)$$

Therefore

$$\frac{d}{ds}\left[(s - s_2)(s - s_3)(s - s_4)\right] = (s - s_2)\left[(s - s_3) + (s - s_4)\right] + (s - s_3)(s - s_4)$$

and

$$B'(s) = (s - s_1)\left\{(s - s_2)\left[(s - s_3) + (s - s_4)\right] + (s - s_3)(s - s_4)\right\} + (s - s_2)(s - s_3)(s - s_4)$$

Finally the coefficients can be condensed to the expression

$$\beta_k = \frac{A(s_k)}{B'(s_k)} = \frac{c_5 s_k^2 + c_6}{\prod_{p=1}^{p=4} (s_k - s_p)}, \qquad p \neq k \tag{F-6}$$

APPENDIX G

CHECK TO SEE THAT SOLUTIONS SATISFY THE GOVERNING DIFFERENTIAL EQUATIONS

The governing differential equations have the form

$$f_8 \frac{d^2U}{d\phi^2} + e_1 \frac{dW}{d\phi} + f_7 \frac{d^2\psi}{d\phi^2} = 0 \tag{G-1}$$

$$e_1 \frac{dU}{d\phi} - (f_3 - r\lambda^2) \frac{d^2W}{d\phi^2} - \epsilon\lambda \frac{dW}{d\phi} + e_o W - e_3 \frac{d\psi}{d\phi} = -q_o \left\{ H(-\phi) - H[-(\phi + d)] \right\} \tag{G-2}$$

$$f_7 \frac{d^2U}{d\phi^2} - e_3 \frac{dW}{d\phi} + f_7 \frac{d^2\psi}{d\phi^2} - e_3\psi = 0 \tag{G-3}$$

First find the second derivatives.

$$F_k''(\phi) = (-b_k + ia_k)^2 F_k(\phi) = -s_k^2 F_k(\phi)$$

$$_wF_k''(\phi) = \frac{-is_k\beta_k}{c_q\alpha_k} F_k(\phi)$$

$$_uF_k''(\phi) = \frac{c_6}{c_9} F_k(\phi) \tag{G-4}$$

Substituting into the first

$$f_8 \left\{ -\frac{c_5}{c_9} \left[\sum_k - s_k^2 F_k(\phi) \right] + \sum_k \frac{c_6}{c_9} F_k \right\} + e_1 \sum_k \frac{\beta_k}{c_a\alpha_k} F_k - f_7 \sum_k s_k^2 F_k \stackrel{?}{=} 0$$

$$\sum_{k=1}^{4} \left\{ \left[f_8 \frac{c_5}{c_9} s_k^2 + \frac{f_8 c_6}{c_9} - \frac{c_1}{c_9} (c_7 s_k^2 + c_8) - f_7 s_k^2 \right] F_k(\phi) \right\} \stackrel{?}{=} 0$$

The bracketed term must be zero if Equation (G-3) is satisfied by the solution.

$$\left(f_8 \frac{c_5}{c_9} - \frac{e_1 c_7}{c_9} - f_7\right) s_k + \frac{f_8 c_6 - e_1 c_8}{c_9} \stackrel{?}{=} 0 \qquad \text{(G-5)}$$

Look at the second term to see if it is zero because both terms in Equation (G-5) must be zero.

$$f_8 c_6 - e_1 c_8 = f_8 c_6 - e_1 e_3 f_8 = f_8 (c_6 - e_1 c_3)$$

$$= f_8 (e_1 e_3 - e_1 e_3) = 0$$

Now the first term is inspected.

$$f_8 c_5 - e_1 c_7 - f_7 c_9 = f_7 [f_8 (e_3 + e_1) - e_1 (f_1 + e_4 \lambda^2) - (e_1 f_7 + e_3 f_8)]$$

$$= f_7 [e_1 (f_8 - f_7 - f_1 - e_4 \lambda^2)]$$

$$= e_1 f_7 [f_0 - r_1 \lambda^2 - D_1 + I_0 \lambda^2 - 1 - F + D_1$$

$$- (I_0 - r_1)\lambda^2] = 0$$

Thus the solution satisfies Equation (G-1). Now Equation (G-3) is checked.

$$\sum_{k=1}^{4} \left\{ \left[f_7 \frac{c_5}{c_9} s_k^2 + \frac{f_7 c_6}{c_9} + e_3 \frac{(c_7 s_k^2 + c_8)}{c_9} - f_7 s_k^2 - e_3 \right] F_k(\phi) \right\} \stackrel{?}{=} 0 \qquad \text{(G-6)}$$

or

$$\left(f_7 \frac{c_5}{c_9} + \frac{e_3 c_7}{c_9} - f_7\right) s_k^2 + \left(\frac{f_7 c_6}{c_9} + \frac{e_3 c_8}{c_9} - e_3\right) \stackrel{?}{=} 0$$

Look at the second term.

$$f_7 c_6 + e_3 (c_8 - c_9) = e_3 (f_7 e_1 + c_8 - c_9) = e_3 (e_1 f_7 - e_1 f_7) = 0$$

Now look at the first term

$$f_7 [c_5 + e_3 (f_1 + e_4 \lambda^2)$$

$$- e_1 f_7 - e_3 f_8] = f_7 [f_7 e_1 + e_3 (f_1 + e_4 \lambda^2 - f_8 + f_7) - f_7 e_1] = 0$$

So Equation (G-3) is satisfied by the solution. Now Equation (G-2) will be checked.

$$e_1\left[-\frac{c_5}{c_9} i \sum_k s_k F_k + \sum_k \left(-\frac{c_6 i}{c_9 s_k} F_k + B_k\right)\right.$$

$$- (f_3 - r\lambda^2)\left[\sum_k - \frac{i s_k (c_7 s_k^2 + c_8)}{c_9} F_k\right]$$

$$- \epsilon\lambda \sum_k \left(-\frac{c_7 s_k^2 + c_8}{c_9} F_k\right) + e_o\left\{\sum_k \left[\frac{i(c_7 s_k^2 + c_8)}{s_k c_9} F_k + A_k\right.\right.$$

$$- e_3 \sum_k (i s_k F_k) \stackrel{?}{=} - \{H(-\phi) - H[-(\phi + d)]\} \qquad \text{(G-7)}$$

where

$$B_k = \frac{\text{sgn}(b_k)\, c_6 \alpha_k}{2 s_k} \{H[\text{sgn}(b_k)\phi] - H[-\text{sgn}(b_k)\phi]$$

$$- H[\text{sgn}(b_k)(\phi + d)] + H[-\text{sgn}(b_k)(\phi + d)]\}$$

$$A_k = \text{sgn}(b_k) \frac{\beta_k}{2 s_k} \{-H[\text{sgn}(b_k)\phi] + H[-\text{sgn}(b_k)\phi]$$

$$+ H[\text{sgn}(b_k)(\phi + d)] - H[-\text{sgn}(b_k)(\phi + d)]\}$$

Collecting terms gives

$$\sum_{k=1}^{4} \left\{\left[\frac{-i e_1 c_5 s_k}{c_9} - i\frac{e_1 c_6}{c_9 s_k} + \frac{f_3 - r\lambda^2)}{c_9} i s_k (c_7 s_k^2 + c_8)\right.\right.$$

$$+ \frac{\epsilon\lambda}{c_9}(c_7 s_k^2 + c_8) + \frac{i e_o}{s_k c_9}(c_7 s_k^2 + c)$$

$$\left.\left. - i e_3 s_k\right] F_k + e_1 B_k + e_o A_k\right\} \stackrel{?}{=} - \{H(-\phi) - H[-(\phi + d)]\}$$

(G-8)

Looking first at the term multiplying F_k, which is

$$i\left\{\frac{c_7}{c_9}(f_3 - r\lambda^2)\, s_k^3 - \left[\frac{e_1c_5 - c_8(f_3 - r\lambda^2) - e_0c_7}{c_9} + e_3\right] s_k\right\}$$

$$+ \frac{\epsilon\lambda c_7}{c_9} s_k + \frac{\epsilon\lambda c_8}{c_9} + i\frac{(e_0c_8 - e_1c_6)}{c_9}$$

Multiply and divide this by (is_k) and get

$$\frac{1}{c_9 i s_k}\{-c_7(f_3 - r\lambda^2)\, s_k^4 + i\epsilon\lambda c_7\, s_k^3 + s_k^2[e_1c_5 - c_8(f_3 - r\lambda^2) - e_0c_7 + e_3c_9]$$

$$+ i\epsilon\lambda c_8\, s_k - (e_0c_8 - e_1c_6)\}$$

Look at the coefficients on powers of s_k

$$\underline{-e_0c_8 + e_1c_6} = -e_0(e_3f_8) + e_1(e_1e_3)$$

$$= -e_3(f_8e_3 - e_1^2) = \underline{-c_0}$$

$$\underline{\epsilon\lambda c_8} = e_3f_8\epsilon\lambda = \underline{-c_1}$$

$$\underline{e_1c_5 - c_8(f_3 - r\lambda^2) - e_0c_7 + e_3c_9} = f_7e_1(e_3 + e_1) - e_3f_8(f_3 - r\lambda^2) - e_0f_7c + e_3(e_1f_7 + e_3f_8)$$

$$= -f_7(e_0c - e_1e_3) - e_3f_8(-e_3 + f_3 - r\lambda^2) - f_7(-e_1e_3 - e_1^2)$$

$$= -f_7(e_0c - 2e_1e_3 - e_1^2) - e_3f_8(-G - Pr_0 + G + F - r\lambda^2)$$

$$= -f_7[e_0c - e_1(e_1 + 2e_3)] - e_3f_8(f_2 - r\lambda^2)$$

$$= -f_7(e_0c - e_1e_2) - e_3f_8(f_2 - r\lambda^2) = \underline{-c_2}$$

Similarly

$$\underline{\epsilon\lambda c_7} = \underline{-c_3}$$

$$\underline{-c_7 (f_3 - r\lambda^2)} = \underline{-c_4}$$

so the term multiplying F_k is the characteristic equation which is evaluated at $s = s_k$. Of course this equation goes to zero for all roots s_k.

The remaining identity which has to be proven is

$$\sum_{k=1}^{4} (e_1 B_k + c_o A_k) = -\{H(-\phi) - H[-(\phi + d)]\} \qquad \text{(G-9)}$$

Noting the identity

$$\frac{\text{sgn}(b_k)}{2}\{H[\text{sgn}(b_k)\,\phi] - H[-\text{sgn}(bk)\,\phi] - H[\text{sgn}(bk)\,(\phi + d)] + H[-\text{sgn}(bk)\,(\phi + d)]\} \equiv -\{H(-\phi) - H[-(\phi + d)]\} \qquad \text{(G-10)}$$

which holds whether b_k is less than or greater than zero, the remaining statement which is to be proved is

$$\sum_{k=1}^{4} \left(\frac{e_1 c_6 \alpha_k}{s_k} - \frac{e_o \beta_k}{s_k} \right) = 1$$

or

$$\sum_{k=1}^{4} \frac{\alpha_k}{s_k} [e_1 c_6 - e_o (c_7 s_k^2 + c_8)] = 1$$

Substituting for c_i ($i = 6, 7, 8$) gives

$$\sum_{k=1}^{4} \frac{\alpha_k}{s_k} [e_o f_7 (f_1 + e_4 \lambda^2) s_k^2 + c_o] \equiv -c_4 \qquad \text{(G-11)}$$

This is an identity and is programmed to be checked with each case calculated using the computer program.

APPENDIX H

COMPUTER PROGRAM FOR DEFLECTION AND STRESS CALCULATIONS

The computer program DEFSTR calculates the deflections and stresses in the cylinder. There are two required functions to perform in order to operate the program as set up for operation on the General Electric Company Mark II Fortran time sharing system. The first is the establishment of a data file (called EMDATA in the program). This file has ten elements on each line of the file. The first element is the line number and following that are the dimensionless data h/R, E_{θ_0}/E_{x_0}, G_{xz_0}/E_{x_0}, E_{ν_0}/E_{x_0}, P, F, ϵ, λ^2, and d.

When the data file has been established and the program DEFSTR called and asked to run, a request for data is received which must be in the form: KEY1, KEY2. KEY1 and KEY2 are integer values which allow the selection of the type of analysis to be done and the type of output desired. KEY1 deals with the inclusion or neglection of inertia terms; KEY2 allows the amount of analysis and output to be regulated as shown in Table H-1.

Table H-1. Options Available for Program DEFSTR

	Mode of Operation of the Computer Program
KEY1	
1	Neither Axial Inertia nor Rotatory Inertia is Neglected
2	Both Axial Inertia and Rotatory Inertia Are Neglected
3	The Axial Inertia Is Neglected
4	The Rotatory Inertia Is Neglected
5	Neither and Then Both Inertias Are Neglected
6	Neither and Then Both Inertias Are Neglected
7	Neither and Then the Rotatory Inertia Is Neglected
8	Neither, Then Axial, Then Rotatory
9	Neither, Then Axial, Then Rotatory, Then Both
KEY2	
1	The Deflections Are Printed
2	Deflections and the Individual Stresses Are Printed
3	Deflections, Individual and Surface Stresses Printed
4	Deflections and Surface Stresses Printed
5	Only Surface and Individual Stresses Printed
6	Only Individual Stresses Printed
7	Only Surface Stresses Printed
8	Only the Roots of the Characteristic Equation Printed

A listing of the program is included here.

DEFSTR

```
100 FUNCTION MULT(AX,B)
110 REAL MULT
```

```
120 IF(AX.EQ.0)GØTØ 7000;IF(B.EQ.0)GØTØ 7000
130 AL=ALØG(ABS(AX));BL=ALØG(ABS(B))
140 ALIM=-80.0
150 IF(AL+BL.LT.ALIM)GØTØ 7000
160 PRØD=AX*B;GØTØ 7010
170 7000 PRØD=0
180 7010 MULT=PRØD
190 RETURN;END
200 FUNCTIØN DIV(AX,B,C,D)
210 REAL MULT
220 Y1=MULT(AX,C);Y2=MULT(B,D)
230 CL=Y1+Y2
240 Y3=MULT(C,C);Y4=MULT(D,D)
250 DL=Y3+Y4
260 IF(CL.EQ.0)GØTØ 7015
270 AL=ALØG(ABS(CL))
280 7015 AL=0
290 BL=ALØG(ABS(DL))
300 ALIM=-80.0
310 IF(AL-BL.LT.ALIM)GØTØ 7020
320 QUØT=CL/DL;GØTØ 7030
330 7020 QUØT=0
340 7030 DIV=QUØT
350 RETURN;END
```

The steps in lines 100-350 define two functions for the multiplication and division of complex numbers.

```
360 REAL MULT
370 DIMENSION A(5),AI(5),RR(4),CR(4),DRR(3),DCR(3),RA(4),
380 &CB(4),0(121),EP1R(4),EP1I(4),EP2R(4),EP2I(4),SGN(4),
390 &FP2R(4),FP2I(4),FPR(4),FPI(4),FLR(4),FLI(4),FR(4),FI(4),
400 &WFP1I(4),WFP2R(4),WFP2I(4),WFPR(4),WFPI(4),WFR(4),
410 &DFI(4),DWFR(4),DWFI(4),DEP1R(4),DEP1I(4),DEP2R(4),
420 &DUFR(4),DUFI(4),UFP1R(4),UFP1I(4),UFP2R(4),UFP2I(4),
430 & UFPI(4),UFLR(4),UFLI(4),P00R(121),P00I(121),W00R(121),
440 &U00R(121),U00I(121),SXM(121),STM(121),SXB(121),STB(121),
450 &SX0(121),ST0(121),SXI(121),STI(121)
460 &,UFR(4),UFI(4),RR1(4),CR1(4),RR2(4),CR2(4)
465 & CA(4),RB(4),FP1R(4),FP1I(4),WFP1R(4),WFI(4),DFR(4),
467 & DEP2I(4),UFPR(4),W00I(121),SXZ(121)
470 INPUT,KEY1,KEY2
480 5 READ("EMDATA",10)DUMV,H,ET0EX,GXZ0EX,E1U,P,F,EP,V,D
490 10 F0RMAT(V)
500 PRINT 15
510 15 F0RMAT("   H  ETHETA/EX  GXZ/EX  ENU/EX      P
520 &         F      EPSIL0N  LAMBDA**2  D")
530 PRINT 20,H,ET0EX,GXZ0EX,E1U,P,F,EP,V,D
540 20 F0RMAT(F6.4,5F9.6,F8.6,F8.3,F5.2)
550 PRINT 30
560 30 FORMAT("**********************************
570 &**********************"//)
```

The above steps reserve the required locations for the program variables and request for the input KEY1, KEY2. Then the first set of data is printed and calculations begin.

```
580 N=4
590 L3=0
600 IF(P-0)7,8,8
610 7 R0=H/2;GØTØ 9
620 8 R0=-H/2
630 9 D1=(H**2)/12
640 XKX= 3.14159/(12.)↑.5
650 G=(XKX)↑2*GXZØEX
660 EOU=ETØEX*(1+H↑2/12)
670 R=H
680 L=0
690 GØTØ(40,46,44,42,40,40,40,40,40),KEY1
700 40 XIO=(H**3)/12
710 R1=H
720 GØTØ 48
730 42 PRINT 41
740 41 FØRMAT(" NEGLECTING RØTATØRY INERTIA GIVES:"//)
750 XIO=0
760 R1=H
770 GØTØ 48
780 44 PRINT 43
790 43 FØRMAT(" NEGLECTING AXIAL INERTIA GIVES:"//)
800 XIO=(H**3)/12
810 R1=0
820 GØTØ 48
830 46 PRINT 47
840 47 FØRMAT(" NEGLECTING AXIAL AND RØT. INERTIA GIVES:"//)
```

```
850 XIO=0
860 R1=0
870 GØTO 48
880 48 L=L+1
```

The logic in lines 580-880 establishes the inertia terms to be used based upon the keyed input.

```
890 E0=E0U+P*R0
900 E1=E1U-P
910 E2=E1U-P+2*(G+P*R0)
920 E3=G+P*R0
930 E4=XI0-R1
940 F1=1+F-D1
950 F2=F-P*R0
960 F0=1+F
970 F3=G+F
980 E5=E0*F1-E1*E2
990 E6=E0*F0-E1*E1
1000 F4=D1*R1+XI0*F0
1010 F5=R1*F2+R*F0
1020 F6=E4*D1-XI0*F1
1030 F7=D1-XI0*V
1040 F8=F0-R1*V
1050 C=F1+E4*V
1060 C0=E3*(F8*E0-E1*E1)
1070 C1=-EP*((V)**.5)*E3*F8
1080 C2=F7*(E0*C-E1*E2)+E3*F8*(F2-R*V)
1090 C3= -EP*((V)**.5)*F7*C
1100 C4=F7*C*(F3-R*V)
```

```
1110 C5=(F7*(E3+E1))/C4
1120 C6=(E1*E3)/C4
1130 C7=(F7*(F1+E4*V))/C4
1140 C8=(E3*F8)/C4
1150 C9=(E1*F7+E3*F8)/C4
1160 PRINT 100
1170 100 FØRMAT("       C0,C5         C1,C6         C2,C7
1180 &C3,C8         C4,C9")
1190 PRINT 110,C0,C1,C2,C3,C4,C5,C6,C7,C8,C9
1200 110 FØRMAT(1P5E14.6)
1210 N=4
1220 CHK=0
1230 A(1)=C0;A(2)=0;A(3)=C2;A(4)=0;A(5)=C4
1240 AI(1)=0;AI(2)=C1;AI(3)=0;AI(4)=C3;AI(5)=0
1250 120 CALL CDØWNH(A,AI,N,RR,CR)
1260 140 PRINT 150
1270 150 FØRMAT(/"           REAL PART         IMAG. PART
1280 &              REAL PART     IMAG. PART")
1290 PRINT 160,RR(1),CR(1),RR(2),CR(2)
1300 160 FØRMAT(" RØØT 1 "1P2E14.7,", RØØT 2 "1P2E14.7)
1310 PRINT 170,RR(3),CR(3),RR(4),CR(4)
1320 170 FØRMAT(" RØØT 3 "1P2E14.7,", RØØT 4 "1P2E14.7)
1330 PRINT 180
1340 180 FØRMAT(/" THE RECØN. CØEFF. ØF THE PØLYN. ARE:")
1350 PRINT 190
1360 190 FØRMAT(/" RE/IM--C0            C1              C2
1370 &     C3            C4")
1380 PRINT 110,A(1),A(2),A(3),A(4),A(5)
```

Lines 890-1380 direct the calculation of the coefficients, the solution of the Characteristic Equation for the roots and the printing of the reconstructed coefficients.

```
1390 IF(EP)1100,1100,205
1400 205 CONTINUE
1410 PRINT 110,AI(1),AI(2),AI(3),AI(4),AI(5)
1420 1100 IF(KEY2-8)200,1000,200
1430 1000 GØTØ(1010,1020,1030,1040),L
1440 1010 GØTØ(790,790,790,790,46,44,42,44,44),KEY1
1450 1020 GØTØ(790,790,790,790,790,790,790,42,42),KEY1
1460 1030 GØTØ(790,790,790,790,790,790,790,790,46),KEY1
1470 1040 GØTØ 790
1480 200 DØ 204 K=1,4
1490 RR1(K)=RR(K)
1500 204 CR1(K)=CR(K)
1510 DØ 700 J=1,51
1520 Ø(J)=-1.02+.02*J
1530 DØ 500 K=1,4
```

The logic in lines 1390-1530 uses the keyed input to direct control to the desired location.

```
1540CCALCULATIØN ØF ALPHA(K)
1550 IF (J.GT.1)GØTØ 209
1560 I=1
1570 DØ 206 M=1,4
1580 IF(K-M)208,206,208
1590 208 DRR(I)=RR(K)-RR(M)
1600 DCR(I)=CR(K)-CR(M)
1610 I=I+1
1620 206 CØNTINUE
1630 AR=DRR(1);XAI=DCR(1);BR=DRR(2);BI=DCR(2)
1640 XCR=MULT(AR,BR)-MULT(XAI,BI);CI=MULT(AR,BI)+MULT(XAI,BR)
1650 AR=XCR;XAI=CI;BR=DRR(3);BI=DCR(3)
1660 XCR=MULT(AR,BR)-MULT(XAI,BI);CI=MULT(AR,BI)+MULT(XAI,BR)
1670 AR=1.0;XAI=0;BR=XCR;BI=CI
1680 XCR=DIV(AR,XAI,BR,BI);CI=DIV(XAI,-AR,BR,BI)
1690 RA(K)=XCR;CA(K)=CI
```

If the deflections or stresses are requested, the coefficient α_k (used in the calculation of the partial fraction expansion of the Characteristic Equation) is determined in lines 1540-1690.

```
1700C CHECK TØ SEE IF SØLUTIØN SATISFIES THE DIFF. EQUATIØNS
1710 AR=RR(K);XAI=CR(K);BR=RR(K);BI=CR(K)
1720 XCR=MULT(AR,BR)-MULT(XAI,BI);CI=MULT(AR,BI)+MULT(XAI,BR)
1730 RNUM=XCR;CNUM=CI;AR=RA(K);XAI=CA(K)
1740 XCR=DIV(AR,XAI,BR,BI);CI=DIV(XAI,-AR,BR,BI)
1750 AR=E0*C7*C4*RNUM+C0;XAI=E0*C7*C4*CNUM
1760 BR=XCR;BI=CI
1770 XCR=MULT(AR,BR)-MULT(XAI,BI);CI=MULT(AR,BI)+MULT(XAI,BR)
1780 CHK=XCR+CHK
1790 IF(K.NE.4)GØTØ 6001
1800 ULIM=ABS(CHK+C4);IF(ULIM-EPSILØN)6001,6003,6003
1810 6003 PRINT 6004
1820 6004 FØRMAT(/" THE D.E. IS NØT SATISFIED BY THE SØL.")
```

The expression derived in Appendix G, Equation (G-11) is checked in the above logic to ascertain that the solution satisfies the Differential Equations.

```
1830CCALCULATIØN ØF BETA(K)
1840 6001 CØNTINUE
1850 AR=RR(K);XAI=CR(K);BR=RR(K);BI=CR(K)
1860 XCR=MULT(AR,BR)-MULT(XAI,BI);CI=MULT(AR,BI)+MULT(XAI,BR)
1870 AR=(C7*XCR)+C8
1880 XAI=C7*CI
1890 BR=RA(K);BI=CA(K)
1900 XCR=MULT(AR,BR)-MULT(XAI,BI);CI=MULT(AR,BI)+MULT(XAI,BR)
1910 RB(K)=XCR
1920 CB(K)=CI
1930 209 CØNTINUE
1940C CALCULATIØN ØF E TØ THE IS(K)Ø AND IS(K)(Ø+D) PØWERS
1950 AR= -Ø(J)*CR(K);XAI=Ø(J)*RR(K)
```

```
1960 DELTA=-20
1970 IF(AR.LT.DELTA)GØTØ 211
1980 IF(AR.GT.1)GØTØ211
1990 XCR=MULT(EXP(AR),CØS(XAI));CI=MULT(EXP(AR),SIN(XAI))
2000 GØTØ 212
2010 211 EP1R(K)=0;EP1I(K)=0
2020 GØ TØ 217
2030 212 EP1R(K)=XCR;EP1I(K)=CI
2040 217 CØNTINUE
2050 AR= -(Ø(J)+D)*CR(K); XAI=(Ø(J)+D)*RR(K)
2060 IF(AR.LT.DELTA)GØTØ 213
2070 IF(AR.GT.1)GØTØ 213
2080 XCR=MULT(EXP(AR),CØS(XAI));CI=MULT(EXP(AR),SIN(XAI))
2090 GØTØ 214
2100 213 EP2R(K)=0;EP2I(K)=0
2110 GØTØ 218
2120 214 EP2R(K)=XCR;EP2I(K)=CI
2130 218 CØNTINUE
```

The β_k and exponential terms are calculated above.

```
2140C CALCULATION OF SGN(B(K)) AND THE HEAVISIDE FUNCTIONS
2150 IF(J.GT.1)GOTO 325
2160 AV=ABS(CR(K))
2170 IF(AV.LT.1E-4)CR(K)=0
2180 295 IF(CR(K))300,310,320
2190 310 IF(L3.EQ.0)GO TO 311
2200 DO 318 L4=1,4
2210 RR(L4)=RR2(L4)
2220 318 CR(L4)=CR2(L4)
2230 GOTO 288
2240 311 M=1
2250 EP=SMALLV
2260 GOTO 270
2270 260 EP=10*Z
2280 270 C1=-EP*((V)**.5)*E3*F8
2290 C3=-EP*((V)**.5)*F7*C
2300 AI(1)=0;AI(2)=C1;AI(3)=0;AI(4)=C3;AI(5)=0
2310 CALL CDOWNH(A,AI,N,RR,CR)
2320 L3=1+L3
2330 DO 273 L2=1,4
2340 RR2(L2)=RR(L2)
2350 273 CR2(L2)=CR(L2)
2360 PRINT 275,M,EP,RR(1),CR(1),RR(2),CR(2),RR(3),CR(3),
2365 &RR(4),CR(4)
2370 275 FORMAT(I2,F7.4,1P4E15.7/9X,1P4E15.7)
2380 288 IF(CR(K))300,290,320
2390 290 M=M+1;Z=EP;GOTO260
2400 300 SGN(K)=-1
```

```
2410 GØTØ 325
2420 320 SGN(K)=1
2430 325 IF(SGN(K))330,360,360
2440 330 IF(Ø(J))340,350,350
2450 340 HØ=1; HØN=0
2460 GØTØ 390
2470 350 HØ=0; HØN=1
2480 GØTØ 390
2490 360 IF(Ø(J))370,380,380
2500 370 HØ=0; HØN=1
2510 GØTØ 390
2520 380 HØ=1; HØN=0
2530 390 IF(SGN(K))400,430,430
2540 400 IF(Ø(J)+D)410,420,420
2550 410 HØD=1;HØDN=0
2560 GØTØ 460
2570 420 HØD=0;HØDN=1
2580 GØTØ 460
2590 430 IF(Ø(J)+D)440,450,450
2600 440 HØD=0;HØDN=1
2610 GØTØ 460
2620 450 HØD=1;HØDN=0
2630 460 DØ 465 L1=1,4
2640 RR(L1)=RR1(L1)
2650 465 CR(L1)=CR1(L1)
```

The sgn function and the Heaviside step functions are determined in steps 2140-2650.

```
2660C CALCULATE F(K) AND F(K)PRIME
2670 FP1R(K)=H0*EP1R(K); FP1I(K)=H0*EP1I(K)
2680 FP2R(K)=H0D*EP2R(K) ;FP2I(K)=H0D*EP2I(K)
2690 FPR(K)=FP1R(K)-FP2R(K)
2700 BR=FPR(K)
2710 FPI(K)=FP1I(K)-FP2I(K)
2720 BI=FPI(K)
2730 FLR(K)=SGN(K)*C9*CA(K)
2740 AR=FLR(K)
2750 FLI(K)=-SGN(K)*C9*RA(K)
2760 XAI=FLI(K)
2770 XCR=MULT(AR,BR)-MULT(XAI,BI);CI=MULT(AR,BI)+MULT(XAI,BR)
2780 FR(K)=XCR; FI(K)=CI
2790 AR=-CR(K);XAI=RR(K);BR=FR(K);BI=FI(K)
2800 XCR=MULT(AR,BR)-MULT(XAI,BI);CI=MULT(AR,BI)+MULT(XAI,BR)
2810 DFR(K)=XCR; DFI(K)=CI
2820C CALCULATION OF WF(K)
2830 WFP1R(K)=(-.5+EP1R(K))*H0 +(.5)*H0N
2840 WFP1I(K)=EP1I(K)*H0
2850 WFP2R(K)=(-.5+EP2R(K))*H0D+(.5)*H0DN
2860 WFP2I(K)=EP2I(K)*H0D
2870 WFPR(K)=WFP1R(K)-WFP2R(K)
2880 WFPI(K)=WFP1I(K)-WFP2I(K)
2890 AR=RB(K);XAI=CB(K);BR=RR(K);BI=CR(K)
2900 XCR=DIV(AR,XAI,BR,BI);CI=DIV(XAI,-AR,BR,BI)
2910 AR=SGN(K)*XCR;XAI=SGN(K)*CI;BR=WFPR(K);BI=WFPI(K)
2920 XCR=MULT(AR,BR)-MULT(XAI,BI);CI=MULT(AR,BI)+MULT(XAI,BR)
2930 WFR(K)=XCR; WFI(K)=CI
2940 AR=RB(K);XAI=CB(K);BR=FR(K);BI=FI(K)
```

```
2950 XCR=MULT(AR,BR)-MULT(XAI,BI);CI=MULT(AR,BI)+MULT(XAI,BR)
2960 BR=-C9*RA(K);BI=-C9*CA(K);AR=XCR;XAI=CI
2970 XCR=DIV(AR,XAI,BR,BI);CI=DIV(XAI,-AR,BR,BI)
2980 DWFR(K)=XCR; DWFI(K)=CI
2990C CALCULATIØN ØF UF(K) AND THE DERIVATIVE ØF UF(K)
3000 UFP1R(K)=(-.5*(1-CR(K)*Ø(J))+EP1R(K))*HØ
3010 & +(.5)*(1-CR(K)*Ø(J))*HØN
3020 UFP1I(K)=(-.5*RR(K)*Ø(J)+EP1I(K)*HØ+
3025 & .5*(1+RR(K)*Ø(J))*HØN
3030 UFP2R(K)=(-.5*(1-CR(K)*(Ø(J)+D))+EP2R(K))*HØD
3040 & +(.5)*(1-CR(K)*(Ø(J)+D))*HØDN
3050 UFP2I(K)=(-.5*RR(K)*(Ø(J)+D)+EP2I(K))*HØD
3060 & +.5*RR(K)*(Ø(J)+D)*HØDN
3070 UFPR(K)=UFP1R(K)-UFP2R(K)
3080 UFPI(K)=UFP1I(K)-UFP2I(K)
3090 BR=RR(K);AR=RR(K);BI=CR(K);XAI=CR(K)
3100 XCR=MULT(AR,BR)-MULT(XAI,BI);CI=MULT(AR,BI)+MULT(XAI,BR)
3110 AR=-SGN(K)*C6*CA(K); XAI=SGN(K)*C6*RA(K);BR=XCR;BI=CI
3120 XCR=DIV(AR,XAI,BR,BI);CI=DIV(XAI,-AR,BR,BI)
3130 UFLR(K)=XCR;UFLI(K)=CI;AR=XCR;XAI=CI;BR=UFPR(K);
3135 & BI=UFPI(K)
3140 XCR=MULT(AR,BR)-MULT(XAI,BI);CI=MULT(AR,BI)+MULT(XAI,BR)
3150 UFR(K)=XCR; UFI(K)=CI
3160 AR=RR(K);XAI=CR(K);BR=RR(K);BI=CR(K)
3170 XCR=MULT(AR,BR)-MULT(XAI,BI);CI=MULT(AR,BI)+MULT(XAI,BR)
3180 AR=WFR(K);XAI=WFI(K);BR=C7*XCR+C8;BI=C7*CI
3190 XCR=DIV(AR,XAI,BR,BI);CI=DIV(XAI,-AR,BR,BI)
3200 DUFR(K)=-C6*XCR;DUFI(K)=-C6*CI
```

The F_k functions and their derivatives are calculated in lines 2660-3200.

```
3210 500 CONTINUE
3220C CALCULATIØN ØF DISPLACEMENTS
3230 PØØR(J)=FR(1)+FR(2)+FR(3)+FR(4)
3240 PØØI(J)=FI(1)+FI(2)+FI(3)+FI(4)
3250 WØØR(J)=WFR(1)+WFR(2)+WFR(3)+WFR(4)
3260 WØØI(J)=WFI(1)+WFI(2)+WFI(3)+WFI(4)
3270 UØØR(J)=-(C5*PØØR(J))/C9+UFR(1)+UFR(2)+UFR(3)+UFR(4)
3280 UØØI(J)=-(C5*PØØI(J))/C9+UFI(1)+UFI(2)+UFI(3)+UFI(4)
3290C CALCULATIØN ØF THE DERIVATIVES ØF THE DISPLACEMENTS
3300 DP=DFR(1)+DFR(2)+DFR(3)+DFR(4)
3310 DW =DWFR(1)+DWFR(2)+DWFR(3)+DWFR(4)
3320 DUF=DUFR(1)+DUFR(2)+DUFR(3)+DUFR(4)
3330 DU=-(C5*DP)/C9+DUF
3340C CALCULATIØN ØF THE STRESSES
3350 SXM(J)=E1U*WØØR(J)+D1*DP+DU
3360 STM(J)=EØU*WØØR(J)+E1U*DU
3370 SXB(J)=.5*H*(DU+DP)
3380 STB(J)=(.5*H)*(E1U*DP-ETØEX*WØØR(J))
3390 SXZ(J)=G*(PØØR(J)+DW)
3400 SXØ(J)=SXM(J)-SXB(J);STØ(J)=STM(J)-STB(J)
3410 SXI(J)=SXM(J)+SXB(J);STI(J)=STM(J)+STB(J)
3420 700 CØNTINUE
3430 GØTØ(505,505,505,505,540,540,580),KEY2
3440 505 DØ 522 J=1,51
3450 IF(J.GT.1)GØTØ 515
3460 PRINT 510
```

```
3470 510 FØRMAT(/ 6X,1HØ,15X,1HW,20X,1HU,18X,3HPSI)
3480 515 PRINT 520,Ø(J),WØØR(J),UØØR(J),PØØR(J)
3490 520 FØRMAT(1F10.5,1P3E20.6)
3500 522 CØNTINUE
3510 GØTØ(1000,540,540,580),KEY2
3520 540 DØ 575 J=1,51
3530 IF(J.GT.1)GØTØ 560
3540 PRINT 550
3550 550 FØRMAT(/3X,1HØ,8X,3HSXM,10X,3HSXB,10X,3HSTM,10X,
3560 &3HSTB,10X,3HSXZ)
3570 560 PRINT 570,Ø(J),SXM(J),SXB(J),STM(J),STB(J),SXZ(J)
3580 570 FØRMAT(1F6.2,1P5E13.6)
3590 575 CØNTINUE
3600 GØTØ(1000,1000,580,580,580,1000),KEY2
3610 580 DØ 610 J=1,51
3620 IF(J.GT.1)GØTØ 600
3630 PRINT 590
3640 590 FØRMAT(/3X,1HØ,8X,3HSXØ,10X,3HSTØ,10X,3HSXI,10X,
3650 &3HSTI,10X,3HSXZ)
3660 600 PRINT 570,Ø(J),SXØ(J),STØ(J),SXI(J),STI(J),SXZ(J)
3670 610 CØNTINUE
3680 GØTØ 1000
3690 790 PRINT 800
3700 800 FØRMAT(////////)
3710 810 GØTØ 5
3720 820 STØP;END
```

The displacements and stresses are calculated and printed as requested and control is diverted to EMDATA to pick up other cases as directed in lines 3210-3720.

APPENDIX I

RELATIONSHIPS BETWEEN ANALYSIS PARAMETERS

Dimensionless and Physical Parameter Relationships

Prestress

$$P = \frac{N}{E_x} = \frac{N}{E_{x_o} h} \tag{I-1}$$

$$F = \frac{T}{E_x} = \frac{T}{E_{x_o} h} \tag{I-2}$$

Material Properties

$$G = \frac{G_x}{E_x} = \frac{K_x^2 G_{xz_o} h}{E_{x_o} h} = K_x^2 \frac{G_{xz_o}}{E_{x_o}} \tag{I-3}$$

$$E_o = \frac{E_\theta}{E_x}\left(1 + \frac{D_\theta}{E_\theta R^2}\right) = \frac{E_{\theta_o}}{E_{x_o}}\left[1 + \frac{(h/R)^2}{12}\right] \tag{I-4}$$

$$E_1 = \frac{E_\nu}{E_x} = \frac{E_{\nu_o}}{E_{x_o}} \tag{I-5}$$

Other

$$D_1 = \frac{D_x}{R^2 E_x} = \frac{E_{x_o} I_2}{R^2 E_{x_o} h} = \frac{h^3}{12R^2 h} = \frac{(h/R)^2}{12} \tag{I-6}$$

$$I_o = \frac{(h/R)^3}{12} \tag{I-7}$$

$$r_1 = \frac{h}{R} \tag{I-8}$$

For external pressure

$$h_o = \frac{h}{2} \tag{I-9}$$

$$r_o = \frac{(h/R)}{2} \tag{I-10}$$

Isotropic Material

Hooke's Law for a homogeneous isotropic material can be written

$$\sigma_x = \frac{E}{1 - \mu^2} (e_x + \mu e_\theta) \tag{I-11}$$

$$\sigma_\theta = \frac{E}{1 - \mu^2} (e_\theta + \mu e_x) , \tag{I-12}$$

assuming the normal stress is zero. Comparing these expressions with the assumed stress-strain relationships given by Equation (2-10)

$$E_{x_o} = E_{\theta_o} = \frac{E}{1 - \mu^2} \tag{I-13}$$

$$E_{\nu_o} = \mu E_{x_o} \tag{I-14}$$

$$\frac{G_{xz_o}}{E_{x_o}} = \frac{E}{2(1 + \mu)} \frac{(1 - \mu^2)}{E} = \frac{1 - \mu}{2} \tag{I-15}$$

BIBLIOGRAPHY

1. N.E. Munch and E. Mangrum, Jr., "Application of Advanced Structural Technologies and Materials to Large Launch Vehicles," Society of Automotive Engineers Preprint 680695, Presented at the Aeronautic and Space Engineering and Manufacturing Meeting, Los Angeles, California, October 7-11, 1968.

2. J.P. Jones and P.G. Bhuta, "Response of Cylindrical Shells to Moving Loads," Journal of Applied Mechanics, Volume 31, Trans. ASME, Volume 86, Series E, 1964, pp. 105-111.

3. P. Mann-Nachbar, "On the Role of Bending in the Dynamic Response of Thin Shells to Moving Discontinuous Loads," Journal of the Aerospace Sciences, Volume 29, 1962, pp. 648-657.

4. H. Reismann, "Response of a Prestressed Cylindrical Shell to Moving Pressure Load," Developments in Mechanics, Proc. 8th Midwestern Mech. Conf. at Case Institute of Technology, April 1-3, 1963, Pergamon Press, Elmsford, New York.

5. H. Reismann, "Response of a Prestressed Elastic Plate Strip to a Moving Pressure Load," Journal of the Franklin Institute, Volume 277, No. 7, July 1964.

6. G.A. Hegemier, "Instability of Cylindrical Shells Subjected to Axisymmetric Moving Loads," Journal of Applied Mechanics, ASME, June 1966.

7. G. Herrmann and E.H. Baker, "Response of Cylindrical Sandwich Shells to Moving Loads," Journal of Applied Mechanics, March 1967.

8. Sing-Chih Tang, "Response of Viscoelastic Cylindrical Shells to Moving Loads," Journal of the Acoustical Society of America, Volume 40, No. 4, 1966, pp. 793-800.

9. G. Herrmann and A.E. Armenakas, "Dynamic Behavior of Cylindrical Shells Under Initial Stress," Proceedings of the Fourth U.S. National Congress of Applied Mechanics (American Society of Mechanical Engineers, New York, 1962).

10. E.H. Baker and G. Herrmann, "Vibrations of Orthotropic Cylindrical Sandwich Shells Under Initial Stress," AIAA Journal, Volume 4, No. 6, June 1966, pp. 1063-1070.

11. I. Mirsky and G. Herrmann, "Nonaxially Symmetric Motions of Cylindrical Shells," Journal of the Acoustical Society of America, Volume 29, No. 10, October 1957, pp. 1116-1123.

12. F.B. Hildebrand, Advanced Calculus for Engineers, Prentice-Hall, Inc., Englewood Cliffs, New Jersey, 1948.

13. J.D. Achenbach and C.T. Sun, "Moving Load on a Flexibly Supported Timoshenko Beam," Int. J. Solids and Structures, 1965, Volume 1, pp. 353-370, Pergamon Press Ltd., Great Britain.

14. S. Timoshenko and S. Woinowsky-Krieger, Theory of Plates and Shells, Second Edition, McGraw-Hill Book Company, Inc., 1959.

15. G.A. Korn and T.M. Korn, Mathematical Handbook for Scientists and Engineers, McGraw-Hill Book Company, Inc., 1961.

16. Yu Chen, Vibrations: Theoretical Methods, Addison-Wesley Publishing Company, Inc., Reading, Massachusetts, 1966.

ADDITIONAL REFERENCES

W.A. Nash, "Instability of Thin Shells," Applied Mechanics Surveys, Edited by Abramson et al., Spartan Books, New York, New York, 1966.

H.E. Lindberg, "Buckling of a Very Thin Cylindrical Shell Due to an Impulsive Pressure," J. App. Mech., Volume 31, Trans. ASME, Volume 86, Series E, 1964, pp. 267-272.

J.N. Goodier and I.K. McIvor, "The Elastic Cylindrical Shell Under Nearly Uniform Radial Impulse," J. App. Mech., Volume 31, Trans. ASME, Volume 86, Series E, 1964, pp. 259-266.

W. Stuiver, "On the Buckling of Rings Subject to Impulsive Pressures," Trans. ASME 32 E (J. App. Mech.) 3, September 1965.

M.H. Lock et al., "Experiments on the Snapping of a Shallow Dome Under a Step Pressure Load," AIAA Journal 6, 7, pp. 1320-1326, July 1968.

D.L. Anderson and H.E. Lindberg, "Dynamic Pulse Buckling of Cylindrical Shells Under Transient Lateral Pressures," AIAA Journal 6, 4, pp. 589-598, April 1968.

J.C. Yao, "Nonlinear Elastic Buckling and Parametric Excitation of a Cylinder Under Axial Loads," Trans. ASME 32 E (J. App. Mech.) 1, pp. 109-115, March 1965.

N.M. Gregoryants, "Problems of Equilibrium Stability of Cylindrical Shells Under Suddenly Applied Loads," Priklodnaya Mekhanika 2, 2, pp. 49-56, 1966.

R.R. Archer and C.G. Lange, "Nonlinear Dynamic Behavior of Shallow Spherical Shells," AIAA Journal 3, 12, pp. 2313-2317, December 1965.

M.P. Bieniek et al., "Dynamic Stability of Cylindrical Shells," AIAA Journal, Volume 4, No. 3, pp. 495-500, March 1966.

V.L. Prisekin, "The Stability of Cylindrical Shell Subjected to a Moving Load" (in Russian), Izvestiyn Akademii Nauk SSSR, Otdelenie Tekhnicheskikh Nauk (Mekhanika i Mashinostroenic), No. 5, 1961, pp. 133-134.

Sing-Chih Tang, "Dynamic Response of a Thin-Walled Cylindrical Tube Under Internal Moving Pressure," PhD Dissertation, The University of Michigan, January 1968.

P.G. Bhuta, "Transient Response of a Thin Elastic Cylindrical Shell to a Moving Shock Wave," Journal of the Acoustical Society of America, Volume 35, 1963, pp. 25-30.

H. Reismann, "Response of a Cylindrical Shell to an Inclined, Moving Pressure Discontinuity (Shock Wave)," Journal Sound Vib., 1968, 8 (2), pp. 240-255.

H. Reismann and J. Medige, "Forced Motion of Cylindrical Shells," Journal Engr. Mech. Div., Proc. Am. Soc. Civil Engr., EM5, October 1968.

Atis A. Liepins, "Asymmetric Nonlinear Dynamic Response and Buckling of Shallow Spherical Shells," NASA CR-1376, June 1969.

BIOGRAPHICAL SKETCH

Elmer Mangrum, Jr., was born July 6, 1936, at Buffalo Valley, Oklahoma, and in June 1954 was graduated from Buffalo Valley High School. In June 1956 he received his Associate in Science degree from Eastern Oklahoma A&M College at Wilburton, Oklahoma. In January 1959 he received the degree of Bachelor of Science with a major in Mechanical Engineering from Oklahoma State University. He joined the General Electric Company in January 1959, and qualified for the Advanced Engineering Program offered by the General Electric Company. This program is an intense, three-year training program which requires the solution of practical engineering problems using advanced mathematical methods. This was in addition to the training on the job which gave a broad exposure to different disciplines through six job assignments in various departments. Mr. Mangrum specialized in solid mechanics and graduated from the Advanced Engineering Program in June 1962.

In 1962 he transferred to Daytona Beach, Florida, and later enrolled in the Graduate School at the University of Florida. Part-time studies were begun, initially through the Florida Institute for Continuing Educational Studies, and later through the Graduate Engineering Education System (GENESYS). He was in the first graduating class of four people from GENESYS in December 1965 when he received the Master of Engineering Degree from the University of Florida with a major in Engineering Science and Mechanics and a minor in Mathematics. Mr. Mangrum continued part-time study and in September 1968 took a year's leave of absence from the General Electric Company to attend the University of

Florida to pursue the work toward the degree of Doctor of Philosophy. Since September 1969 he has been actively engaged in research to complete the requirements for this degree.

Elmer Mangrum, Jr., is married to the former Rita Anice Chesnut and they have one child. He is a member of Phi Theta Kappa, Pi Tau Sigma, and the ASME.

This dissertation was prepared under the direction of the chairman of the candidate's supervisory committee and has been approved by all members of that committee. It was submitted to the Dean of the College of Engineering and to the Graduate Council, and was approved as partial fulfillment of the requirements for the degree of Doctor of Philosophy.

August 1970

Dean, College of Engineering

Dean, Graduate School

Supervisory Committee:

Chairman

C. O. Luehr

Gene W. Hemp